Justus-Liebig-Universität Gießen
Institut für Anorganische und Analytische Chemie
Fachbereich Biologie und Chemie

Synthesis and investigation of copper(I) complexes with a thioether ligand system

Kumulativ-Dissertation zur Erlangung

des Doktorgrades der Naturwissenschaften

Dr. rer. nat.

vorgelegt von

Thomas

Rotärmel

aus Gießen

2023

Selbstständigkeitserklärung

Ich erkläre: Ich habe die vorgelegte Dissertation selbstständig und ohne unerlaubte fremde Hilfe und nur mit den Hilfen angefertigt, die ich in der Dissertation angegeben habe. Alle Textstellen, die wörtlich oder sinngemäß aus veröffentlichten Schriften entnommen sind, und alle Angaben, die auf mündlichen Auskünften beruhen, sind als solche kenntlich gemacht. Ich stimme einer evtl. Überprüfung meiner Dissertation durch eine Antiplagiat-Software zu. Bei den von mir durchgeführten und in der Dissertation erwähnten Untersuchungen habe ich die Grundsätze guter wissenschaftlicher Praxis, wie sie in der „Satzung der Justus-Liebig-Universität Gießen zur Sicherung guter wissenschaftlicher Praxis“ niedergelegt sind, eingehalten.

_____	_____
Ort, Datum	Thomas Rotärmel

Erstgutachter: Prof. Dr. Siegfried Schindler

Zweitgutachter: Prof. Dr. Richard Göttlich

Danksagung

Ich möchte mich bei Prof. Dr. Siegfried Schindler für die Aufnahme in seine Arbeitsgruppe, die Möglichkeit zu promovieren und die angenehme Zusammenarbeit während meiner Promotion bedanken. Des Weiteren möchte ich mich bei Prof. Dr. Richard Göttlich für das Zweitgutachtung dieser Arbeit bedanken.

Weiterhin möchte ich mich bei Dr. Jonathan Becker für den Kristallographie-Kurs und das Messen sowie Lösen zahlreicher Kristalle bedanken.

Ich möchte mich bei der gesamten Arbeitsgruppe Lars Schneider, Alexander Petrillo, Alexander Granichny, Florian Ritz, Anna Scholl und Stefan Schaub, sowie bei meinen ehemaligen Arbeitskollegen Dr. Pascal Specht, Dr. Tim Brückmann, Dr. Miriam Wern, Dr. Markus Lerch und Dr. Andrea Miska für die angenehme Arbeitsatmosphäre und die tolle Zusammenarbeit während meiner Promotion bedanken.

Auch möchte ich mich bei meinen ehemaligen Kommilitonen und Freunden bedanken, die mir immer mit Rat und Tat zur Seite standen.

Besonderer Dank gilt meiner Freundin Anna, die mich in den guten sowie in den schwierigen Zeiten meiner Promotion unterstützt und motiviert hat. Du warst mir immer eine große Stütze.

Zum Schluss möchte ich noch vor allem meinen Eltern und meiner Schwester Kristina danken, ohne die ich nie so weit gekommen wäre. In all den Jahren meines Studiums und meiner Promotion habt ihr mich immer unterstützt, mir immer geholfen und mich immer begleitet. Vielen Dank!

„Was wir wissen, ist ein Tropfen. Was wir nicht wissen, ist ein Ozean.“

Isaac Newton

Table of contents

1. Introduction 1

1.1 Catalytic selective oxidation in the chemical industry 1

1.2 Activation of molecular dioxygen 2

1.3 Oxygenase and Oxidase 5

1.4 Copper-containing metal enzymes 5

1.5 Tyrosinase and catechol oxidase 8

1.6 PHM, D*β*M, and T*β*M 9

1.7 Copper dioxygen binding modes and model complexes 11

1.8 Thioether ligated copper model systems 14

1.9 Closed shell ligand systems 22

2. Research goals 23

3. Investigation of the reactivity of copper(I) complexes with a N_3S thioether ligand-system 25

4. Syntheses and investigation of metal complexes with macrocyclic polythioether ligands 36

5. Summary 53

6. References 57

1. Introduction

1.1 Catalytic selective oxidation in the chemical industry

The selective oxidation reaction is an important field in the chemical industry for the functionalization of hydrocarbons and many other organic raw materials.[1] About 20 % of all processes in the chemical industry are based on oxidation reactions and around 600 million tons of chemicals per year are produced by oxidation reactions.[2] An important and known example is the production of adipic acid, which is a precursor for the synthesis of nylon-6,6.[3] In general, adipic acid is synthesized in a two-step process starting with cyclohexane (Scheme 1).[4]

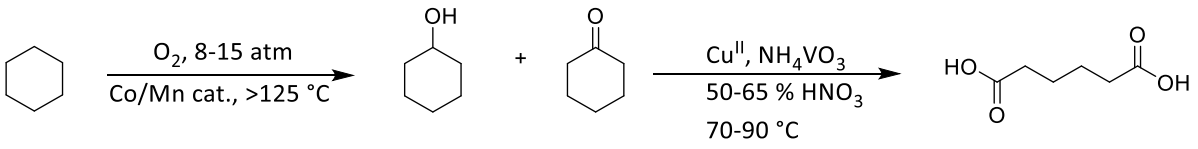

Scheme 1: Two-step process for the synthesis of adipic acid.[5]

At first, in the presence of a cobalt or manganese catalyst, cyclohexane is reacted with dioxygen at high temperature (>125 °C) and pressures (8-15 atm) to yield a mixture of cyclohexanol and cyclohexanone (KA oil). In the second step, the KA oil is then converted to adipic acid by oxidation with nitric acid in the presence of copper and vanadium catalysts. Succinic and glutaric acid are usually formed as side products. However, the use of nitric acid in the two-step oxidation process of cyclohexane poses environmental constraints by emission of nitrous oxide as ozone decomposing greenhouse gas and the formation of side products. For this reason, using green oxidants such as molecular dioxygen is gathering increasing interest not only for cyclohexane oxidation but for oxidation reactions in general.[5,6] In fact, molecular dioxygen is an ideal oxidant due it is abundantly available, inexpensive, and environmentally friendly. Over the past decades, organometallic compounds have emerged as useful catalysts for the efficient assembly of new chemical bonds. However, combining organometallic catalysts with dioxygen to produce selective oxidized organic compounds has proven challenging. A large barrier in the ability to design catalyst that utilizes molecular dioxygen is a relatively limited understanding of

how dioxygen reacts with transition metal complexes.[7] To better understand how dioxygen is transferred to organic substrates, naturally occurring enzymes, which represent the best catalysts engineered for selective oxidation reactions and dioxygen activation, are taken as role models.

1.2 Activation of molecular dioxygen

Metal active sites play an important role in the activation of molecular dioxygen for organic substrate oxidation.[8] However, without being activated, atmospheric molecular dioxygen doesn't react with most of the organic molecules, due to the thermodynamic stability of molecular dioxygen in its triplet ground state and because almost all organic molecules possess singlet ground states (paired electrons).[9] Therefore, at first molecular dioxygen ($^3O_2$), which is a diradical (two unpaired electrons, Scheme 2), has to be converted into an activated state ($^1O_2$, Singlet Dioxygen). Otherwise, the reaction between a triplet ground state molecule and a singlet ground state molecule would be spin forbidden. This kinetic barrier makes life possible.[10]

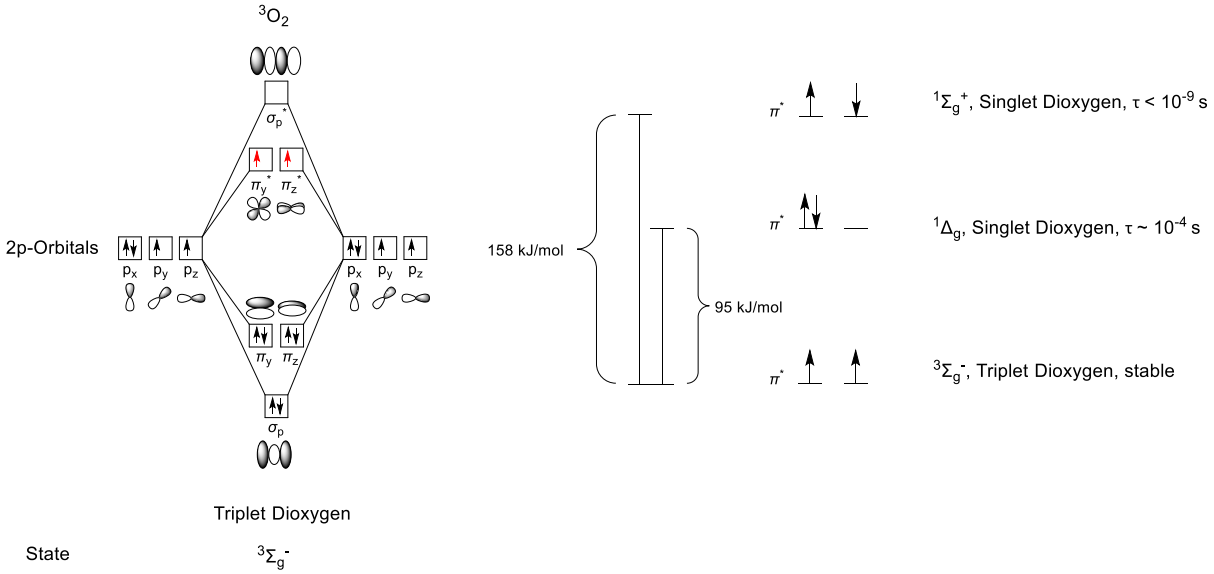

Scheme 2: Orbital diagram of the triplet ground state as well as two singlet excited states of molecular dioxygen showing the participating atom orbitals from each of the two oxygen atoms. The resulting molecule orbitals are shown in the diagram and are the result of the overlap of each atom orbital. The lowest 1s and 2s molecular orbitals are filled and omitted for clarity.

Besides the triplet state, molecular dioxygen can occur in two singlet excited states, which are 95 kJ/mol ($^1\Delta_g$) and 158 kJ/mol ($^1\Sigma_g^+$) above the triplet state as shown in Scheme 2. However, comparing the electronic configurations of the three demonstrated orbital diagrams in Scheme 2 shows that these three states only vary in the occupation of the *π*-antibonding orbitals. Due to the fact, that the transition from $^1\Delta_g$ to $^3\Sigma_g^-$ is spin forbidden, the $^1\Delta_g$ dioxygen species is relatively long stable. In contrast to that is the $^1\Sigma_g^+$ dioxygen species a short-lived state, because the spin allowed a transition between the $^1\Sigma_g^+$ and $^3\Sigma_g^-$ species.[11]

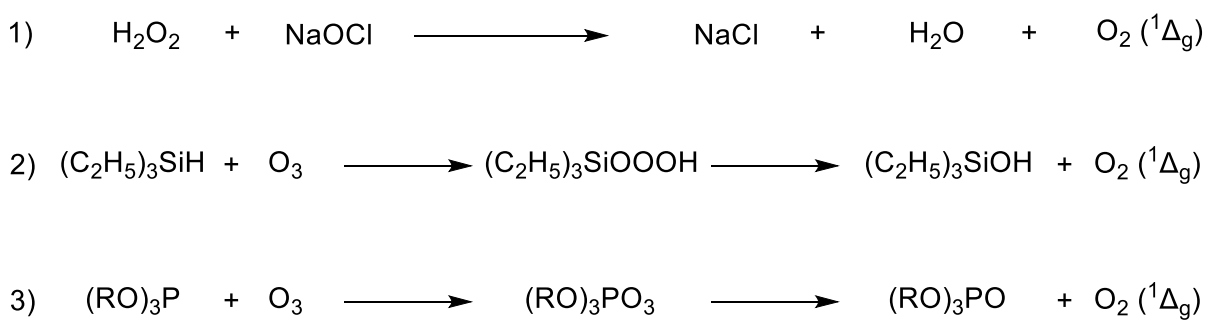

Scheme 3: Generation of singlet dioxygen $^1\Delta_g$ via three different chemical methods.[12–14]

The formation of singlet dioxygen can be realized with different methods. One way for the generation of $^1O_2$ is the photochemical method. In this method irradiation of a triplet dioxygen occurs with the light of an appropriate wavelength in the presence of a capable photosensitizer, which can absorb the light and use the energy to excite dioxygen to its singlet state. Besides the photochemical method, singlet dioxygen $^1O_2$ can also be produced by the reaction of hydrogen peroxide with sodium hypochlorite (Scheme 3, 1)).[12] Another chemical method uses triethylsilane and ozone (Scheme 3, 2))[13] or triphenyl phosphite (Scheme 3, 3)) and ozone to generate dioxygen in a singlet state configuration.[14]

In addition to the photochemical and chemical method of activating molecular dioxygen, dioxygen activation can also occur via transition metal ions. In this context, various enzymes are involved in dioxygen activation for the oxidation of organic substrates with a metal active site.[15–17] The enzyme thereby activates dioxygen by forming a metal oxygen adduct complex. The complex center of the adduct complex

removes a part of the electron density of the O-O bond, resulting in a weakened O-O bond. A closer look at the energetic states is provided by the molecular orbital (MO) Scheme 4. When dioxygen reacts with a metal center, the metal ion is oxidized and dioxygen is reduced, whereby the additional electrons occupy the antibonding molecular orbital π^*, thus weakening the O-O bond. Ground-state triplet dioxygen is a paramagnetic diradical with two electrons occupying π^* orbitals with parallel spins (Scheme 2). Reduction of dioxygen can lead to a superoxide- (Scheme 4, A) or peroxide-anion (Scheme 4, B). The superoxide-anion has three electrons in the π^* orbitals and the peroxide-anion has four electrons in the π^* orbitals.[18]

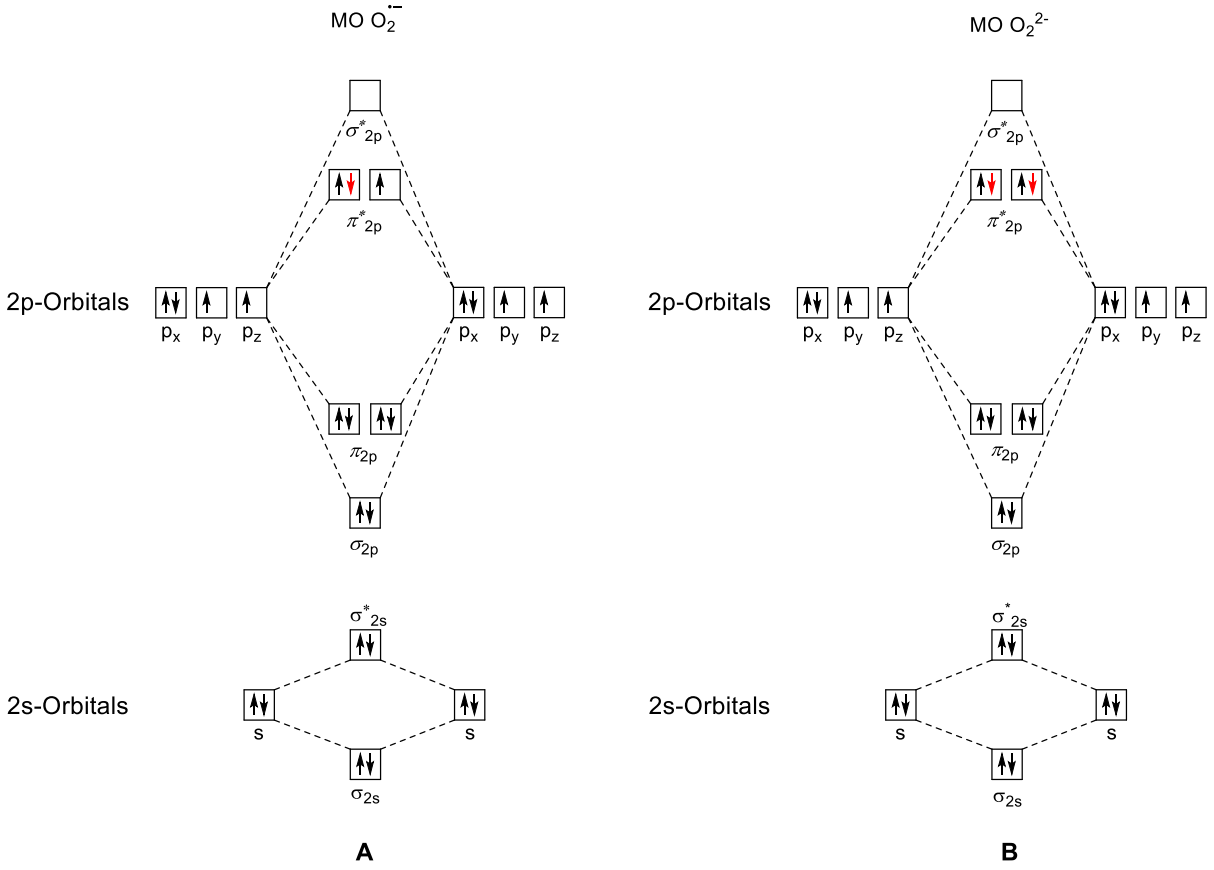

Scheme 4: Molecular orbital diagram for the superoxide-anion (A) and the peroxide-anion (B).[18]

The activation of dioxygen by metal proteins, the mechanism of dioxygen binding, and substrate oxidation are subjects of the following chapters and will be described in detail below.

1.3 Oxygenase and Oxidase

In search for a new possible metal catalyst for dioxygen activation, the metal enzymes in nature represent the best catalyst engineer for selective oxidation reactions. In biology, most of the selective oxidation reactions are performed by oxygenases and oxidases, which differ in the catalytic mechanism of aerobic oxidation. While the oxidases use molecular oxygen as an electron/proton acceptor in substrate (Sub) oxidation (Scheme 5, pathway a)), the oxygenases transfer oxygen-atom from dioxygen to the substrate (Scheme 5, pathway b)). Depending on whether only one or both oxygen atoms are incorporated into the substrate, the oxygenases are divided into monooxygenases and dioxygenases.[19,20]

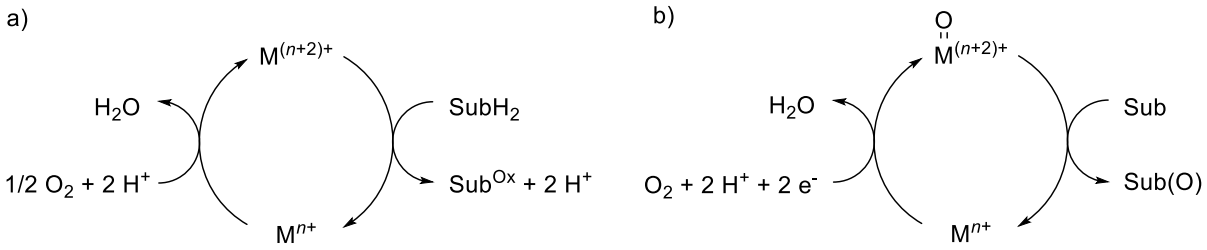

Scheme 5: Aerobic oxidation catalyzed by metalloenzymes via oxidase pathway a) and oxygenase pathway b).[20]

1.4 Copper-containing metal enzymes

Metal-containing enzymes that react with dioxygen play a central role in many biological processes. The most common metals incorporated in enzymes are zinc, iron, and copper, but only the iron- and copper-containing enzymes exhibit redox activity. Over 25 copper-containing enzymes are known today, their function range from electron transfer, dioxygen binding and transport to oxidation catalysis and nitrous oxide reduction (Scheme 6).[21,22] The copper-containing enzymes in Scheme 6 can be classified as types 1, 2, or 3 copper centers according to their visible, UV, and electron paramagnetic resonance (EPR) spectra.[16,21,23,24]

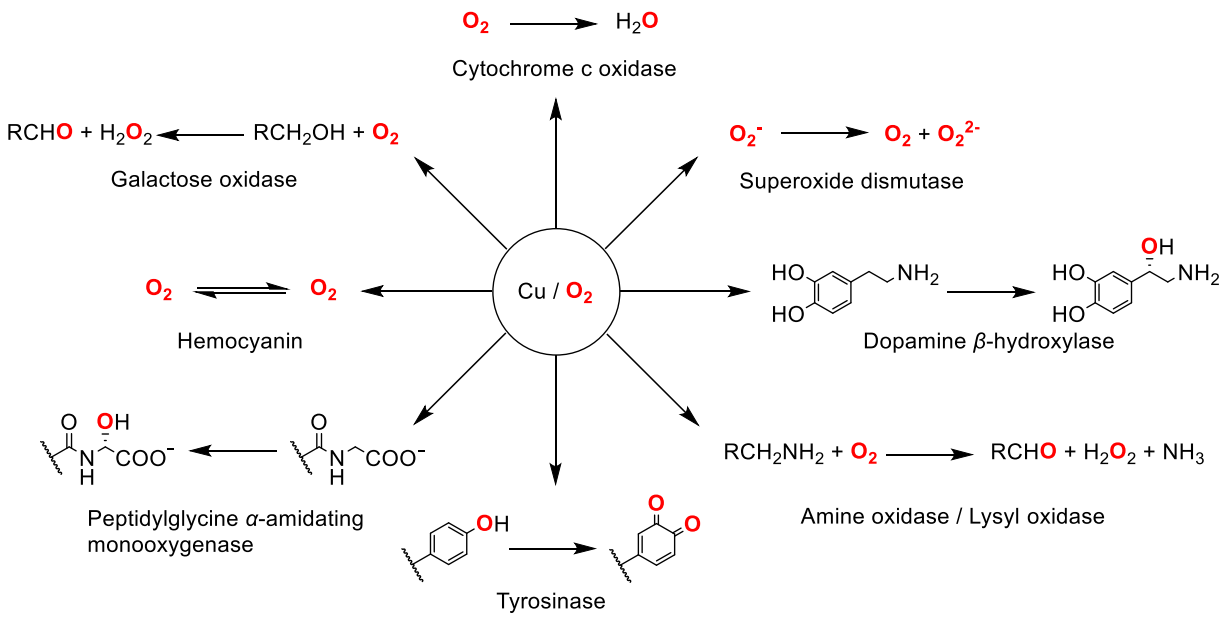

Scheme 6: Copper-containing enzymes in biological processes.[22]

Type 1 copper centers ("blue" copper proteins) are characterized by a strong absorption band in the visible region around 600 nm, which is responsible for the blue color in the electron absorption spectrum. This band is a consequence of the cysteine sulfur-to-copper ligand-to-metal charge transfer (LMCT) transition.[25] The "blue" copper proteins are found as mononuclear compounds involved in electron transfer processes. The copper atom in the active site is distorted tetrahedrally coordinated by two histidine (His) N-donors, a cysteine (Cys) thiolate S-donor and a fourth weakly bound variable ligand, in most cases a methionine (Met) residue. Instead of methionine also glutamine (Gln) or leucine (Leu) are found in some cases. Examples of type 1 proteins are azurin, plastocyanin (Scheme 7, type 1), and amicyanin.[26–28]

In contrast, to type 1 copper centers, type 2 copper centers are referred to as "non-blue" or "normal" copper enzymes. Most type 2 copper centers are either square planar or distorted tetrahedral coordinated by four N-donor atoms from for example histidine and/ or O-donor atoms from a water molecule.[28] Due to the absence of sulfur-to-copper charge transfer the color of these proteins is light blue caused by weak d-d transitions of the copper(II) ion. Examples of type 2 proteins are superoxide dismutase, dopamine-*β*-hydroxylase, and galactose oxidase (Scheme 7, type 2),

which are mostly involved in catalysis, selective hydroxylation, and C-H bond activation.[29,30]

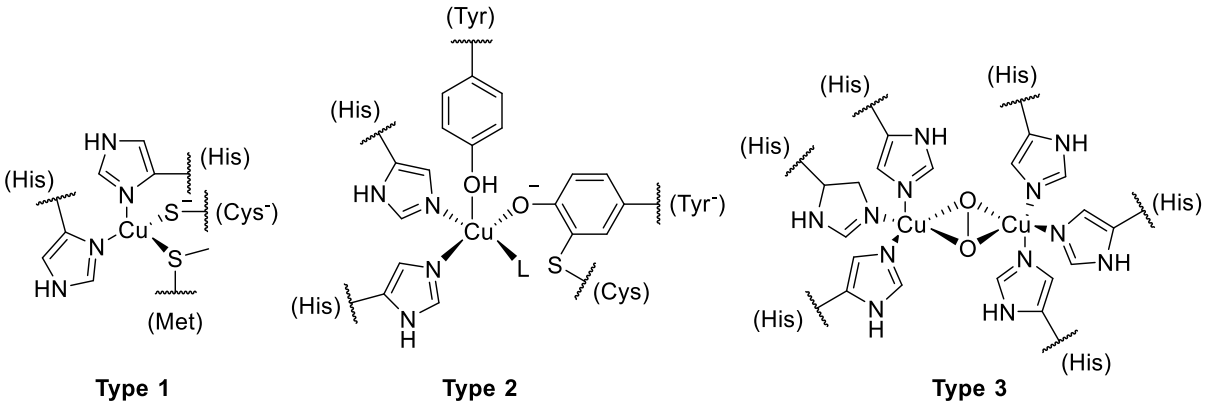

Scheme 7: Examples of selected copper centers for each type: plastocyanin (type 1)[26], galactose oxidase (type 2)[30], and hemocyanin in oxy form (type 3).[31]

Type 3 copper centers are compared to the type 1 and 2 centers characterized by two copper ions that are antiferromagnetically coupled. Due to the interaction between two paramagnetic copper ions, which results in a diamagnetic state, no contribution to EPR (electron paramagnetic resonance) spectra will be observed. Each copper ion is coordinated tetragonal by three nitrogen donor atoms of histidine.[22] Proteins with a type 3 copper center can incorporate reversibly dioxygen between the two copper ions, for which reason they can serve either as oxygenase, oxidase, or as a dioxygen transport protein. In their oxy form, a strong absorption band in the range of the UV region can be observed for the type 3 copper centers.

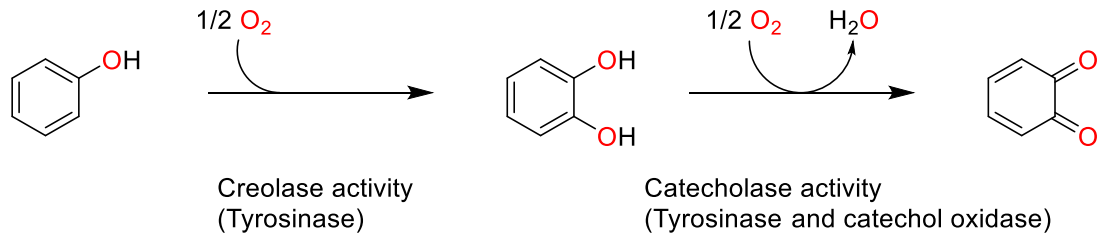

Scheme 8: Reaction pathway of phenol to *o*-diquinone by creolase- and catecholase activity.[32]

Examples of type 3 proteins are hemocyanin (Scheme 7, type 3), tyrosinase, and catechol oxidase.[31,33] Hemocyanin, an example of an oxygen carrier protein, can be divided into the arthropodan hemocyanins (lobsters and spiders) and the molluscan hemocyanins (octopus and snails). At first, only a crystal structure for arthropodan

hemocyanins (spiny lobster and horseshoe crab) was known, but in 1998 also a subunit from a molluscan hemocyanin (giant octopus) could be crystallized and investigated.[34]

1.5 Tyrosinase and catechol oxidase

Tyrosinase, which represents another member of the type 3 copper active center, exhibits monooxygenase activity as shown in Scheme 5 a) and Scheme 8 in the first step of the reaction pathway of phenol to *o*-quinones. In the second step, catechol oxidase, another member of the type 3 copper active site, catalyzes the prior produced catechol to the corresponding *o*-quinones. While tyrosinase can be found in plants, fungi, bacteria, mammalians, crustaceans, and insects, catechol oxidase can be isolated from plant tissues, insects, and crustaceans.[23,35]

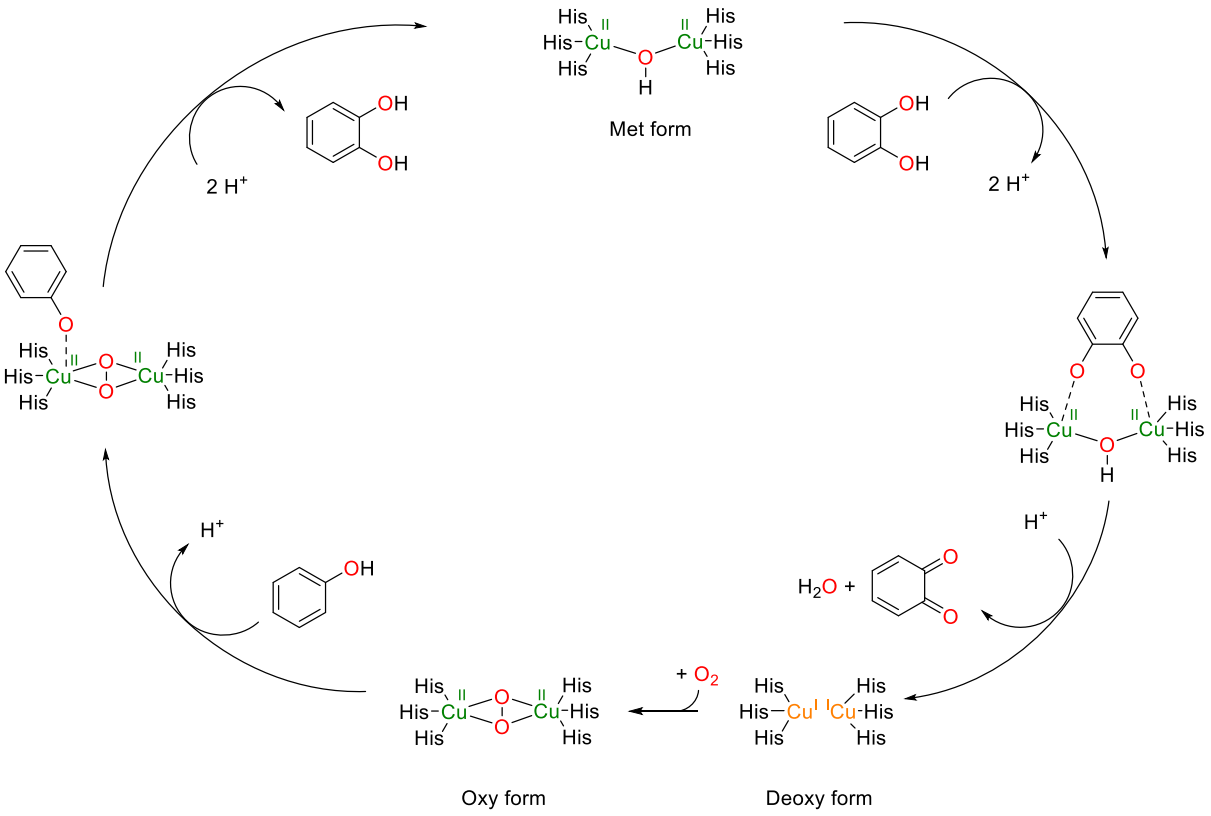

Scheme 9: Proposed mechanism for the reaction pathway of phenol to *o*-quinones. In the first step, the cresolase activity occurs followed by the catecholase activity.[32]

Already in 1996 Solomon and co-workers could purpose a proposed mechanism for the creolase and catecholase activities of the enzyme tyrosinase. In the first step of the cresolase activity, after the deoxy form reacts with dioxygen to the oxy form (Scheme 9), a phenol substrate binds in an axial fashion to one of the copper centers of the oxy form and gets monooxygenated to catechol. In the second step, the catecholase activity, the generated *o*-diphenol substrate binds to the met form in a bidentate fashion and gets oxidized to the corresponding *o*-quinone. Moreover, the deoxy form of the enzyme is generated again and can repeat the mechanism cycle.[23,32]

1.6 PHM, D*β*M, and T*β*M

Peptidylglycine-*α*-hydroxylating monooxygenase (PHM), dopamine-*β*-monooxygenase (D*β*M), and tyramine-*β*-monooxygenase (T*β*M) are important mononuclear copper-containing enzymes responsible for the stereospecific C-H *α*-hydroxylation of hormones and glycine-extended neuropeptides for neurotransmitter regulation and hormone biosynthesis.[17] In amino acid sequence, active site coordination, and reactivity, these three monooxygenases show many similarities. PHM, D*β*M, and T*β*M are distinguished by two distinct Cu sites (Cu_M and Cu_H), that are separated in the protein by an ~11 Å distance. In contrast to the coupled binuclear copper monooxygenases tyrosinase and hemocyanin, PHM, D*β*M, and T*β*M are so-called “non-coupled” binuclear copper monooxygenases, because of the lack of magnetic coupling between the Cu_M and Cu_H sites.

The Cu_M site is coordinated by one methionine and two histidine residues and the Cu_H site by three histidine residues. The activation of dioxygen and the hydroxylation reaction takes place at the Cu_M site, however, the Cu_H side is responsible for the electron transfer.[36] While PHM hydroxylates the C-terminus of a glycine residue of a glycine-extended prohormone, D*β*M manages the oxidation of dopamine to norepinephrine, two important neurotransmitters in the human body. In addition to that, T*β*M hydroxylates tyramine to octopamine (Scheme 10).[37]

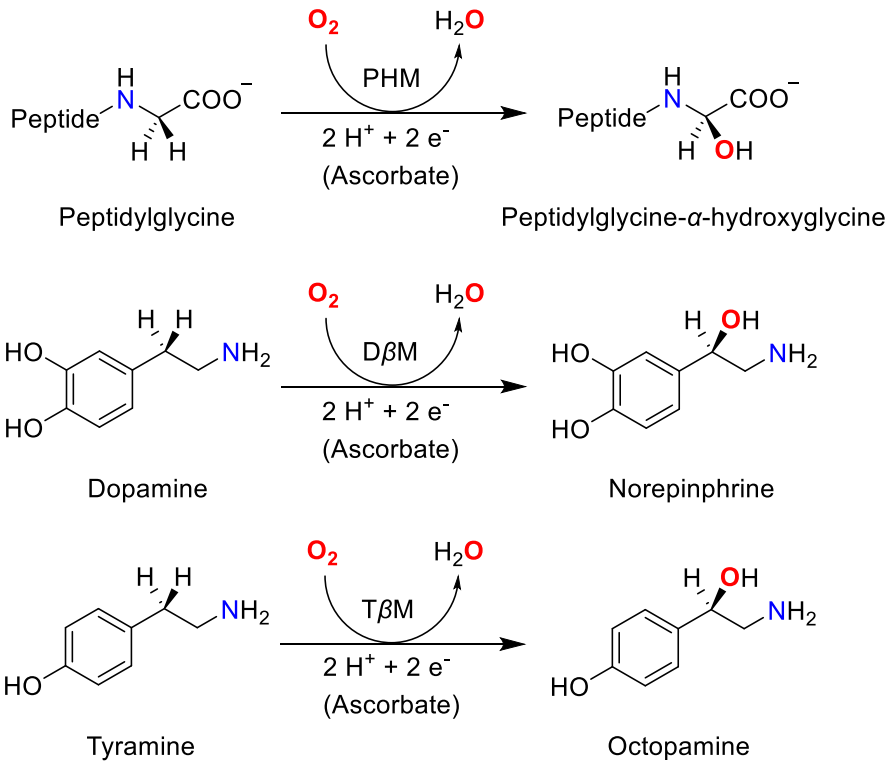

Scheme 10: Catalytic reactions of the monooxygenases PHM, DβM, and TβM.[38]

Several studies have dealt with the possible mechanism of substrate hydroxylation for the PHM, DβM, and TβM enzymes. In the predominant proposed mechanism, the Cu_M site is coordinated by dioxygen resulting in oxidation of the copper center and reduction of the dioxygen. The formed *end-on* copper(II) superoxido adduct is the active species for the hydrogen atom transfer (HAT) reaction from the substrate, followed by the formation of a copper(II) hydroperoxido adduct and a substrate radical.[38] The next step can be divided into two pathways. In pathway 1 (Scheme 11, pathway a)), a cupric oxyl intermediate is formed by homolytically cleavage of the O-O bond of the copper(II) hydroperoxido adduct. The substrate radical and the cupric oxyl intermediate rebound in the next step to give the product bound to the copper center. In pathway 2, the copper(II) hydroperoxido adduct reacts directly with the substrate radical by cleaving the O-O bond and hydroxylating the substrate (Scheme 11, pathway b)). The substrate product and the cupric oxyl species can then be reduced and protonated to yield a copper(II) hydroxido complex. In both pathways, the starting copper(I) complex can be regained by an external proton and electron.[37]

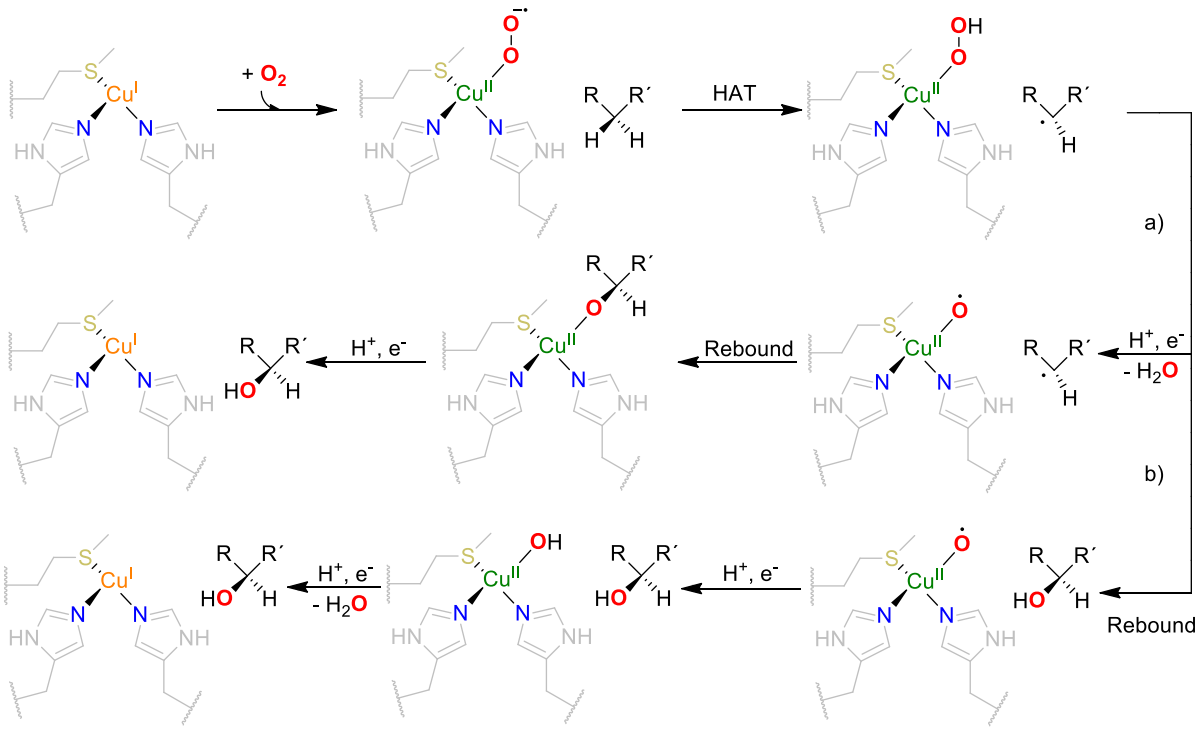

Scheme 11: Proposed mechanism for the enzymatic substrate reaction of PHM. D*β*M and T*β*M.[37]

1.7 Copper dioxygen binding modes and model complexes

Understanding the relationship between structure and reactivity is still a central challenge in copper dioxygen chemistry. Already in 1993, the crystal structure of hemocyanin protein could be solved.[39] In this structure, dioxygen was found to bridge between both copper ions in a *side-on* μ-η^2:η^2-peroxide fashion (Scheme 7, type 3). Extensive studies have been made to prepare model complexes, which mimic the active center of copper proteins to get more information about the effect of the binding mode of molecular oxygen in oxyhemocyanin. In this context, many copper oxygen intermediates with different binding modes could be found and have been investigated in terms of spectroscopy and reactivity. In 1988 Karlin *et al.* described the first crystallographic characterization of a copper dioxygen species with the tripodal ligand system TMPA (tris(2-pyridylmethyl)amine, Scheme 12 a)).[40] In comparison to the μ-η^2:η^2 dioxygen binding mode of oxyhemocyanin, the X-ray data showed a *trans*-μ-1,2-peroxido group between the two copper ions, that is only stable below −70 °C. Moreover, strong absorption bands at 440, 525, and 590 nm and

Raman vibrations at 561 and 832 cm^{-1} could be observed, which does not fit to the spectroscopic data of a *side-on* μ-η^2:η^2-peroxide binding mode.[41,42]

A short time later, in 1989, Kitajima and co-workers reported a copper dioxygen complex with a crystal structure of an oxygen-bridged dicopper species in a *side-on* μ-η^2:η^2-peroxide fashion.[43] With the anionic tripodal ligand HB(3,5-*i*Pr$_2$pz)$_3$ (tris(3,5-diisopropylpyrazolyl)borate, Scheme 12 b)) ligand, the copper dioxygen adduct is a stable solid at room temperature or in a non-coordinating solvent below −10 °C and shows similar spectroscopic features like the oxyhemocyanin. The model complex shows absorption bands at 349 and 551 nm, and Raman vibration at 741 cm^{-1}, while for the oxyhemocyanin absorption bands at 340 and 551 nm, and Raman vibration at 744-752 cm^{-1} were reported.[44]

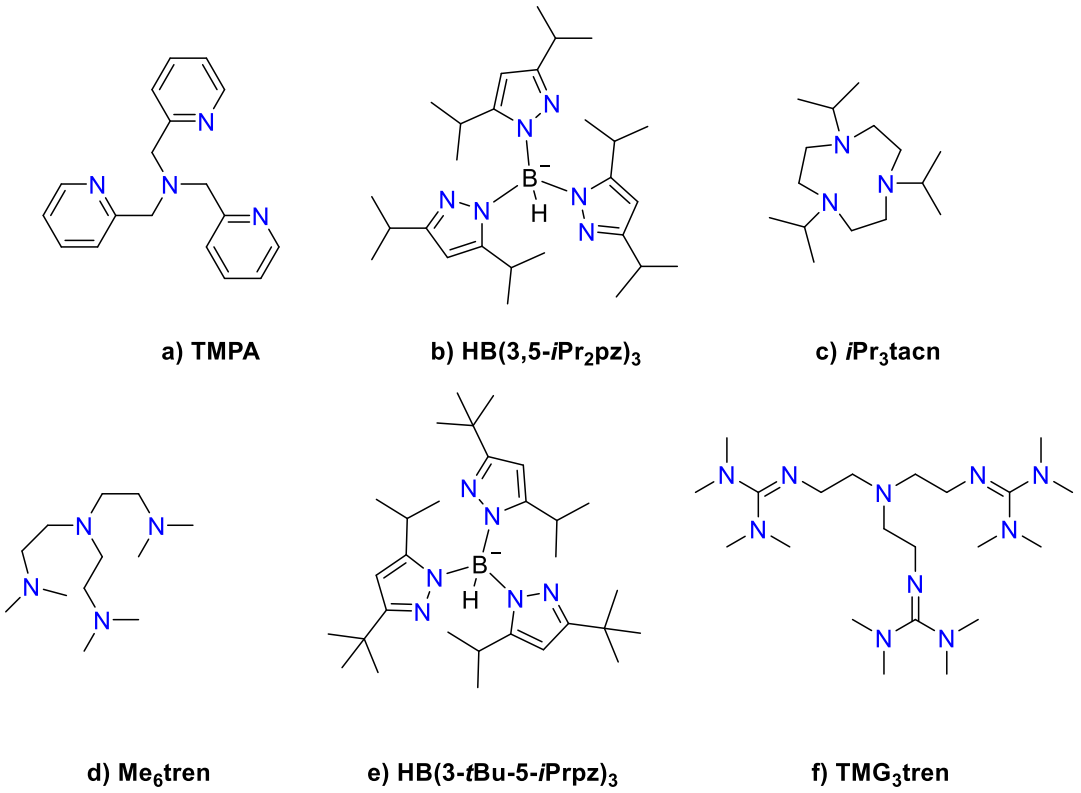

Scheme 12: Ligand systems used for model complexes.[40,41,43–50]

In 1996, a new copper dioxygen binding mode could be described by the working group of Tolman. In their work, they used the ligand *i*Pr$_3$tacn (1,4,7-triisopropyl-1,4,7-triazacyclononane, Scheme 12 c)) and revealed the structure and bonding of a bis(μ-oxido) copper(III) complex derived from crystallographic data, spectroscopic measurements and theoretical studies as well as the existence of an equilibrium

between a bis(*μ*-oxido) copper(III) and *side-on* *μ*-η^2:η^2-peroxido copper(II) complex.[45,46]

In contrast to the *side-on* *μ*-η^2:η^2-peroxido and *trans*-*μ*-1,2-peroxido complex, the dioxygen in the bis(*μ*-oxido) copper(III) complex is fully reduced by four electrons and the O-O-bond has been cleaved. Intensive absorption bands at 324 and 448 nm could be received and differ as well as the Raman vibration (600 cm^{-1}) from the previously described peroxido complexes.[45,46,51]

The formation of mononuclear *end-on* copper(II) superoxido species was first suggested as an initial reaction step in the reaction mechanism proposed for copper-containing monooxygenases like dopamine-*β*-hydroxylase,[52] phenylalanine hydroxylase[53] and peptidylglycine-*α*-amidating enzyme.[54] However, the first mononuclear copper dioxygen model complex was reported in 1991 by Karlin and co-workers using the TMPA ligand system (Scheme 12 a)). Although this mononuclear copper dioxygen species could initially only be proven spectroscopically, they could describe the first 1:1 copper dioxygen development, either in biological or model systems. In addition to that, the reaction of the mononuclear copper dioxygen complex to the *trans*-*μ*-1,2-peroxido complex could be investigated by means of kinetic, thermodynamic, and spectral parameters.[55] In this context, in 1999, Schindler *et al*. demonstrated spectroscopically the formation of a more stable copper(II) superoxido species than during a similar reaction of the copper(I) complex with the TMPA ligand using the aliphatic tripodal amine Me_6tren (tris(2-dimethyl-aminoethyl)amine, Scheme 12 d)).[50]

In 1994 and 2006, two crystal structures of mononuclear *end-on* copper(II) superoxido model complexes were reported. While the copper(I) complex with the ligand HB(3-*t*Bu-5-*i*Prpz)$_3$ (Scheme 12 e)) led to the formation of superoxide binding in η^2 fashion,[48] the crystal structure with the super basic tren derivate TMG_3tren (tris(tetramethylguanidino)tren, Scheme 12 f)) ligand showed a dioxygen species in η^1 fashion.[49] Only in 2004, structural characterization of the copper monooxygenase in PHM could show unambiguously a mononuclear *end-on* copper(II) superoxido complex in η^1 fashion in the active site.[56]

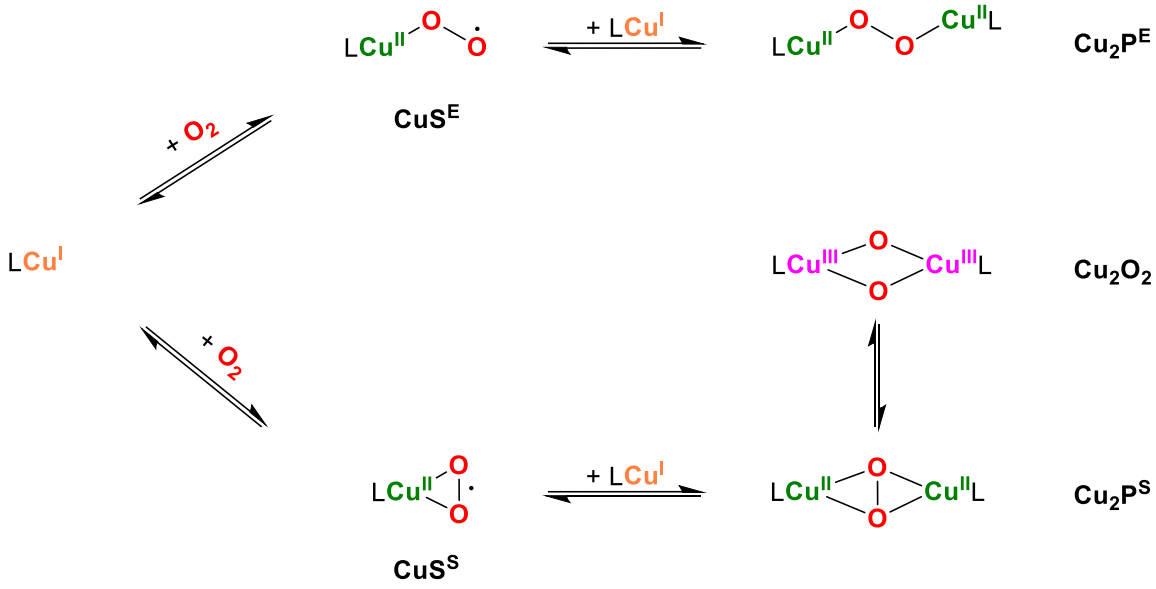

Scheme 13: Different copper dioxygen binding modes.[57]

In Scheme 13 are shown summarized the possible reaction pathways for the generation of different copper dioxygen species referred to copper enzymes starting from a copper(I) complex.[57,58] In the first step, a copper(I) complex reacts with dioxygen and delivers a mononuclear copper dioxygen species such as *side-on* copper(II) superoxido complex (CuS^S) or *end-on* copper(II) superoxido (CuS^E) complex. The structure of the resulting mononuclear species (CuS^S or CuS^E) is mainly depending on the ligand system.[16,59] The mononuclear copper species can react with another copper(I) complex to a *μ*-peroxido dicopper(II) complex in either a *side-on* Cu_2P^S or *end-on* Cu_2P^E fashion mode. The *side-on* Cu_2P^S can react further to a bis(*μ*-oxido) copper(III) species (Cu_2O_2) or can be in an equilibrium with the *side-on* Cu_2P^S species. Various parameters, such as the solvent, counterion effects, or ligand structure can have an influence on the equilibrium and be decisive for which species is favored to form.[47]

1.8 Thioether ligated copper model systems

Most of the copper dioxygen adducts investigated in the literature contain all nitrogen ligands.[16] However, the binding and activation of dioxygen at a copper center with a thioether ligand system as described in chapter **1.6** for PHM, D*β*M, and T*β*M are uncommon, for the reason that this kind of thioether ligation is characteristic for type

1 copper centers and is not presented in other dioxygen activating copper proteins.[23,27,60] Biochemical and biophysical investigation has already shown that the Cu_H center receives and passes electrons to the Cu_M center, where dioxygen and substrate binding occur.[61,62] Without a doubt, the thioether residue plays an important role in determining the electronic structure and functions of the Cu_M site leading to C-H bond activation. In order to get more information about the effect of the thioether residue, studies have been made to mimic the active site of the copper enzymes PHM, D*β*M, and T*β*M. Inspired by the biochemistry of copper enzymes with sulfur ligand residues, a variety of ligand scaffolds with $N_2S_{(thioether)}$ and $N_3S_{(thioether)}$ have been synthesized and investigated regarding their reactivity towards dioxygen.

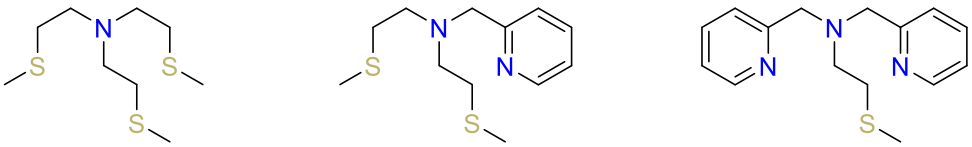

TMMEA **PMMEA** **BPMMEA**

Scheme 14: Sulfur containing tripodal ligands TMMEA (tris((methylthio)ethyl)amine), PMMEA (2-pyridylmethylbis(2-methylthioethyl)amine) and BPMMEA (bis(2-pyridylmethyl)-2-methylthioethylamine) included in Rorabachers work.[63,64]

The start in this area was made by Rorabacher and co-workers, who studied the influence of coordination geometry, the mechanism of complex formation, and the redox potentials of sulfur-containing ligand systems (Scheme 14).[63,64]

In 2006, Tolman *et al.* investigated a copper(I) complex with an anionic $N_2S_{(thioether)}$ ligand system $Me_2L^{iPr,SR}H$ (Scheme 15, a)) probing the effect of thioether substituents on the dioxygen reactivity *β*-diketiminate-copper(I) complexes and the role of the methionine ligand in copper monooxygenases. Low-temperature experiments of a copper(I) solution and dioxygen led to the formation of stable 1:1 Cu/O_2 adducts, which based on UV/Vis, Raman spectroscopic data, and DFT calculations propose a *side-on* η^2 dioxygen binding mode with negligible copper-thioether bonding and significant peroxido-copper(III) character.

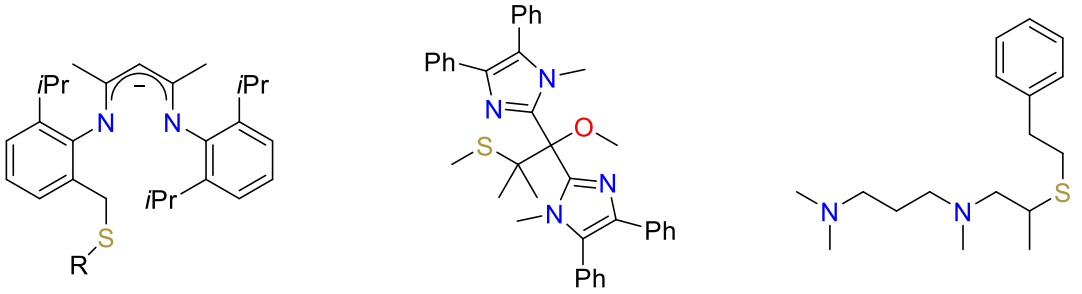

a) $Me_2L^{iPr,SR}H$ **b) $BIT^{OMe,SMe}$** **c) ANS**

R = Me, Ph

Scheme 15: $N_2S_{(thioether)}$ ligand system used for investigation of the active site of sulfur-containing copper enzymes.[65–67]

However, adding argon to the solution results in the formation of a bis(*μ*-oxdio) copper(III) species confirmed by spectroscopy and theory.[65] Copper(I) complexes with imidazolyl ligand $BIT^{OMe,SMe}$ (1-Methoxy-2-methyl-1,1-bis(*N*-methyl-4,5-diphenyl-2-imidazolyl)-2-methylthiopropane, Scheme 15, b)) were investigated by Zhou and co-workers, but no discrete copper dioxygen adducts were formed.[66,68] Karlin *et al.* reported with the linear N_2S tridentate ligand ANS (Scheme 15 c)) the formation of a *side-on* μ-η^2:η^2-peroxido copper(II) species with thioether coordination. This was the first case of thioether coordination within a *side-on* μ-η^2:η^2-peroxido copper(II) structure type, which indicated that it was possible to study ligand systems containing sulfur-containing ligand residues.[67] Nevertheless, the formation of a mononuclear *end-on* copper(II) superoxido species was not reached with these ligands (Scheme 15).

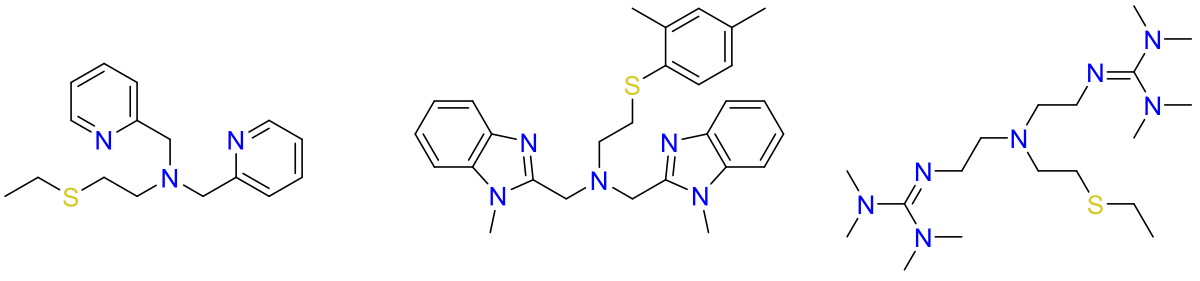

d) BPMEEA **e) Bis(1-methyl-2-methylbenzimidazolyl)-(2,4-dimethylphenylthioethyl)amine** **f) $(TMG_{Et})_2N_{Et}SEt$**

Scheme 16: $N_3S_{(thioether)}$ ligand system used for investigation of the active site of sulfur-containing copper enzymes.[69–72]

Within the $N_3S_{(thioether)}$ family of ligands, also the reaction of copper(I) complexes with dioxygen has been studied. Based on the TMPA ligand system Karlin and co-workers investigated the tetradentate BPMEEA ligand with two pyridyl residues, one amine donor, and one thioether residue (bis(2-pyridylmethyl)-2-ethylthioethylamine, Scheme 16, d)). Their findings showed, that the copper(I) complex reacts reversibly with dioxygen in dichloromethane and acetone (at −80 °C) or in 2-methyltetrahydrofuran (2-MeTHF, at −128 °C) producing a *trans*-*μ*-1,2-peroxido complex with a sulfur thioether ligation (Scheme 17). UV/Vis and Resonance Raman spectroscopy confirmed the formation of a *trans*-*μ*-1,2-peroxido structure. In addition, direct evidence for thioether ligation was derived from EXAFS (extended X-ray absorption fine structure) spectroscopy.[69,70]

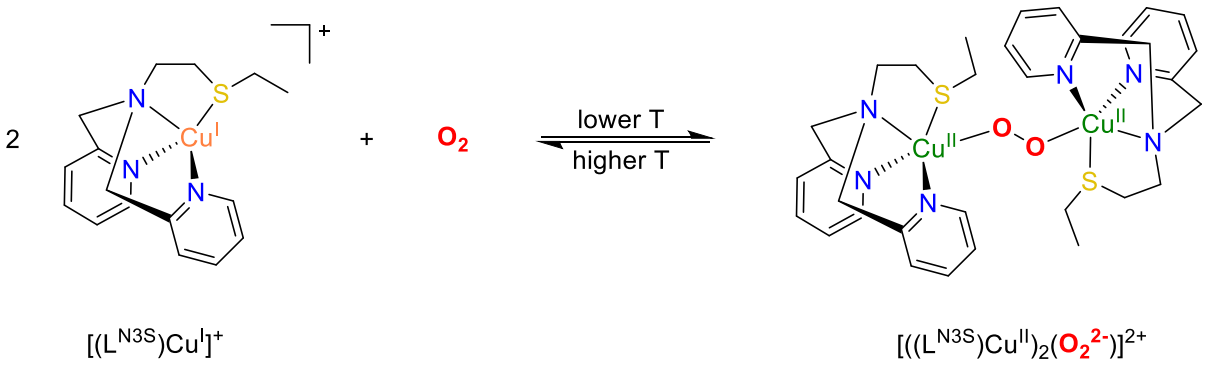

Scheme 17: Schematic representation of the reversible reaction of a copper(I) complex with the BPMEEA ligand and dioxygen.[69,70]

No copper dioxygen adduct could be observed for oxidation reactions of copper(I) complexes with several $N_3S_{(thioether)}$ benzimidazole-containing ligands (Scheme 16 e)) by Castilla and co-workers.[71] In 2013, Schindler and co-workers looked into the ligand $(TMG_{Et})_2N_{Et}SEt$ (2´,2´-(((2-ethylthio)ethyl)azanediyl)bis(ethane-2,1-diyl))bis-(1,1,3,3-tetramethyl-guanidine, Scheme 16 f)), a tren guanidine derivate. While the TMG_3tren ligand led to the formation of a mononuclear *end-on* copper(II) superoxido complex in η^1 fashion, the reaction behavior of the copper(I) complex with the $(TMG_{Et})_2N_{Et}SEt$ ligand was quite different. Time-resolved UV/Vis spectra for the reaction of the copper(I) complex with dioxygen in acetone at −76 °C led to the formation of a *side-on* μ-η^2:η^2-peroxido copper(II) species that subsequently

isomerized to an equilibrium mixture with a bis(*μ*-oxido) copper(III) species (Scheme 18).[49,72]

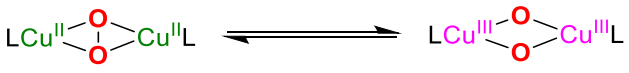

Scheme 18: Equilibrium between a *side-on* μ-η^2:η^2-peroxido copper(II) and bis(*μ*-oxido) copper(III) species.[72]

However, in contrast to the monooxygenases PHM, D*β*M, and T*β*M under these conditions no formation of an *end-on* copper(II) superoxido complex could be observed.

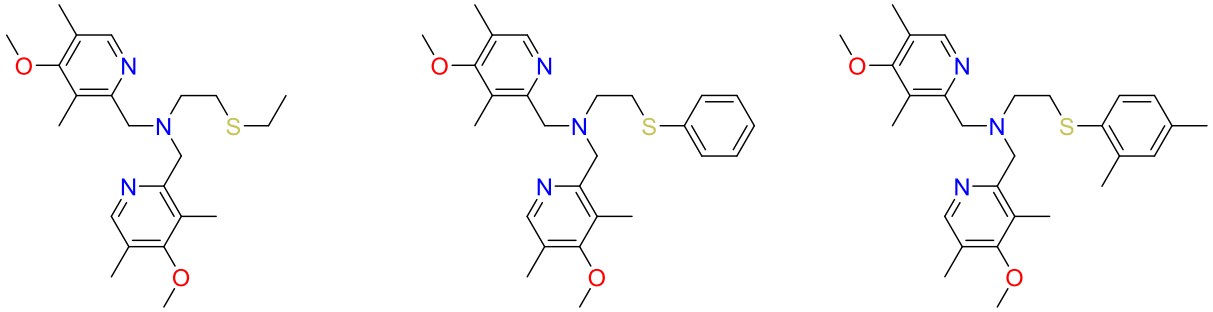

a) ^{DMM}**ESE** **b)** ^{DMM}**ESP** **c)** ^{DMM}**ESDP**

Scheme 19: Tuning an $N_3S_{(thioether)}$-based ligand by its thioether donor group.[73]

Further investigation on the $(TMG_{Et})_2N_{Et}SEt$ ligand by Bhadra *et al.* led to the formation of an *end-on* copper(II) superoxido complex, with a proven Cu^{II}-S interaction and hydrogen atom abstraction (HAA) reactivity. They probed lower temperatures by changing the solvent from acetone to 2-MeTHF, also requiring a change to tetrakis(pentafluorophenyl)borate ($B(C_6F_5)_4^-$) as counterion. Under these conditions, dioxygen was added to a precooled copper(I) complex solution in 2-MeTHF resulting in the formation of a brilliant green color. Intensive absorption bands at 442, 642 and 742 nm could be received and the presence of an *end-on* copper(II) superoxido complex was further confirmed by resonance Raman spectroscopy.[74] The measurement on a frozen 2-MeTHF sample revealed bands at 446 and 1105 cm^{-1}, which can be assigned as the Cu-O and as the superoxide O-O

stretch.[61,75] Variable temperature dioxygen binding studies revealed that the superoxide formation only forms below −90 °C.[74]

Further detailed studies with $N_3S_{(thioether)}$-based ligands containing two electron-rich 4-methoxy-3,5-dimethylpyridin (DMM, Scheme 19) residues and different thioether residues could show the influence of the thioether group on the Cu-S bond.

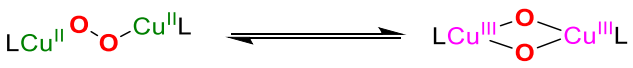

Scheme 20: Equilibrium between a *trans*-*μ*-1,2-peroxido copper(II) and bis(*μ*-oxido) copper(III) species.[73]

While a *trans*-*μ*-1,2-peroxido intermediate is favored for the ^{DMM}ESE ligand, a change to a more demanding thioether donor group causes a weakening of the Cu-S bond, which results in the stabilization of a bis(*μ*-oxido) copper(III) species for the ^{DMM}ESP and ^{DMM}ESDP ligand systems with S-aryl substituents (ethyl in ^{DMM}ESE a), phenyl in ^{DMM}ESP b), or 2,4-dimethylphenyl in ^{DMM}ESDP c), Scheme 19). Besides the formation of a bis(*μ*-oxido) copper(III) species, an equilibrium mixture between the oxido species and a *trans*-*μ*-1,2-peroxido species (Scheme 20) for the ^{DMM}ESP ligand was observed, that is the first example supported by a ligand system with a thioether donor group.[73] These findings of an equilibrium between a *trans*-*μ*-1,2-peroxido copper(II) and bis(*μ*-oxido) copper(III) species differs from previously observed results, that only a *side-on* *μ*-η^2:η^2-peroxido copper(II) species could be in equilibrium with a bis(*μ*-oxido) copper(III) species (Scheme 13).[16,59,76]

The addition of the coordinating anion methylsulfonate ($CH_3SO_3^-$) led to a spectroscopically pure bis(*μ*-oxido) copper(III) species (by UV/Vis-spectroscopy), stabilizing the bis(*μ*-oxido) copper(III) species relative to the *trans*-peroxido species in contrast to the effect of coordination anions on the equilibrium between a *side-on* *μ*-η^2:η^2-peroxido copper(II) and bis(*μ*-oxido) copper(III) species reported previously.[73] With bidentate ligand systems, Stack and co-workers showed that the addition of coordinating anions converts an equilibrium between a *side-on* *μ*-η^2:η^2-peroxido copper(II) and bis(*μ*-oxido) copper(III) species to an anion bridged *side-on* peroxido species.[77] In addition to this, Masuda and co-workers also demonstrated the stabilization of the *side-on* peroxido species, when a coordinating anion is added

additionally.[78] However, the ligand system ^{DMM}ESP demonstrates a new strategy to reversible cleave an O-O bond, which can be useful for the development of a synthetic, copper-based water-splitting catalyst.[79]

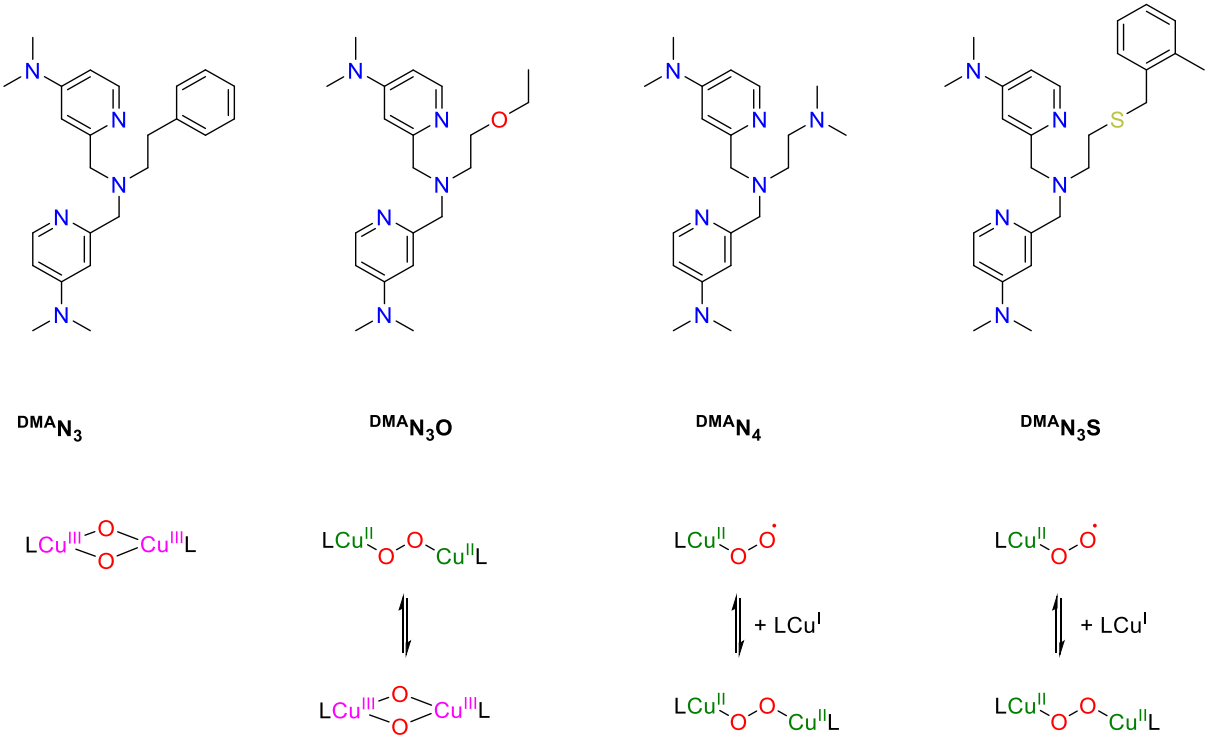

Scheme 21: Four structurally analogous ligands with different donor atoms and oxygenated products of copper(I)-complexes.[61]

Based on the TMPA ligand system further investigation to optimize the electronic and steric structure was carried out by Karlin and co-workers to stabilize the *end-on* copper(II) superoxido complex. The new ligand system varies in comparison to the DMM ligand system (Scheme 19) by the two pyridyl groups and the thioether residue. On the one hand, highly electron-rich dimethylamino (DMA) groups at the para position of both pyridyl groups were inserted. This kind of ligand design was based on the N_4 analog (Scheme 21 $^{DMA}N_4$) to stabilize a mononuclear *end-on* copper(II) superoxido complex reported previously.[80] On the other hand, the thioether residue was featured with a more demanding *o*-methyl benzyl substituent to slow the further reaction from the mononuclear *end-on* copper(II) superoxido complex to the dinuclear *trans-μ*-1,2-peroxido copper(II) complex similar to the previously described ^{DMM}ESDP ligand system (Scheme 19).[73]

The copper(I) complex with the ligand $^{DMA}N_3S$ can activate dioxygen in 2-MeTHF at −135 °C as a mononuclear *end-on* copper(II) superoxido complex, that rapidly converted to the thermodynamically more stable dinuclear *trans*-*μ*-1,2-peroxido copper(II) species confirmed by UV/Vis and Resonance Raman spectroscopy. Furthermore, it was shown that polar or hydrogen-bonding solvents like acetone, ethanol, or methanol have an important effect on the stabilization of the *end-on* copper(II) superoxido complex due to the formation of a hydrogen bond between an oxygen atom of the superoxido ligand and a polar solvent. This results in a shift of the equilibrium constant to the mononuclear *end-on* copper(II) superoxido complex over the dinuclear *trans*-*μ*-1,2-peroxido copper(II) complex.

Further investigations on the influence of the Cu-S interaction were carried out by comparing copper dioxygen species with different donor atoms binding (Scheme 21). Under identical reaction conditions like for the $^{DMA}N_3S$ ligand, the copper(I) complexes with the ligands $^{DMA}N_3$, $^{DMA}N_3O$, and $^{DMA}N_4$ (Scheme 21) were oxygenated. While the copper(I) complex with the ligand $^{DMA}N_3$ formed a bis(*μ*-oxido) copper(III) species, the copper(I) complex with the $^{DMA}N_3O$ ligand led to the formation of a *trans*-*μ*-1,2-peroxido copper(II) species, which converts to a bis(*μ*-oxido) copper(III) species with a similar UV/Vis spectrum as for the $^{DMA}N_3$ ligand, indicating an extremely weak interaction between the copper atom and the oxygen atom of the ether arm in $^{DMA}N_3O$. As in the case of the copper(I) complex with the $^{DMA}N_3S$ ligand, an *end-on* copper(II) superoxido complex and *trans*-*μ*-1,2-peroxido copper(II) complex were generated for the copper(I) complex with the $^{DMA}N_4$ ligand leading to the suggestion, that the S-donor atom from the thioether residue of $^{DMA}N_3S$ is coordinated to the *end-on* copper(II) superoxido complex and *trans*-*μ*-1,2-peroxido copper(II) complex.

These findings showed again the importance of ligand design and tuning. Redesign and modification of previously reported N_3S ligand systems led to the stabilization of an *end-on* copper(II) superoxido product with thioether ligation. This complex mimics the active site of the copper monooxygenase PHM and exhibits furthermore enhanced reactivity towards O-H (2,6-di-*tert*-butyl-4-methoxyphenol) and C-H (*N*-methyl-9,10-dihydroacridine) substrates in comparison to the nitrogen analogs ^{DMA}TMPA and ^{DMM}TMPA.[61]

1.9 Closed shell ligand systems

In addition to the open shell ligand systems described in the previous chapters, macrocyclic (closed shell) structures generated continuous interest in coordination chemistry. Macrocyclic ligand systems exhibit new properties beyond those anticipated from noncyclic open shell ligand systems. Besides the possibility to bind a wide variety of metals, they are versatile ligands in the biomimetic chemistry of dioxygen activation and show increased stability of metal coordination over open shell structures.[81] This effect is called the macrocyclic effect and makes closed shell ligand systems extremely favorable for metal complexation.[82] In this regard, TMC (1,4,8,11-tetramethyl-1,4,8,11-tetraazacyclotetradecane, Scheme 22) is one of the most used closed shell ligand systems, which can complex various metal ions with high thermodynamic and kinetic stability with respect to metal ion dissociation.[83]

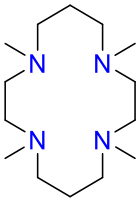

TMC

Scheme 22: Closed shell ligand system TMC.

A variety of metal-oxygen adducts with the TMC ligand system have been synthesized and characterized. In the case of iron, TMC complexes of oxido, superoxido, and peroxido ligands were successfully obtained with hydrogen peroxide (H_2O_2) or iodosylbenzene (PhIO) as an oxygenation agent.[84] In 2018, Schindler *et al.* could structurally characterize an iron(IV) oxido complex with the TMC ligand system and a water molecule as an additional ligand. In their efforts to trap the iron(IV) oxido complex, they use ozone as an oxygenation agent and could show that ozone enables a clean preparation of the oxido complex.[85] However, oxygenation with ozone is well known for iron and manganese porphyrinoid complexes,[86,87] but studies on the reactions of ozone and copper(I) complexes have not been reported so far.

2. Research goals

The goal of the research project presented herein was the synthesis and investigation of model complexes for the PHM enzyme using sulfur-containing thioether ligand systems. As described in the introduction, the *end-on* copper(II) superoxido complex reacts rapidly to form the thermodynamically more stable *trans*-*μ*-1,2-peroxido copper(II) complex, which makes the stabilization of this species difficult. Therefore, the motivation was the development of new ligands by modification of already known ligand systems to stabilize the *end-on* copper(II) superoxido complex and prevent dimerization.

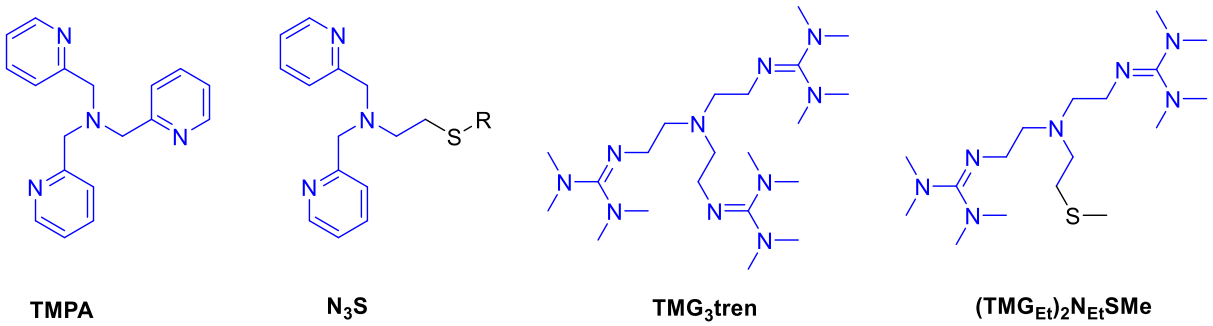

Scheme 23: Tetradentate ligands that are discussed in this work. R can be a methyl-, ethyl-, *tert*-butyl, benzyl-, 4-methoxybenzyl- or furfuryl-group.

In this regard, my research was initially started based on the open shell ligand systems TMPA and TMG_3tren. To create a model complex for the PHM enzyme, the TMPA and TMG_3tren ligand systems were first modified by replacing a pyridine group in the TMPA ligand system and a guanidine group in the TMG_3tren ligand system with a thioether residue (Scheme 23). By attaching different sterically demanding thioether residues, the influence of the thioether group on the stability of the oxygen species should be investigated. Therefore, the reaction of the copper(I) complexes with dioxygen was investigated using low-temperature-stopped-flow techniques. Furthermore, electrochemical and crystallographic analyses were executed to determine the impact of ligand modification on dioxygen activation. These results were reported in the European Journal of Inorganic Chemistry and are described in **Chapter 3**.

As described in the introduction**,** macrocyclic closed shell ligand systems offer increased stability in complex coordination and versatility in the biomimetic chemistry of dioxygen activation. The aim was for that reason to investigate the difference between open-shell ligand systems and closed-shell systems on the stability of the oxygen complexes. For this purpose, incorporation of sulfur in the cyclam N_4 ligand system should be performed to receive the sulfur-containing ligands dithiacylam N_2S_2 and tetrathiacyclam S_4 shown in Scheme 24.

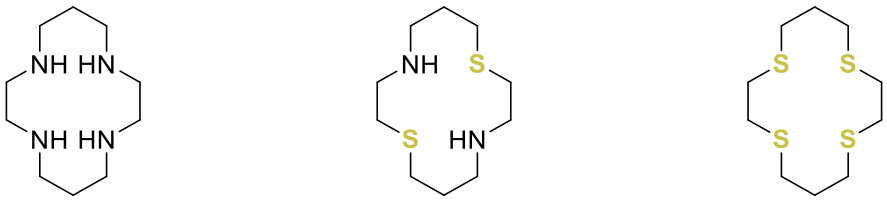

N_4 **N_2S_2** **S_4**

Scheme 24: Sulfur-containing ligands N_2S_2 and S_4 derived from cyclam ligand N_4.

The reactivity towards dioxygen was investigated using low-temperature-stopped-flow techniques and should provide further insights into a possible mechanism of the reaction between the metal complexes and dioxygen. In addition, it has been shown that ozone can be used as another oxygenation agent besides dioxygen to generate oxygen adduct complexes.[85,86] The investigation of the more reactive ozone as an oxidant agent, in case of a successful reaction with the copper(I) complex, should lead to new copper-oxygen adducts like an ozonido complex. The results are described in **Chapter 4** and have been reported in Faraday Discussions.

3. Investigation of the reactivity of copper(I) complexes with a N_3S thioether ligand-system

This work has been published in

European Journal of Inorganic Chemistry

Thomas Rotärmel, Pascal Specht, Jonathan Becker, Adam Neuba, and Siegfried Schindler

Eur. J. Inorg. Chem., **2022**, e202200626

European Journal of Inorganic Chemistry 10.1002/ejic.202200626

WILEY-VCH

RESEARCH ARTICLE

Investigations of the reactivity of copper(I) complexes with a N_3S thioether ligand-system

Thomas Rotärmel,[a] Pascal Specht,[a] Jonathan Becker,[a] Adam Neuba[b], and Siegfried Schindler[a*]

Dedicated to the 90th birthday of Prof. Dr. Horst Elias

[a] *T. Rotärmel, Dr. P. Specht, Dr. J. Becker, Prof. Dr. S. Schindler*
Institute for Inorganic and Analytical Chemistry,
Justus-Liebig-University Gießen,
Heinrich-Buff-Ring 17, 35392 Gießen, Germany
E-mail: Siegfried.schindler@ac.jlug.de
https://www.uni-giessen.de/fbz/fb08/Inst/laac/schindler
[b] *A. Neuba*
Department of Chemistry
University of Paderborn
Warburger Straße 100, 33098 Paderborn, Germany

Supporting information for this article is given via a link at the end of the document.

Abstract: In the active site of several copper monooxygenases, thioether residues are coordinated through the sulfur atom, e. g. dopamine-β-monooxygenase (DβM). The reaction of dioxygen with a series of copper(I) complexes with thioether groups in tripodal ligands based on either derivatives of tris(2-pyridylmethyl)amine (TMPA) or a guanidine system were investigated by low-temperature stopped-flow measurements. The formation of labile intermediates, an *end-on* superoxido complex, and μ-1,2-peroxodicopper(II) complexes were spectroscopically detected and a kinetic analysis allowed the calculation of activation parameters for these reactions supporting the postulated mechanism. Most interesting was the finding that replacing the ethyl group in the tren-guanidine derivative ($^{TMG}Et)_2(SEt^{Et})N$ with a methyl group allowed a dramatic increase in the stability of the formed superoxido copper complex. Measurements with ozone were performed in an effort to find an alternative way to obtain and stabilize the labile intermediates.

Introduction

Copper-mediated activation of molecular dioxygen is essential in various synthetic, industrial, and biological processes.[1] The binding of dioxygen to copper in the form of η^1-superoxido (A), peroxido (B and D), or oxido (C) complexes (Scheme 1) has been intensively studied for years because of the biological occurrence in proteins such as hemocyanin (Hc), the O_2-carrier for arthropods and mollusks,[2] and monooxygenases including dopamine-β-monooxygenase (DβM) and peptidyl-glycine-α-monooxygenase (PHM), enzymes that play a crucial role in the biogenesis of neurotransmitters and hormones.[3] In previous work, for example by Karlin, Stack, Tolman, and Itoh as well as by us, it was demonstrated that copper-dioxygen complex formation and its reactivity are highly dependent on the nature of the ligand.[4,5] Most copper-dioxygen adduct complexes reported in the literature contain ligands with nitrogen donors. However, in recent years, studies of contemporary interest in Cu^I/O_2 include the influence of thioether sulfur ligation inspired by the unique active-site of the monooxygenases DβM and PHM, containing thioether ligand residues, such as cysteine (Cys) and methionine (Met).[5–7]

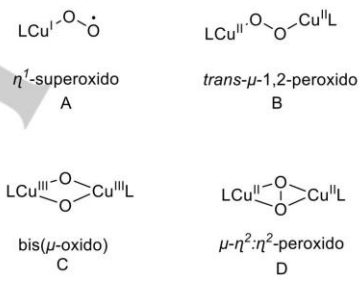

Scheme 1: Different binding modes of copper-dioxygen adducts.

Therefore, several different thioether ligands have already been investigated previously.[8–10] In 2006 Karlin et al. described reversible copper(I)-O_2 binding and adduct formation of a trans-μ-1,2-peroxodicopper(II) complex (Scheme 1, B) in a sulfur ligand environment employing a tetradentate $N_3S_{(thioether)}$ ligand, similar to the tripodal tetradentate ligand tris(2-pyridylmethyl)amine (TMPA, Scheme 2).[11,12] However, this is not a binding mode so far observed in nature. To get closer to mimicking the active site (a monomolecular *end-on*-superoxido copper complex, Scheme 1, A) of PHM[6], Bhadra et al. used a thioether derivative ($^{TMG}Et)_2(SEt^{Et})N$ Scheme 2, R = Et) of the tripodal ligand tris(tetramethyl-guanidino)tren (TMG_3tren, Scheme 2). With this ligand, an *end-on*-superoxido copper complex with an experimentally proven Cu-S bond demonstrated hydrogen atom abstraction (HAA) reactivity.[13] Based on these results and inspired by the biochemistry of the corresponding enzymes, we decided to investigate the role of the thioether residues in PHM and DβM by synthesizing a variety of ligand scaffolds based on the TMPA and TMG_3tren (Scheme 2) ligand system and test their reactivity towards dioxygen and ozone.

European Journal of Inorganic Chemistry 10.1002/ejic.202200626

WILEY-VCH

RESEARCH ARTICLE

Results and Discussion

Synthesis and characterization of a copper(I) complex with a TMG$_3$tren-derivative

As described in the introduction, Bhadra et al. succeeded in mimicking the active site of the enzymes PHM and DβM.[13] However, it was necessary to perform these investigations in 2-MeTHF at -135 °C to observe the formation of the end-on superoxido complex.[13,14] We assumed that the ethyl group at the sulfur atom suppresses strong coordination to the copper(II) ion. In the molecular structure of the copper(II) complex [(^{TMG}Et)$_2$(SEt^{Et})NCuCl]Cl the sulfur atom is not bound to the copper(II) ion most likely due to sterical reasons.[15] Therefore, it seemed likely that replacing the ethyl group with the sterically less demanding methyl group should allow the stabilization of the *end-on* superoxido complex. (^{TMG}Et)$_2$(SEt^{Me})N (Scheme 2: TMG$_3$tren-derivative with R = Me) was synthesized in a four-step synthesis based on the ligand synthesis of the (^{TMG}Et)$_2$(SEt^{Et})N ligand with some modifications (Scheme 3, see Experimental Section).[15] However, purification of **1** turned out tedious.

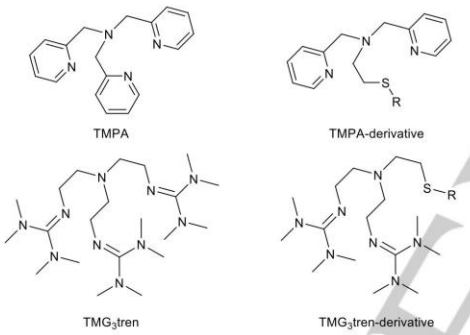

Scheme 2: Tetradentate ligands that are discussed in this work.

During our efforts to obtain **1**, we got the ligand in the form of its sodium complex [Na(**1**)]PF$_6$ (the molecular structure and crystallographic data are reported in the Supporting Information 1.2). Treatment of [Na(**1**)]PF$_6$ with [Cu(MeCN)$_4$]PF$_6$ in acetone led to the isolation of a light yellow solid. Single crystals could be grown by slow solvent evaporation. As shown in Figure 1 (crystallographic data are reported in Supporting Information), the copper(I) complex could be obtained via an exchange reaction. The crystal structures revealed that the sodium and the copper complex are coordinated distorted trigonal pyramidally by three N-donor atoms and one sulfur-donor atom. The Cu-S bond length in the copper-complex (2.2684(6) Å) falls in the normal range for Cu^I-S$_{thioether}$ complexes. According to literature copper(I) complexes containing at least one thioether ligand reveal typical Cu-S bond distances between 2.20 and 2.44 Å.[16,17,18] This distorted trigonal pyramidal geometry presents an open coordination site for further ligand binding. The Cu-S (2.2684(6) Å) and Cu-N bond distances (2.0183(18), 2.0209(18), and 2.2035(17) Å) are comparable with the bond lengths of the copper complex with (^{TMG}Et)$_2$(SEt^{Et})N (Cu-S 2.2709(5), Cu-N 2.0362(15), 2.0436(15) and 2.1987(14) Å).[13] The molecular structures of the copper(II) complexes [(**1**)CuCl]Cl and [(**1**)CuCl]BPh$_4$ have been reported previously and show that in the solid state the sulfur atom is coordinated, supporting our findings.[19]

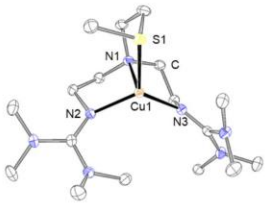

Figure 1: ORTEP representation of the copper complex described in the molecular structures of [Cu(**1**)]$^+$. H atoms and counter ion were omitted for clarity, anisotropic displacement ellipsoids were plotted at 50% probability. Selected bond lengths (Å): Cu1-S1: 2.268, Cu1-N1: 2.204, Cu1-N2: 2.018, Cu1-N3: 2.021. Selected bond angles (°): N1-Cu1-S1: 89.09, N1-Cu1-N2: 84.59, N2-Cu1-N3: 119.78, N3-Cu1-S1: 123.29.

Oxygenation reactions of [Cu(1)]PF$_6$

Quite surprisingly, [Cu^I(**1**)]$^+$ with different anions tetrakis(3,5-bis(trifluoromethyl)phenyl)borate ([Bar$^F{}_4$]$^-$ and tetrakis(pentafluorophenyl)borate B(C$_6$F$_5$)$_4^-$) did not dissolve in 2-MeTHF, so that a direct comparison with the reaction of [(^{TMG}Et)$_2$(Set^{Et})NCu]B(C$_6$F$_5$)$_4$ with dioxygen under identical conditions was not possible. However, [Cu^I(**1**)]PF$_6$ could be reacted with dioxygen in acetone at -90 °C (Scheme 4). Bubbling dioxygen through a cooled complex solution led to the formation of a dark green colored solution under these conditions indicating the formation of an *end-on* superoxido complex. This was confirmed by the UV-vis spectrum of this compound which is characterized by an absorbance maximum at 432 nm (Figure 2) and is similar to the ethyl-derivative (442 nm) and the N$_4$-analog (442 nm).[13,20] In contrast, the reaction of dioxygen with [(^{TMG}Et)$_2$(Set^{Et})NCu]OTf in acetone did not allow the observation of the end-on superoxido complex.[15]

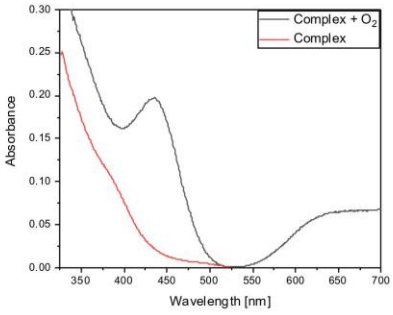

Figure 2. UV-vis spectrum of [Cu^I(**1**)]PF$_6$ ($c_{complex}$ = 0.75 mmol/L, red line) and after the reaction with dioxygen at -90 °C (black line).

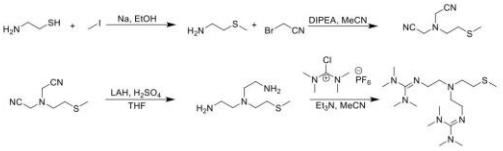

Scheme 3: Ligand Synthesis of (^{TMG}Et)$_2$(SEt^{Me})N.

European Journal of Inorganic Chemistry 10.1002/ejic.202200626

WILEY-VCH

RESEARCH ARTICLE

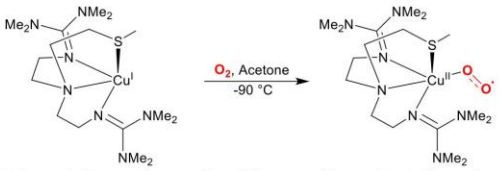

Scheme 4: Oxygenation reaction of the copper(I) complex to the end-on copper(II) superoxido complex.

To gain more information about the improved stability of the end-on superoxido complex $[Cu^{I}(\mathbf{1})O_2]PF_6$ low-temperature stopped-flow measurements were performed. Time-resolved UV-vis spectra (Fig. 3) were collected in acetone between -90 °C and -75 °C. Measurements were performed under pseudo first order conditions ($[O_2]$ >> [complex]) and the formation of the absorbance band at 432 nm over time could be fitted to a single exponential function, indicating first order for the complex concentration in the rate law. A plot of k_{obs} vs. dioxygen concentration showed a linear dependence with an intercept (see Supporting Information), indicating first order in $[O_2]$ and reversibility of the reaction (see Supporting Information). An Eyring plot based on the second order rate constants (see Supporting Information) allowed to calculate activation parameters $\Delta H^{\ddagger}$ = 4.9 ± 1 kJ · mol^{-1} and $\Delta S^{\ddagger}$ = -164 ± 1 J · mol^{-1} K^{-1}. The negative activation entropy indicates an associative mechanism in line with previous results. Stopped-flow measurements in acetonitrile were performed as well to investigate the stability of the *end-on* superoxido copper complex at higher temperatures. However, no reaction was observed at -40 °C in acetonitrile with dioxygen. Additionally, the reaction of ozone with $[Cu^{I}(\mathbf{1})]PF_6$ in acetone showed the same reaction as with dioxygen under the same conditions. Nearly the same behavior had been observed for the reaction of $[Cu(tet\ b)]PF_6$ with dioxygen and ozone reported previously by us.[21] Unfortunately and in contrast to the quite stable copper superoxido complex with the TMG_3tren ligand, the complex $[Cu^{II}(\mathbf{1})O_2]PF_6$ started to decompose immediately after its formation and therefore, no additional experiments were performed with this system.

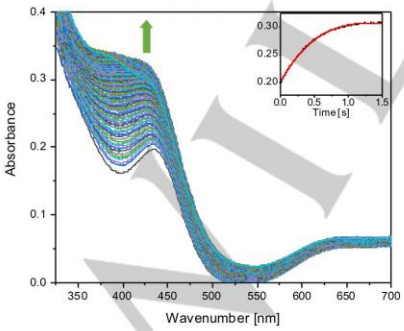

Figure 3. Time-resolved UV-vis spectra of the reaction of dioxygen ($c_{dioxygen}$ = 5.7 · 10^{-3} mol/L)[22] with $[Cu^{I}(\mathbf{1})]PF_6$ in acetone ($c_{complex}$ = 0.75 mmol/L after mixing) at -90 °C. The inset displays the time dependent change in absorbance at 432 nm (black: experimental, red: exponential fit).

Synthesis and characterization of copper(I/II) complexes with TMPA- and related derivatives

With regard to our success to stabilize the superoxido complex with a thioether derivative of TMG_3tren described above by simply replacing the ethyl group in $[(^{TMG}Et)_2(SEt^{Et})NCu]^+$ with a methyl group we decided to extend this approach to the TMPA ligand system. Previous work by Karlin and co-workers already had shown the importance and influence of the ligand design. The first synthetic attempts to obtain an *end-on*-superoxido copper complex with a modified TMPA ligand (Scheme 5, R = Et), however, had led to the formation of a binuclear μ-1,2-peroxodicopper(II) complex as described in the introduction.[8,18] Redesign and modification of their previous investigated N_3S ligand systems resulted in the formation of a mononuclear *end-on*-superoxido copper complex in the presence of a thioether.[9] The preparation of selected thioether-amine N_3S ligands used for the present study was performed according to the literature and is reported in the Experimental Section (Scheme 6).[8] Several ligands with two pyridyl groups and different thioether residues were synthesized. The thioether residue was modified from R = Me (Scheme 5, **2**) to sterically more demanding groups R (Scheme 5, **3-6**).

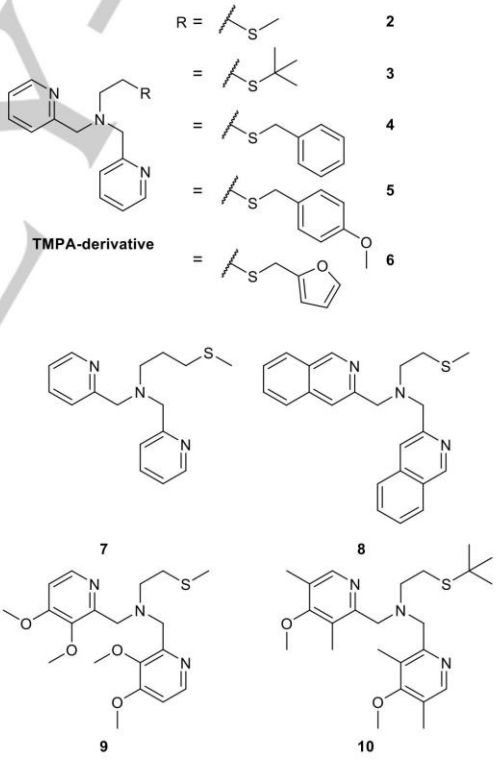

Scheme 5: Modification of the TMPA-derivative with different thioether- and pyridine-residues.

European Journal of Inorganic Chemistry 10.1002/ejic.202200626

WILEY-VCH

RESEARCH ARTICLE

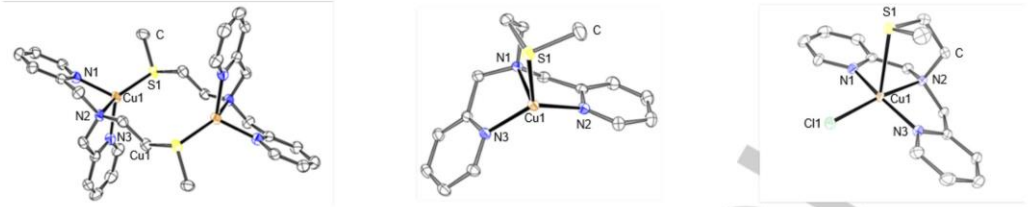

Figure 4. ORTEP representations of the dimeric Cu(I) complex (a), the monomeric Cu(I) complex (b) and the monomeric Cu(II) complex (c) described in the molecular structures of (a) $[Cu^{I}(\mathbf{2})]^{+}_{2}$, (b) $[Cu^{I}(\mathbf{2})]^{+}$ and (c) $[Cu^{II}(\mathbf{2})Cl]^{+}$. H atoms and counter ions were omitted for clarity, anisotropic displacement ellipsoids were plotted at 50% probability. Selected bond lengths (Å) for (a): Cu1-S1: 2.184, Cu1-N1: 2.048, Cu1-N2: 2.173, Cu1-N3: 2.047. Selected bond angles (°) for (a): S1-Cu1-N1: 119.03, N1-Cu1-N2: 80.96, N2-Cu1-N3: 82.35, N3-Cu1-S1: 122.33. Selected bond lengths (Å) for (b): Cu1-S1: 2.257, Cu1-N1: 2.203, Cu1-N2: 2.002, Cu1-N3: 2.020. Selected bond angles (°) for (b): S1-Cu1-N1: 91.44, N1-Cu1-N2: 82.40, N2-Cu1-N3: 121.84, N3-Cu1-S1: 116.83. Selected bond lengths (Å) for (c): Cu1-S1: 2.742, Cu1-N1: 1.976, Cu1-N2: 2.049, Cu1-N3: 1.987, Cu1-Cl1: 2.243. Selected bond angles (°) for (c): S1-Cu1-N1: 84.63, S1-Cu1-N2: 84.37, S1-Cu1-N3: 104.48, S1-Cu1-Cl1: 102.91, N1-Cu1-N2: 84.11, N2-Cu1-N3: 82.35, N3-Cu1-Cl1: 94.64, Cl1-Cu1-N1: 97.51.

The reaction of **2** with $[Cu^{I}(MeCN)_4]PF_6$ in acetone as well as in dichloromethane led to the precipitation of a yellow colored solid in high yields. The formation of $[Cu^{I}(\mathbf{2})]PF_6$ was confirmed by electrospray ionization mass spectrometry (ESI-MS), revealing the characteristic peak at *m*/*z* = 336.0594 for the $[Cu^{I}(\mathbf{2})]^{+}$ cation. Furthermore, suitable single crystals for X-ray structural characterization were obtained. The molecular structure revealed the complex as a dimer, $[Cu^{I}(\mathbf{2})]_2(PF_6)_2$ in the solid state, where each copper ion is coordinated distorted tetrahedrally by one ligand via the three N- donors and by the other ligand via its thioether donor atom (Figure 4a). While this type of complex dimerization in the solid state has been already observed for a number of three- and four-coordinated complexes with a thioether residue[18,23], the formation of a mononuclear form was often only indicated in solution by NMR measurements.[8]

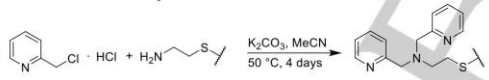

Scheme 6: Ligand Synthesis of different TMPA-derivatives.

We were able to obtain the corresponding mononuclear species in an unusual and somewhat unexpected way. The copper(I) complex had been reacted with sulfur to prepare a disulfido or trisulfido complex as described previously, however, no sulfido complex was obtained.[24] Instead $[Cu^{I}(\mathbf{2})]PF_6$ presented in Figure 4b was obtained (crystallographic data are reported in the Supporting Information) and revealed that the copper(I)-ion has a distorted trigonal-pyramidal geometry with three N-donor atoms and one sulfur-donor atom in the coordination sphere. Following the same synthetic protocol, four further ligands (Scheme 5) were synthesized. A central feature of these ligands was the introduction of more sterically demanding thioether residues with *tert*-butylthioether (in **3**), benzylthioether (in **4**), 4-methoxybenzylthioether (in **5**), and furylmethylthioether (in **6**). With these ligands, only the copper(I) complex $[Cu^{I}(\mathbf{3})]_2(BPh_4)_2$ could be crystallized (Supporting Information) and the molecular structure of this dimer is similar to that of $[Cu^{I}(\mathbf{2})]_2(PF_6)_2$. Complexes $[Cu^{I}(\mathbf{5})]_2(BPh_4)_2$ and $[Cu^{I}(\mathbf{6})]_2(OTf)_2$ were characterized by ESI-MS and elemental analysis.

Copper(II) complexes with ligands **2**, **3** and **4** could be structurally characterized, no suitable crystals with ligands **5** and **6** could be obtained. The molecular structures of $[Cu^{II}(\mathbf{2})Cl]PF_6$ (Fig 4c), $[Cu^{II}(\mathbf{3})Cl]OTf$ and $[Cu^{II}(\mathbf{4})Cl]PF_6$ (crystallographic data are reported in the Supporting Information) revealed a chloride anion as an additional ligand. This is a consequence of well-known chloride abstraction quite often observed by a reaction of copper(I) complexes with this solvent.[25] The crystal structure of $[Cu^{II}(\mathbf{2})Cl]PF_6$ (Fig 4c) revealed a distorted square pyramidal coordination geometry with the thioether group in an axial position with a Cu-S bond distance of 2.7418(6) Å for $[Cu^{II}(\mathbf{2})Cl]PF_6$ (Figure 4), 2.7171(7) for $[Cu^{II}(\mathbf{3})Cl]OTf$ and 2.7174(5) Å for $[Cu^{II}(\mathbf{4})Cl]PF_6$. The Cu-S bond distances are comparable with data reported previously for structurally characterized $[Cu^{II}(\mathbf{2})(Cl)](BF_4)$ by Rorabacher and co-workers who furthermore investigated redox potentials, kinetics of complex formation, and catalytic catechol oxidations.[17,26] While ligands **1** - **6** only differ in the type of thioether residues, the effect of chelate ring size was studied with ligand **7** (Scheme 5). The influence of modifications of the pyridine residue was investigated furthermore by applying ligands **8**, **9,** and **10** (Scheme 5). Reaction of the ligands **7** and **8** with copper(I)salts in an acetone/dichloromethane mixture caused the formation of yellow-colored solids, formulated as $[Cu^{I}(\mathbf{7})]BPh_4$ and $[Cu^{I}(\mathbf{8})]PF_6$, on the basis of crystal structure analysis (crystallographic data are reported in the Supporting Information). In comparison with previously described structures, the complexes turned out to be mononuclear with a Cu-S bond of 2.2031(6) and 2.2297(5) Å. Copper(II) complexes suitable for crystallographic characterization were not obtained. In contrast to copper(I) complexes with these two ligands. It was not possible to obtain copper(I) complexes with ligands **9** and **10**. During the reaction of these two ligands with different copper(I) salts, a disproportionation reaction occurred and only the corresponding copper(II) complexes could be isolated. However, it was possible to crystallize the copper(II) complexes by slow solvent evaporation (the molecular structures and the crystallographic data are presented in the Supporting Information). No secondary weak interactions in the crystal structures were detected.

Electrochemical studies

The copper(I) complexes were characterized by cyclic voltammetry to gain more information on the influence of the different thioether residues with regard to their redox potentials. The redox potentials were determined at a complex concentration of 2 mM in acetonitrile under anaerobic conditions starting from

European Journal of Inorganic Chemistry 10.1002/ejic.202200626

WILEY-VCH

RESEARCH ARTICLE

the copper(I) complex. Ferrocene was used as standard ($E_{1/2}$ = 0.65 V under these conditions). The cyclic voltammograms for the complexes with the ligands **2** - **5** are presented in Figure 5 while cyclic voltammograms of the complexes with the ligands **6** - **10** are reported in the Supporting Information. Redox potentials are reported in Table 1. All complexes (with the exception of [Cu(**7**)]BPh_4 and [Cu(**10**)]BPh_4) showed reversible behavior and the potentials of nearly all copper(I) complexes are quite similar with a value of $E_{1/2}$ close to 0.1 V. However, the half-wave potentials of complexes with the ligands **2** – **6** indicate that sterically more demanding residues (except for **4**) result in a higher value of $E_{1/2}$. While the larger distance of the N-donor atom and the S-donor atom in Ligand **7** and the additional substitution of the pyridyl-groups in ligand **10** caused irreversibility, the modification of only the pyridyl groups with sterically demanding groups resulted in a shift to more positive oxidation values. The value of $E_{1/2}$ for the complex with ligand **2** is comparable to the results obtained by Rorabacher and co-workers in 1999. In contrast to our work, they determined the potential in an aqueous solution with ferroin as an external standard. Nevertheless changing the methyl group to the sterically more demanding ethyl group led to a higher $E_{1/2}$ value as well.[17]

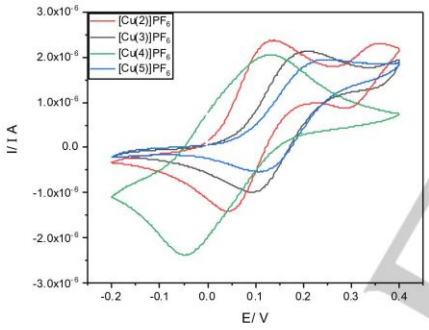

Figure 5: Cyclic voltammograms of the copper(I) complexes with ligands **2**, **3**, **4** and **5** in acetonitrile ($c_{complex}$ = 2 mmol L^{-1}; $c_{electrolyte}$ = 0.1 mol L^{-1}).

Table 1. Potentials of the copper(I) complexes.

Complex	E_p^{red} [V]	E_p^{ox} [V]	$E_{1/2}$ [V]	ΔE [mV]
[Cu(**2**)]BPh_4	0.044	0.140	0.092	96
[Cu(**3**)]BPh_4	0.094	0.200	0.147	106
[Cu(**4**)]BPh_4	-0.050	0.130	0.040	180
[Cu(**5**)]BPh_4	0.114	0.250	0.182	136
[Cu(**6**)]BPh_4	0.204	0.326	0.265	122
[Cu(**7**)]BPh_4	–	–	–	–
[Cu(**8**)]BPh_4	0.134	0.250	0.192	116
[Cu(**9**)]BPh_4	-0.030	0.100	0.035	130
[Cu(**10**)]BPh_4	–	–	–	–

Oxygenation reactions of copper(I) complexes

As described in the introduction a number of $N_3S_{(thioether)}$ ligands, containing two pyridyl-, one amine- and one thioether-donor, have been investigated previously and showed that Cu^I/O_2 reactivity often led to the formation of *μ*-1,2-*trans*-peroxo dicopper(II) species.[8,12,18] However, further modifications of the ligand system by Karlin and co-workers allowed to generate a mononuclear copper(II) superoxido complex possessing a thioether ligation.[9] When copper(I) complexes with ligands **2** – **6** were reacted with dioxygen, here as well, only the formation of the corresponding *μ*-1,2-*trans*-peroxo dicopper(II) complexes could be spectroscopically observed. Thus dioxygen reacts with $[Cu^I(\mathbf{3})]^+$ in acetone at -90 °C, forming the dark blue colored *μ*-1,2-*trans*-peroxo dicopper(II) species (Scheme 8).

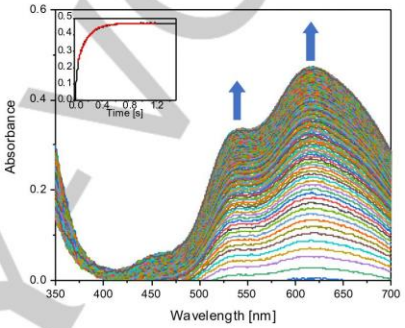

Figure 6. Time-resolved UV-vis spectra of the reaction of dioxygen ($c_{dioxygen}$ = 5.7 · 10^{-3} mol/L)[22] with $[Cu^I(\mathbf{3})]BPh_4$ in acetone ($c_{complex}$ = 0.2 mmol/L after mixing) at -90 °C. The inset displays the time dependent change in absorbance at 616 nm (black: experimental, red: exponential fit).

Time resolved UV-vis spectra are presented in Figure 6. Absorbance maxima at 455 nm, 541 nm and 616 nm are consistent with the formation of the peroxido complex similar to other *trans*-peroxido complexes, e.g. $[((Cu^{II}(TMPA))_2(\mu\text{-}1,2\text{-}O_2)]$ reported previously.[11] However, as can be seen in Figure 6, no formation of an *end-on* superoxido copper complex could be detected.

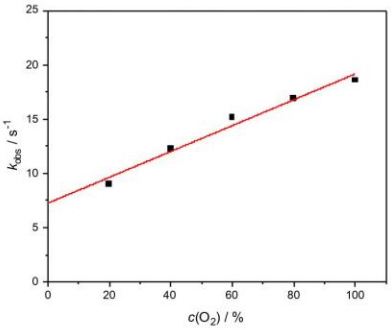

Figure 7. k_{obs} vs. $c(O_2)$ at -80 °C.

European Journal of Inorganic Chemistry 10.1002/ejic.202200626

WILEY-VCH

RESEARCH ARTICLE

The absorbance vs. time trace at 616 nm (as well as at other wavelengths) obtained under pseudo first order conditions could be fitted to a one exponential function, indicating first order for the complex concentration in the rate law. A plot of k_{obs} vs. [O_2] showed a linear dependence in line with first order of dioxygen concentration as well (Fig. 7). The intercept is the consequence of the reversibility of the reaction. The overall reaction sequence can be described according to Scheme 7.

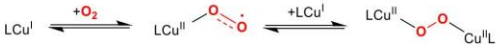

Scheme 7: Formation of the μ-1,2-*trans*-peroxo dicopper(II) species via a mononuclear copper(II) superoxido complex.

While it is sometimes possible to observe the superoxido complex as an intermediate,[27] this is not the case if the formation of this species is rate-determining (followed by a very fast consecutive step). A description of the kinetics of this type of mechanism has been described previously in great detail.[28]

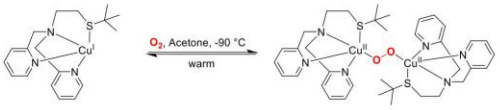

Scheme 8: Reversible dioxygen binding of [Cu^{I}(**3**)]BPh$_4$.

An Eyring plot (Fig. 8) allowed the calculation of the activation parameters to $\Delta H^{\ddagger}$ = 21 ± 1 kJ · mol^{-1} and $\Delta S^{\ddagger}$ = -70 ± 3 J · mol^{-1} K^{-1} and is in line with previous measurements of related complexes. The negative activation entropy indicates an associative mechanism. Kinetic measurements were also performed for complexes [Cu^{I}(**4**)]$^+$ and [Cu^{I}(**6**)]$^+$ (Supporting Information) and activation parameters could be obtained (Table 2). Due to the similarity of all these reactions no detailed kinetic investigations were performed for complexes [Cu^{I}(**2**)]$^+$ and [Cu^{I}(**5**)]$^+$.

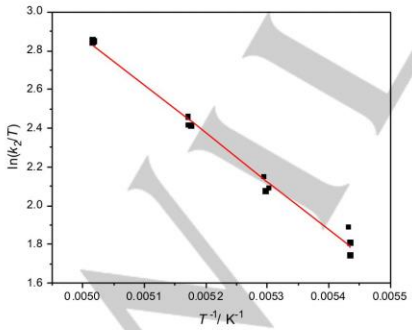

Figure 8. Eyring plot for k_2 values obtained from the temporal evolution of the absorbance at 616 nm between -89 °C and -73 °C for the reaction of [Cu^{I}(**3**)]BPh$_4$ with O_2 in acetone.

Further reactions with dioxygen were performed at -140 °C in MeTHF/THF which also only allowed to spectroscopically detect the formation of the dinuclear peroxido copper complex again.

Table 2. Calculated activation parameters for the O_2-interaction in acetone at -90 °C.

Parameter[a]	[Cu^{I}(**3**)]$^+$	[Cu^{I}(**4**)]$^+$	[Cu^{I}(**6**)]$^+$
$\Delta H^{\ddagger}$ (kJ·mol^{-1})	+21 ± 1	+29 ± 1	+21 ± 1
$\Delta S^{\ddagger}$ (J·mol^{-1} K^{-1})	-70 ± 3	-29 ± 4	-66 ± 4

Previously, we observed that ozone could be applied to generate an *end-on*-superoxido copper complex.[21] Therefore, ozone was reacted with [Cu^{I}(**3**)]$^+$ in acetone at -90 °C. While there was an indication that a superoxido complex might have formed briefly it was not possible to really detect and characterize this species. Switching the solvent to MeTHF/THF and lowering the temperature to -140 °C allowed the observation of the formation of a dark green colored species followed by an immediate color change to dark blue right afterwards. While the green color strongly indicates the formation of an end-superoxido copper complex, attempts to analyze this species failed due to the instability of the compound. The UV-vis spectrum of the dark blue species with absorbance maxima at 540 and 616 nm (Fig. 9) are in line with the formation of the μ-1,2-*trans*-peroxido dicopper(II) complex.

The interaction of [Cu(**9**)]$^+$ and [Cu(**10**)]$^+$ with dioxygen (in acetone) and ozone (in MeTHF/THF) could not be analyzed due to the fact that both complexes tend to disproportionate.

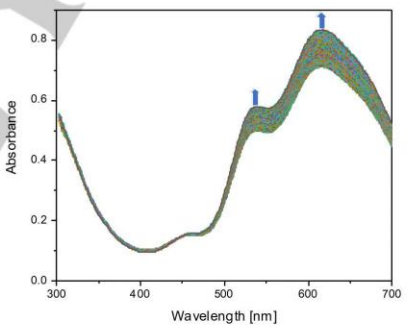

Figure 9: UV-vis spectra of the reaction of [Cu^{I}(**3**)]BPh$_4$ with ozone in MeTHF/THF at -140 °C.

In comparison to these complexes, the copper(I) complexes of **7** and **8** did not react with dioxygen at all. The addition of O_2 at low temperature led to no spectroscopic changes and even at room temperature no color change was observed, indicating that a seemingly minor ligand modification (larger distance between the N-donor and S-donor atom in **7** and addition of a steric more demanding pyridyl group in **8**), effects the Cu$^{I}O_2$ chemistry and stability of these complexes highly.

Summary and Conclusion

The results reported herein demonstrate the importance and influence of ligand design and ligand modification in Cu^{I}/O_2-

European Journal of Inorganic Chemistry 10.1002/ejic.202200626

WILEY-VCH

RESEARCH ARTICLE

chemistry. Copper(I) complexes with ligands based on TMPA (= tris(2-pyridylmethyl)amine) behaved quite differently. While some complexes could not even be studied due to disproportionation in solution, other ones (e. g. due to larger chelate rings leading to a stabilization of Cu(I) complexes) did not react at all with dioxygen. In contrast, other complexes of the investigated series did form *μ*-1,2-*trans*-peroxido dicopper(II) that could be spectroscopically observed at low temperatures in stopped-flow measurements. However, in none of these reactions, it was possible to observe an *end-on* superoxido copper complex prior to the consecutive reaction to the peroxido complex. Kinetic measurements showed that the formation of the superoxido complex is rate-determining and therefore, it was not possible to detect this species. Different from previous investigations by us, reactions with ozone did not provide any advantage for the systems studied here. A dark green colored species was observed in one reaction with ozone at -140 °C, however, this species was extremely short-lived and only the dark blue colored *μ*-1,2-*trans*-peroxido complex, formed immediately afterward, could be spectroscopically detected.

However, most interesting was the finding that replacing the ethyl group in the tren-guanidine derivative ($^{TMG}Et)_2(SEt^{Et})N$ with a methyl group allowed a dramatic increase in the stability of the superoxido copper complex that only could be observed with ($^{TMG}Et)_2(SEt^{Et})N$ at – 135 °C in contrast to the -90 ° (or even a bit higher) with ($^{TMG}Et)_2(Set^{Me})N$. This is important for further investigations to apply copper complexes in selective oxygenation reactions.

Experimental Section

General: All reagents and solvents used were of p.a. quality and were purchased from Sigma Aldrich and AcrosOrganics. The solvents were purified by distillation with a drying agent by standard procedures. The air sensitive syntheses of the metal complexes were performed under inert conditions in a glove box by MBraun (H_2O and O_2 concentrations less than 0.1 ppm) under an argon atmosphere. Stopped-flow measurements were carried out with a HI-Tech SF-61SX2 and CSF-61DX2 low-temperature stopped-flow unit equipped with a diode array spectrophotometer. Kinetic data were analyzed with the software Kinetic Studio (TgK Scientific). NMR measurements were performed with a Bruker Avance II 400 MHz (AV II 400). The NMR analysis of the copper(I) complexes were carried out on a Bruker Avance Neo 700 NMR spectrometer. For Electrospray-ionization MS (ESI-MS) measurements a Bruker microTOF mass spectrometer was used. UV/Vis spectra were recorded with an Agilent 8453 spectrometer. The CHN elemental analysis was performed using the CHN-Analysator: Thermo FlashEA – 1112 Series.

Electrochemistry: Cyclic voltammetry measurements were performed with a glassy carbon electrode as working electrode, a platinum/titanium electrode (counter electrode) and an Ag/AgCl reference electrode. MeCN was used as solvent and NBu_4BF_4 was applied as conducting salt. Ferrocene was used as standard ($E_{1/2}$ = 0.65 V) and the electrochemical data were recorded with an e-corder 410 edaq (eDAQ, Colorado Springs, US) and the programm eChem.

Crystallography: Experimental data by single-crystal X-ray diffraction measurements were collected using a Bruker D8 Venture system, equipped with dual IμS-sources (Mo/Cu), a PHOTON 100 or PHOTON II detector and an Oxford Cryostream 700 low temperature system (details are described in the Supporting Information). More detailed information regarding crystallographic results is reported in the Supporting Information. Depositions Numbers 2193634 (for [Cu(**1**)](PF_6)), 2195195 (for [Cu_2(**2**)$_2$](PF_6)$_2$), 2193628 (for [Cu(**2**)](PF_6)), and 2193625 (for [Cu(**2**)Cl](PF_6)) contain the supplementary crystallographic data for this paper. These data are provided free of charge by the joint Cambridge Crystallographic Data Centre and Fachinformationszentrum Karlsruhe Accesss Structures service www.ccdc.cam.ac.uk/structures.

Synthesis of Ligands:

2-(Methylthio)ethanamine: To a solution of Na (4.92 g, 214 mmol) in ethanol (300 mL) 2-aminoethanethiol (15.0 g, 194 mmol) was added and stirred at room temperature for 15 min. Iodomethane (29.0 g, 204 mmol) was added dropwise at 0 °C to the suspension. The reaction mixture was stirred 15 min at room temperature. Afterwards, the mixture was heated under reflux for 3 h and after cooling, distilled water (100 mL) was added. Ethanol was removed under reduced pressure and the aqueous phase was washed with dichloromethane (3 x 100 mL). The organic phase was dried over Na_2SO_4 and the solvent was evaporated under reduced pressure. The resulting yellow oil was purified by Kugelrohr distillation to give a colorless oil (14.6 g, 0.160 mol, 83 % yield). ^{1}H NMR (400 MHz, $CDCl_3$): *δ* (ppm) = 2.89 (dd, *J* = 6.7, 5.9 Hz, 2H), 2.60 (dd, *J* = 6.7, 5.9 Hz, 2H), 2.10 (s, 3H), 1.64 (s, 2H); ^{13}C NMR (100 MHz, $CDCl_3$): *δ* (ppm) = 40.3 (CH_2), 38.2 (CH_2), 15.1 (CH_3). HRMS (ESI): *m*/*z* calcd for $C_3H_{10}NS^+$: 92.0529; found: 92.0525 [M + H]$^+$; $C_3H_9NNaS^+$: 114.0348; found: 114.0357 [M + Na]$^+$.

2,2´-((2-(Methylthio)ethyl)azanediyl)diacetonitrile: To a suspension of 2-(Methylthio)ethaneamine (7.30 g, 80.1 mmol) and diisopropylethylamine (20.7 g, 160 mmol) in acetonitrile bromoacetonitrile (19.2 g, 160 mmol) was added dropwise at 0 °C. Afterwards, the reaction mixture was heated to 60 °C for 3 h. After cooling to room temperature, distilled water (100 mL) was added and the solution was extracted with dichloromethane (3 x 50 mL). The collected organic phases were dried over Na_2SO_4 and the solvent was removed under reduced pressure. The brown oil was extracted with warm diethylether (3 x 100 mL) and the ether phases were dried over Na_2SO_4. The solvent was removed under reduced pressure to give a yellow oil (7.63 g, 45.1 mmol, 56 % yield). ^{1}H NMR (400 MHz, $CDCl_3$): *δ* (ppm) = 3.69 (s, 4H), 2.94 – 2.90 (m, 2H), 2.69 – 2.65 (m, 2H), 2.16 (s, 3H); ^{13}C NMR (100 MHz, $CDCl_3$): *δ* (ppm) = 114.2 (q), 52.6 (CH_2), 42.2 (CH_2), 31.6 (CH_2), 15.8 (CH_3). HRMS (ESI): *m*/*z* calcd for $C_7H_{11}N_3NaS^+$: 192.0566; found: 192.0572 [M + Na]$^+$.

N´-(Aminomethyl)-N´-(2-(methylthio)ethyl)ethane-1,2-diamine: To a suspension of $LiAlH_4$ (9.75 g, 257 mmol) in dry THF (200 mL) at 0°C conc. H_2SO_4 (12.6 g, 128 mmol) was added carefully. After addition of conc. H_2SO_4 the suspension was stirred for 30 min at 0 °C. Afterwards, 2,2´-((2-(Methylthio)ethyl)azanediyl)diacetonitrile (7.25 g, 42.8 mmol) was added dropwise to the suspension and stirred for 24 h at room temperature. Distilled water was added carefully at 0 °C to the suspension until no further gas development was observed. The suspension was filtered and the collected precipitate was washed with THF (200 mL). The solvent was evaporated under reduced pressure. The oil was treated with distilled water (100 mL) and washed with dichloromethane (3 x 50 mL). The organic phases were dried over Na_2SO_4 and the solvent was removed under reduced pressure to give a yellow oil (2.22 g, 12.5 mmol, 29 %). ^{1}H NMR (400 MHz, $CDCl_3$): *δ* (ppm) = 2.75 (dd, *J* = 6.5, 5.3 Hz, 4H), 2.72 – 2.66 (m, 2H), 2.64 – 2.58 (m, 2H), 2.53 (dd, *J* = 6.5, 5.3 Hz, 4H), 2.12 (s, 3H), 1.47 (s, 4H); ^{13}C NMR (100 MHz, $CDCl_3$): *δ* (ppm) 57.3 (CH_2), 53.5 (CH_2), 39.9 (CH_2), 32.6 (CH_2), 15.8 (SCH_3). HRMS (ESI): *m*/*z* calcd for $C_7H_{20}N_3S^+$: 178.1373; found: 178.1385 [M + H]$^+$; $C_7H_{19}N_3NaS^+$: 200.1192; found: 200.1202 [M + Na]$^+$.

2´,2´-(((2-(Methylthio)ethyl)azanediyl)bis(ethane-2,1-diyl))bis-(1,1,3,3-tetramethyl-guanidine = 1): To an solution of N´-(Aminomethyl)-N´-(2-(methylthio)ethyl)ethane-1,2-diamine (0.50 g, 2.8 mmol) and trimethylamine (0.57 g, 5.6 mmol) in dry acetonitrile (50 mL) at 0°C a solution of Chloro-N,N,N´,N´-tetramethylformamidinium hexa-fluorophosphate (1.6 g, 5.6 mmol) in dry acetonitrile was added dropwise.

European Journal of Inorganic Chemistry 10.1002/ejic.202200626

WILEY-VCH

RESEARCH ARTICLE

The reaction mixture was stirred 3 h under reflux. Afterwards, a solution of NaOH (0.27 g, 5.6 mmol) in distilled water (5.6 mL) was added and the solvent was evaporated under pressure. In order to deprotonate the bis-hydrochloride, KOH (50 wt.-%, 50 mL) was added and the ligand was extracted into the acetonitrile phase (3 x 25 mL). The collected organic phases were dried over Na_2SO_4 and the solvent was evaporated under reduced pressure to give a yellow oil (0.910 g, 1.68 mmol, 60 %). ^{1}H NMR (400 MHz, CD_3CN): δ (ppm) = 3.18 – 3.12 (m, 4H), 2.75 – 2.72 (m, 14H), 2.71 – 2.70 (m, 2H), 2.68 (s, 12H), 2.49 – 2.44 (m, 4H), 2.11 (s, 3H); ^{13}C NMR (100 MHz, CD_3CN): δ (ppm) 163.1 (q), 57.4 (CH_2), 53.9 (CH_2), 47.6 (CH_2), 39.4 (NCH_3), 31.7 (CH_2), 14.2 (SCH_3). HRMS (ESI): *m/z* calcd for $C_{17}H_{39}N_3NaS^+$: 396.2880; found: 396.2872 [M + Na]$^+$.

General ligand-synthesis: The (Chloromethyl)pyridine backbone, the thioether residue and potassium carbonate were placed in a Schlenk flask and were dissolved in dry acetonitrile (100 mL). The reaction mixture was stirred for four days under argon at 50-60 °C. After four days, the solvent was removed and the yellow oil was dissolved in dichloromethane (100 mL). The organic phase was washed three times with water (20 mL). After drying over $MgSO_4$, the solution was filtered and the solvent was removed by rotary evaporation. The yellow raw product was purified by column chromatography. The general procedure is based on the ligand synthesis of *DMMESE* published previously by Karlin and co-workers.[8] Applied amounts of reactants, purification, yields and analyses are listed for each ligand.

Bis(2-pyridylmethyl)-2-(methylthio)ethylamine (2):
2-(Chloromethyl)pyridine hydrochloride (0.500 g, 3.05 mmol), 2-(methylthio)ethylamine (0.132 g, 1.45 mmol) and potassium carbonate (2.11 g, 15.3 mmol). The yellow raw product was purified by column chromatography (alumina, 100 % ethyl acetate, R_f = 0.48) yielding a yellow oil (0.277 g, 1.01 mmol, 70 % yield). ^{1}H NMR (400 MHz, $CDCl_3$): δ (ppm) = 8.45 (ddd, *J* = 4.9, 1.8, 0.9 Hz, 2H), 7.59 (td, *J* = 7.6, 1.8 Hz, 2H), 7.51 (dt, *J* = 7.8, 1.2 Hz, 2H), 7.08 (ddd, *J* = 7.4, 4.9, 1.3 Hz, 2H), 3.80 (s, 4H), 2.78 – 2.71 (m, 2H), 2.65 – 2.57 (m, 2H), 1.95 (s, 3H); ^{13}C NMR (100 MHz, $CDCl_3$) δ (ppm) = 158.4 (q), 148.0 (CH), 135.7 (CH), 122.0 (CH), 121.0 (CH), 59.2 (CH_2), 52.4 (CH_2), 30.8 (CH_2), 14.7 (CH_3). HRMS (ESI): *m/z* calcd for $C_{15}H_{20}N_3S^+$: 274.1373; found: 274.1370 [M + H]$^+$, $C_{15}H_{19}N_3NaS^+$: 296.1192; found: 296.1200 [M + Na]$^+$.

Bis(2-pyridylmethyl)-2-(*tert*-butylthio)ethylamine (3):
2-(Chloromethyl)pyridine hydrochloride (1.35 g, 8.25 mmol), 2-(*tert*-Butylthio)ethylamine (0.500 g, 3.75 mmol) and potassium carbonate (3.11 g, 22.5 mmol). The yellow raw product was purified by column chromatography (alumina, 100 % ethyl acetate, R_f = 0.53) yielding a yellow oil (0.680 g, 2.15 mmol, 57 % yield). ^{1}H NMR (400 MHz, $CDCl_3$): δ (ppm) = 8.52 (ddd, *J* = 4.9, 1.8, 1.0 Hz, 2H), 7.66 (td, *J* = 7.6, 1.8 Hz, 2H), 7.58 (dt, *J* = 7.8, 1.2 Hz, 2H), 7.14 (ddd, *J* = 7.3, 4.8, 1.3 Hz, 2H), 3.87 (s, 4H), 2.87 – 2.75 (m, 2H), 2.75 – 2.65 (m, 2H), 1.26 (s, 9H); ^{13}C NMR (100 MHz, $CDCl_3$) δ (ppm) = 159.5 (q), 149.0 (CH), 123.0 (CH), 122.0 (CH), 121.0 (CH), 60.4 (CH_2), 54.5 (CH_2), 42.0 (q), 31.0 (CH_3), 26.0 (CH_2). HRMS (ESI): *m/z* calcd for $C_{18}H_{26}N_3S^+$: 316.1842; found: 316.1838 [M + H]$^+$.

Bis(2-pyridylmethyl)-2-(benzylthio)ethylamine (4):
2-(Chloromethyl)pyridine hydrochloride (1.69 g, 10.3 mmol), 2-(Benzylthio)ethylamine hydrochloride (0.951 g, 4.67 mmol) and potassium carbonate (3.87 g, 28.0 mmol). The yellow raw product was purified by column chromatography (alumina, 1:1 ethyl acetate/hexane, R_f = 0.56) yielding a yellow oil (0.890 g, 2.55 mmol, 55 % yield). ^{1}H NMR (400 MHz, $CDCl_3$): δ (ppm) = 8.51 (ddd, *J* = 4.9, 1.8, 0.9 Hz, 2H), 7.57 (td, *J* = 7.7, 1.8 Hz, 2H), 7.54 (dt, *J* = 7.8, 1.2 Hz, 2H), 7.29 – 7.18 (m, 5H), 7.14 (ddd, *J* = 7.4, 4.9, 1.3, 2H), 3.81 (s, 4H), 3.61 (s, 2H), 2.83 – 2.72 (m, 2H), 2.65 – 2.54 (m, 2H); ^{13}C NMR (100 MHz, $CDCl_3$) δ (ppm) = 159.5 (q), 149.0 (q), 138.4 (CH), 136.4 (CH), 128.8 (CH), 128.5 (CH), 127.0 (CH), 123.0 (CH), 122.0 (CH), 60.4 (CH_2), 53.6 (CH_2), 36.3 (CH_2), 28.9 (CH_2). HRMS (ESI): *m/z* calcd for $C_{21}H_{24}N_3S^+$: 350.168; found: 350.163 [M + H]$^+$, $C_{21}H_{23}N_3NaS^+$: 372.1505; found: 372.1511 [M + H]$^+$.

Bis(2-pyridylmethyl)-2-((4-methoxybenzyl)thio)ethylamine (5):
2-(Chloromethyl)pyridine hydrochloride (0.386 g, 2.35 mmol), 2-((4-Methoxybenzyl)thio)ethylamine hydrochloride (0.250 g, 1.07 mmol) and potassium carbonate (0.887 g, 6.42 mmol). The yellow raw product was purified by column chromatography (alumina, 3:1 ethyl acetate/methanol, R_f = 0.50) yielding a yellow oil (0.151 g, 0.398 mmol. 37 % yield). ^{1}H NMR (400 MHz, $CDCl_3$): δ (ppm) = 8.44 (ddd, *J* = 4.9, 1.8, 0.9 Hz, 2H), 7.57 (td, *J* = 7.6, 1.8 Hz, 2H), 7.47 (dt, *J* = 7.9, 1.1 Hz, 2H), 7.11 – 7.01 (m, 4H), 6.74 – 6.69 (m, 2H), 3.74 (s, 4H), 3.71 (s, 3H), 3.50 (s, 2H), 2.73 – 2.66 (m, 2H), 2.55 – 2.48 (m, 2H); ^{13}C NMR (100 MHz, $CDCl_3$) δ (ppm) = 158.5 (q), 157.5 (q), 148.0 (q), 135.7 (CH), 129.4 (CH), 128.8 (CH), 122.0 (CH), 121.0 (CH), 112.8 (CH), 59.2 (CH_2), 54.2 (CH_2), 52.6 (CH_2), 34.6 (CH_2), 27.8 (CH_3). HRMS (ESI): *m/z* calcd for $C_{22}H_{26}N_3OS^+$: 380.1792; found: 380.1788 [M + H]$^+$.

Bis(2-pyridylmethyl)-2-(furfurylthio)ethylamine (6):
2-(Chloromethyl)pyridine hydrochloride (0.676 g, 4.12 mmol), 2-(Furfurythio)ethylamine (0.296 g, 1.88 mmol) and potassium carbonate (1.56 g, 11.3 mmol). The yellow raw product was purified by column chromatography (alumina, 100 % ethyl acetate, R_f = 0.13) yielding a yellow oil (0.360 g, 1.06 mmol, 56 % yield). ^{1}H NMR (400 MHz, $CDCl_3$): δ (ppm) = 8.52 (ddd, *J* = 4.9, 1.8, 0.9 Hz, 2H), 7.66 (td, *J* = 7.6, 1.8 Hz, 2H), 7.56 (dt, *J* = 7.9, 1.2 Hz, 2H), 7.30 (dd, *J* = 1.9, 0.9 Hz, 1H), 7.15 (ddd, *J* = 7.5, 4.9, 1.3 Hz, 2H), 6.25 (dd, *J* = 3.2, 1.9 Hz, 1H), 6.08 (dd, *J* = 3.1, 0.9 Hz, 1H), 3.84 (s, 4H), 3.62 (s, 2H), 2.82 – 2.74 (m, 2H), 2.73 – 2.64 (m, 2H); ^{13}C NMR (100 MHz, $CDCl_3$) δ (ppm) = 159.4 (q), 151.6 (q), 149.0 (CH), 142.1 (CH), 136.5 (CH), 123.3 (CH), 123.0 (CH), 122.1 (CH), 110.4 (CH), 107.5 (CH), 60.1 (CH_2), 53.5 (CH_2), 29.2 (CH_2), 28.3 (CH_2). HRMS (ESI): *m/z* calcd for $C_{19}H_{22}N_3OS^+$: 340.1479; found: 340.1485 [M + H]$^+$, $C_{19}H_{21}NaN_3OS^+$: 362.1298; found: 362.1300 [M + Na]$^+$.

Bis(2-pyridylmethyl)-3-(methylthio)propylamine (7):
2-(Chloromethyl)pyridine hydrochloride (3.43 g, 20.9 mmol), 3-(methylthio)propylamine (1.00 g, 9.51 mmol) and potassium carbonate (7.89 g, 57.1 mmol). The yellow raw product was purified by column chromatography (alumina, 100 % ethyl acetate, R_f = 0.54) yielding a yellow oil (0.910 g, 3.16 mmol, 33 % yield). ^{1}H NMR (400 MHz, $CDCl_3$): δ (ppm) = 8.53 (ddd, *J* = 4.9, 1.8, 0.9 Hz, 2H), 7.66 (td, *J* = 7.6, 1.8 Hz, 2H), 7.53 (d, *J* = 7.8 Hz, 2H), 7.15 (ddd, *J* = 7.5, 4.9, 1.3 Hz, 2H), 3.85 (s, 4H), 2.67 (t, *J* = 7.1 Hz, 2H), 2.52 – 2.42 (m, 2H), 2.04 (s, 3H), 1.84 (p, *J* = 7.3 Hz, 2H); ^{13}C NMR (100 MHz, $CDCl_3$) δ (ppm) = 159.6 (q), 149.0 (CH), 136.4 (CH), 123.0 (CH), 122.0 (CH), 60.5 (CH_2), 53.3 (CH_2), 32.0 (CH_2), 26.7 (CH_2), 15.4 (CH_3). HRMS (ESI): *m/z* calcd for $C_{16}H_{22}N_3S^+$: 288.1529; found: 288.1528 [M + H]$^+$.

Bis(2-quinolylmethyl)-2-(methylthio)ethylamine (8):
2-(Chloromethyl)quinoline hydrochloride (1.77 g, 8.25 mmol), 2-(methylthio)ethylamine (0.342 g, 3.75 mmol) and potassium carbonate (3.11 g, 22.5 mmol). The yellow raw product was purified by column chromatography (alumina, 1:1 ethyl acetate/hexane, R_f = 0.61) yielding a yellow solid (0.798 g, 2.14 mmol, 57 % yield). ^{1}H NMR (400 MHz, $CDCl_3$): δ (ppm) = 8.14 (dd, *J* = 8.5, 0.8 Hz, 2H), 8.04 (dq, *J* = 8.4, 0.9 Hz, 2H), 7.84 – 7.74 (m, 4H), 7.68 (ddd, *J* = 8.4, 6.9, 1.5 Hz, 2H), 7.50 (ddd, *J* = 8.1, 6.9, 1.2 Hz, 2H), 4.07 (s, 4H), 2.90 (dd, *J* = 8.5, 6.0 Hz, 2H), 2.73 (dd, *J* = 8.3, 5.9 Hz, 2H), 1.97 (s, 3H); ^{13}C NMR (100 MHz, $CDCl_3$) δ (ppm) = 160.2 (q), 147.5 (CH), 136.4 (CH), 129.4 (CH), 129.0 (CH), 127.5 (CH), 127.4 (CH), 126.2 (CH), 121.2 (CH), 61.2 (CH_2), 53.5 (CH_2), 31.9 (CH_2), 15.7 (CH_3). HRMS (ESI): *m/z* calcd for $C_{23}H_{24}N_3S^+$: 374.1686; found: 374.1692 [M + H]$^+$, $C_{23}H_{23}N_3NaS^+$: 396.1505; found: 396.1511 [M + Na]$^+$.

Bis(3,4-dimethoxy-2-pyridylmethyl)-2-methylthioethylamine (9):
2-(Chloromethyl)-3,4-dimethoxypyridine hydro-chloride (1.85 g, 8.25 mmol), 2-(methylthio)ethylamine (0.342 g, 3.75 mmol) and potassium carbonate (3.11 g, 22.5 mmol). The yellow raw product was purified by column chromatography (alumina, 1:1 ethyl acetate/hexane, R_f = 0.61) yielding a yellow solid (0.798 g, 2.14 mmol, 57 % yield). ^{1}H NMR (400 MHz, $CDCl_3$): δ (ppm) = 8.39 (d, *J* = 5.7 Hz, 2H), 6.92 (d, *J* = 5.7 Hz, 2H), 4.17 (s, 4H), 3.94 (s, 6H), 3.83 (s, 6H), 3.09 – 3.01 (m, 2H), 2.77 – 2.70 (m, 2H),

European Journal of Inorganic Chemistry 10.1002/ejic.202200626

WILEY-VCH

RESEARCH ARTICLE

2.02 (s, 3H); ^{13}C NMR (100 MHz, $CDCl_3$) δ (ppm) = 159.4 (q), 150.4 (CH), 144.8 (CH), 144.4 (CH), 107.5 (CH), 61.1 (CH_2), 56.0 (CH_2), 53.6 (CH_3), 53.2 (CH_3), 30.9 (CH_2), 15.4 (CH_3). HRMS (ESI): *m/z* calcd for $C_{19}H_{28}N_3O_4S^+$: 394.1796; found: 394.1801 [M + H]$^+$.

Bis(4-methoxy-3,5-dimethyl--2-pyridylmethyl)-2-(*tert*-butylthio)ethylamine (10): 2-(Chloromethyl)-4-methoxy-3,5-dimethylpyridine hydrochloride (0.916 g, 4.12 mmol), 2-(*tert*-Butylthio)ethylamine (0.251 g, 1.88 mmol) and potassium carbonate (1.56 g, 11.3 mmol). The yellow raw product was purified by column chromatography (alumina, 100 % ethyl acetate, R_f = 0.52) yielding a yellow oil (0.800 g, 1.85 mmol, 98 % yield). ^{1}H NMR (400 MHz, $CDCl_3$): δ (ppm) = 8.08 (s, 2H), 3.69 (s, 4H), 3.65 (s, 6H), 2.68 – 2.60 (m, 2H), 2.55 – 2.46 (m, 2H), 2.15 (s, 6H), 2.06 (s, 6H), 1.12 (s, 9H); ^{13}C NMR (100 MHz, $CDCl_3$) δ (ppm) = 163.0 (q), 156.0 (CH), 147.3 (CH), 125.4 (CH), 124.2 (CH), 58.7 (CH_2), 53.8 (CH_2), 40.9 (CH_2), 30.1 (CH_3), 24.4 (CH_2), 12.2 (CH_3), 9.7 (CH_3). HRMS (ESI): *m/z* calcd for $C_{24}H_{38}N_3O_2S^+$: 432.2680; found: 432.2675 [M + H]$^+$; $C_{24}H_{37}N_3NaO_2S^+$: 454.2499; found: 454.2500 [M + Na]$^+$.

Synthesis of Copper(I) Complexes:

[Cu(1)]PF_6: To a stirred solution of **1** (0.059 g, 0.11 mmol) in 2-MeTHF (2 mL) a solution of $[Cu(MeCN)_4]PF_6$ (0.037 g, 0.10 mmol) in 2-MeTHF (2 mL) was added dropwise. The mixture was stirred over night at room temperature. Slow evaporation of the solvent led to yellow crystals that were suitable for X-ray structural characterisation. Yield: 46.5 mg (0.080 mmol, 80 %). ^{1}H NMR (700 MHz, acetone-*d6*): δ (ppm) = 3.25 (ddd, *J* = 13.9, 7.0, 3.8 Hz, 2H), 3.13 (ddd, *J* = 13.9, 6.9, 3.9 Hz, 2H), 2.94 (dd, *J* = 9.2, 2.8 Hz, 4H), 2.84 – 2.81 (m, 2H), 2.80 – 2.77 (m, 2H), 2.69 (s, 12H), 2.67 (s, 12H), 2.06 (s, 3H). HRMS (ESI): *m/z* calcd for $C_{17}H_{39}CuF_6N_7PS^+$: 581.1925; found: 581.1932 [M + L]$^+$. Anal calcd (%) for $C_{17}H_{39}CuF_6N_7PS \cdot 2.5\ CH_3CN$: C 29.48, H 5.58, N 12.34, found: C 29.06, H 5.22, N 12.73.

[Cu(2)]PF_6: To a stirred solution of **2** (0.050 g, 0.18 mmol) in acetone (2 mL) a solution of $[Cu(MeCN)_4]PF_6$ (0.068 g, 0.18 mmol) in acetone (2 mL) was added dropwise. The mixture was stirred over night at room temperature. Slow evaporation of the solvent led to yellow crystals that were suitable for X-ray structural characterisation. Yield: 74.4 mg (0.155 mmol ,85 %). ^{1}H NMR (700 MHz, acetone-*d6*): δ (ppm) = 7.93 (s, 2H), 7.16 (s, 4H), 7.14 – 7.10 (m, 2H), 4.19 (s, 4H), 3.13 (s, 4H), 1.95 (s, 3H). HRMS (ESI): *m/z* calcd for $C_{15}H_{19}CuN_3S^+$: 336.0591; found: 336.0594 [M + L]$^+$. Anal. calcd (%) for $C_{15}H_{19}CuF_6N_3PS$: C 37.39, H 3.97, N 8.72, found: C 37.88, H 3.85, N 8.44.

[Cu(3)]BPh_4: To a stirred solution of **3** (0.050 g, 0.16 mmol) in dichloromethane (2 mL) a solution of $[Cu(MeCN)_4]PF_6$ (0.058 g, 0.157 mmol) in dichloromethane (2 mL) was added dropwise. After stirring for 2 h, solid $NaBPh_4$ (0.054 g, 0.16 mmol) was added and it was stirred over night at room temperature. The yellow solution was filtered and slow evaporation of the solvent led to colorless crystals that were suitable for X-ray structural characterisation. Yield: 76.6 mg (0.110 mmol, 70 %).^{1}H NMR (700 MHz, acetone-*d6*): δ (ppm) = 7.78 (t, *J* = 7.7 Hz, 2H), 7.48 – 7.38 (m, 4H), 7.21 (dddt, *J* = 8.0, 5.5, 2.8, 1.5 Hz, 9H), 6.79 (t, *J* = 7.4 Hz, 9H), 6.64 (tt, *J* = 7.3, 1.5 Hz, 4H), 4.14 (s, 4H), 3.07 (t, *J* = 5.3 Hz, 4H), 1.14 (s, 9H). HRMS (ESI): *m/z* calcd for $C_{18}H_{25}CuN_3S^+$: 378.1060; found: 378.1062 [M + L]$^+$. Anal. calcd (%) for $C_{42}H_{45}BCuN_3S \cdot 0.6\ CH_2Cl_2$: C 68.29, H 6.22, N 5.61, found: C 68.15, H 6.11, N 5.62.

[Cu(4)]PF_6: To a stirred solution of **4** (0.050 g, 0.14 mmol) in dichloromethane (2 mL) a solution of $[Cu(MeCN)_4]PF_6$ (0.052 g, 0.14 mmol) in dichloromethane (2 mL) was added dropwise. The solution was stirred over night at room temperature. Slow evaporation of the solvent led to yellow crystals that were suitable for X-ray structural characterisation. Yield: 82.9 mg (0.113 mmol ,81 %). HRMS (ESI): *m/z* calcd for $C_{21}H_{23}CuN_3S^+$: 412.0904; found: 412.0904 [M + L]$^+$; $C_{21}H_{23}ClCuN_3S^+$: 447.0592; found: 447.0594 [M + L + Cl]$^+$. Anal. calcd (%) for $C_{21}H_{23}CuF_6N_3PS \cdot 0.5\ CH_2Cl_2$: C 43.01, H 4.03, N 7.00, found: C 43.08, H 3.89, N 7.06.

[Cu(5)]BPh_4: To a stirred solution of **5** (0.021 g, 0.055 mmol) in dichloromethane (2 mL) a solution of $[Cu(MeCN)_4]PF_6$ (0.020 g, 0.054 mmol) in dichloromethane (2 mL) was added dropwise. After stirring for 2 h, solid $NaBPh_4$ (0.019 g, 0.054 mmol) was added and it was stirred over night at room temperature. The yellow solution was filtered and slow evaporation of the solvent led to colorless crystals that were suitable for X-ray structural characterisation. Yield: 32.1 mg (0.0420 mmol, 78 %).^{1}H NMR (700 MHz, acetone-*d6*): δ (ppm) = 8.61 (dt, *J* = 5.1, 1.5 Hz, 2H), 7.78 (td, *J* = 7.7, 1.7 Hz, 3H), 7.36 (dd, *J* = 7.6, 5.0 Hz, 5H), 7.21 – 7.19 (m, 7H), 7.04 – 6.99 (m, 3H), 6.78 (t, *J* = 7.4 Hz, 6H), 6.71 – 6.67 (m, 3H), 6.66 – 6.61 (m, 3H), 4.04 (s, 2H), 3.62 (s, 4H), 3.40 (s, 3H), 2.93 (dd, *J* = 6.8, 4.5 Hz, 2H), 2.85 (dd, *J* = 6.6, 4.7 Hz, 2H). HRMS (ESI): *m/z* calcd for $C_{22}H_{25}CuN_3OS^+$: 442.1009; found: 442.1006 [M + L]$^+$. Anal. calcd (%) for $C_{46}H_{45}BCuN_3OS \cdot 2.5\ CH_2Cl_2 \cdot CH_3CN$: C 59.72, H 5.26, N 5.52, found: C 59.24, H 5.08, N 5.52.

[Cu(6)]OTf: To a stirred solution of **6** (0.100 g, 0.295 mmol) in acetone (2 mL) a solution of $[Cu(MeCN)_4]OTf$ (0.109 g, 0.290 mmol) in acetone (2 mL) was added dropwise. The solution was stirred over night at room temperature. Slow evaporation of the solvent led to a yellow solid. Yield: 109 mg (0.197 mmol , 68 %).^{1}H NMR (700 MHz, acetone-*d6*): δ (ppm) = 7.99 (t, *J* = 7.4 Hz, 5H), 7.43 (d, *J* = 1.9 Hz, 2H), 6.32 (dd, *J* = 3.2, 1.8 Hz, 2H), 6.29 (d, *J* = 3.2 Hz, 2H), 4.94 (s, 2H), 3.86 (s, 4H), 3.22 (s, 4H). HRMS (ESI): *m/z* calcd for $C_{19}H_{21}CuN_3OS^+$: 402.0696; found: 402.0699 [M + L]$^+$. Anal. calcd (%) for $C_{46}H_{45}BCuN_3OS$: C 43.51, H 3.83, N 7.61, found: C 43.48, H 3.78, N 7.42.

[Cu(7)]BPh_4: To a stirred solution of **7** (0.050 g, 0.17 mmol) in dichloromethane (2 mL) a solution of $[Cu(MeCN)_4]PF_6$ (0.065 g, 0.17 mmol) in dichloromethane (2 mL) was added dropwise. The mixture was stirred for 30 min. at room temperature. An acetone solution (2 mL) of sodium tetraphenylborate (0.059 g, 0.17 mmol) was added to the reaction mixture and stirred at room temperature over night. The precipitated solid was filtrated, washed with diethyl ether and dried. Slow evaporation of the solvent led to colorless crystals that were suitable for X-ray structural characterisation. Yield: 89.1 mg (0.133 mg, 77 %). ^{1}H NMR (700 MHz, acetone-*d6*): δ (ppm) = 8.71 (d, *J* = 5.1 Hz, 2H), 7.93 (td, *J* = 7.7, 1.7 Hz, 2H), 7.53 – 7.47 (m, 4H), 7.36 – 7.30 (m, 8H), 6.94 (t, *J* = 7.5 Hz, 8H), 6.79 (tt, *J* = 7.2, 1.5 Hz, 4H), 4.04 (s, 4H), 3.12 – 2.96 (m, 3H), 2.76 – 2.64 (m, 3H), 2.33 (s, 3H). HRMS (ESI): *m/z* calcd for $C_{16}H_{21}CuN_3S^+$: 350.0747; found: 350.0752 [M + L]$^+$. Anal. calcd (%) for $C_{40}H_{41}BCuN_3S \cdot 0.5\ CH_2Cl_2$: C 68.26, H 5.94, N 5.90, found: C 68.49, H 6.02, N 6.36.

[Cu(8)]PF_6: To a stirred solution of **8** (0.050 g, 0.13 mmol) in acetone (2 mL) a solution of $[Cu(MeCN)_4]PF_6$ (0.050 g, 0.13 mmol) in acetone (2 mL) was added dropwise. The solution was stirred over night at room temperature. Slow evaporation of the solvent led to yellow crystals that were suitable for X-ray structural characterisation. Yield: 68.0 mg (0.117 mmol ,88 %). ^{1}H NMR (700 MHz, acetone-*d6*): δ (ppm) = 8.62 (d, *J* = 8.4 Hz, 2H), 8.41 (d, *J* = 8.5 Hz, 2H), 7.94 (d, *J* = 8.1 Hz, 2H), 7.90 – 7.83 (m, 2H), 7.59 (t, *J* = 7.59 Hz, 2H), 7.53 (d, *J* = 8.5 Hz, 2H), 4.60 (d, *J* = 17.4 Hz, 2H), 4.47 (d, *J* = 17.4 Hz, 2H), 3.16 (t, *J* = 5.6 Hz, 2H), 3.06 (t, *J* = 5.5 Hz, 2H), 1.73 (s, 3H). HRMS (ESI): *m/z* calcd for $C_{23}H_{23}CuN_3S^+$: 436.0904; found: 436.0904 [M + L]$^+$. Anal. calcd (%) for $C_{23}H_{23}CuF_6N_3PS$: C 47.46, H 3.98, N 7.22, found: C 46.75, H 3.85, N 7.02.

[Cu(9)]BPh_4: To a stirred solution of **9** (0.030 g, 0.076 mmol) in dichloromethane (2 mL) a solution of $[Cu(MeCN)_4]PF_6$ (0.028 g, 0.076 mmol) in dichloromethane (2 mL) was added dropwise. After stirring for 2 h, solid $NaBPh_4$ (0.026 g, 0.076 mmol) was added and it was stirred over night at room temperature. The yellow solution was filtered and slow evaporation of the solvent led to a yellow solid. Yield: 43.6 mg (0.0560 mmol, 74 %). HRMS (ESI): *m/z* calcd for $C_{19}H_{27}CuN_3O_4S^+$: 456.101; found: 456.104 [M + L]$^+$; $C_{19}H_{27}ClCuN_3O_4S^+$: 491.0707; found: 491.0702 [M + L + Cl]$^+$. Anal. calcd (%) for $C_{43}H_{47}BCuN_3O_4S \cdot 4.5\ CH_2Cl_2 \cdot CH_3CN$: C 49.57 H 4.96 N 4.67, found: C 49.42, H 4.69, N 5.06.

[Cu(10)]PF_6: To a stirred solution of **10** (0.025 g, 0.058 mmol) in dichloromethane (2 mL) a solution of $[Cu(MeCN)_4]PF_6$ (0.021 g, 0.055 mmol) in dichloromethane (2 mL) was added dropwise. The solution was stirred over night at room temperature. Slow evaporation of the solvent led to a yellow solid. Yield: 24.6 mg (0.0390 mmol ,70 %). HRMS (ESI): *m/z* calcd for $C_{24}H_{37}CuN_3O_2S^+$: 494.1897; found: 494.1895 $[M + L]^+$. Anal. calcd (%) for $C_{24}H_{37}CuF_6N_3O_2PS \cdot 0.5\ CH_2Cl_2$: C 43.11, H 5.61, N 6.16, found: C 43.27, H 5.71, N 6.08.

Oxygenation Reactions of Copper(I) Complexes: In the glove box, ca. 100 mg of the copper(I) complex were dissolved in 2 mL acetone (for -90 °C) or MeTHF/THF (for -140 °C). Dioxygen was bubbled 5 min. through the complex solution using a syringe needle.

Ozonolysis of Copper(I) Complexes: Ozonolysis was performed with the OZONOSAN PM 83 K. For the reactions with ozone and the copper(I) complexes absolute dry glassware was used. The complex solutions were prepared in a glove box. Ca. 100 mg of the copper complexes were dissolved in 2 mL acetone (for -90 °C) or MeTHF/THF (for -140 °C). Ozone was bubbled 5 min. through the complex solution with a special homebuilt glass cannula, which allowed bubbling ozone through the complex solution without any contact to the metal of a syringe needle.

Acknowledgements

We gratefully acknowledge support by the Justus-Liebig-Universität Gießen and the Deutsche Forschungsgemeinschaft for financial support (SS, SCHI 377/18-1). Furthermore, we would like to thank Stefan Schaub for his help in the laboratory with ozone handling.

Keywords: Copper • Dioxygen activation • Stopped-Flow • Kinetics • Ozone

References

[1] D. A. Quist, D. E. Diaz, J. J. Liu, K. D. Karlin, *J. Biol. Inorg. Chem.* **2017**, *22*, 253.
[2] a) K. A. Magnus, H. Ton-That, J. E. Carpenter, *Chem. Rev.* **1994**, 727.
[3] a) K. D. Karlin, N. Wei, B. Jung, S. Kaderli, P. Niklaus, A. D. Zuberbuehler, *J. Am. Chem. Soc.* **1993**, *115*, 9506; b) J. P. Klinman, *Chem. Rev.* **1996**, *96*, 2541; c) J. P. Klinman, *J. Biol. Inorg. Chem.* **2006**, *281*, 3013; b) V. Gómez-Vidales, I. Castillo, *Eur. J. Inorg. Chem.* **2022**, *in press: doi.org/10.1002/ejic.202100728*.
[4] a) L. Q. Hatcher, K. D. Karlin, *J. Biol. Inorg. Chem.* **2004**, *9*, 669; b) E. A. Lewis, W. B. Tolman, *Chem. Rev.* **2004**, *104*, 1047; c) Siegfried Schindler, *Eur. J. Inorg. Chem.* **2000**, *2000*, 2311; d) T. Osako, S. Nagatomo, Y. Tachi, T. Kitagawa, and S. Itoh, *Angew. Chem.* **2002**, *114*, 4501.
[5] L. M. Mirica, X. Ottenwaelder, T. D. P. Stack, *Chem. Rev.* **2004**, *104*, 1013.
[6] S. T. Prigge, B. A. Eipper, R. E. Mains, L. M. Amzel, *Science (New York, N.Y.)* **2004**, *304*, 864.
[7] R. E. Cowley, L. Tian, E. I. Solomon, *Proc. Natl. Acad. Sci. USA* **2016**, *113*, 12035.
[8] S. Kim, J. W. Ginsbach, A. I. Billah, M. A. Siegler, C. D. Moore, E. I. Solomon, K. D. Karlin, *J. Am. Chem. Soc.* **2014**, *136*, 8063.
[9] S. Kim, J. Y. Lee, R. E. Cowley, J. W. Ginsbach, M. A. Siegler, E. I. Solomon, K. D. Karlin, *J. Am. Chem. Soc.* **2015**, *137*, 2796.
[10] J. Y. Lee, K. D. Karlin, *Curr. Opin. Chem. Biol.* **2015**, *25*, 184.
[11] R. R. Jacobson, Z. Tyeklar, A. Farooq, K. D. Karlin, S. Liu, J. Zubieta, *J. Am. Chem. Soc.* **1988**, *110*, 3690.
[12] L. Q. Hatcher, D.-H. Lee, M. A. Vance, A. E. Milligan, R. Sarangi, K. O. Hodgson, B. Hedman, E. I. Solomon, K. D. Karlin, *Inorg. Chem.* **2006**, *45*, 10055.
[13] M. Bhadra, W. J. Transue, H. Lim, R. E. Cowley, J. Y. C. Lee, M. A. Siegler, P. Josephs, G. Henkel, M. Lerch, S. Schindler et al., *J. Am. Chem. Soc.* **2021**, *143*, 3707.
[14] T. Hoppe, S. Schaub, J. Becker, C. Würtele, S. Schindler, *Angew. Chem.* **2013**, *52*, 870.
[15] T. Hoppe, P. Josephs, N. Kempf, C. Wölper, S. Schindler, A. Neuba, G. Henkel, *Z. Anorg. Allg. Chem.* **2013**, *639*, 1504.
[16] a) L. Zhou, D. Powell, K. M. Nicholas, *Inorg. Chem.* **2006**, *45*, 3840; b) G. Y. Park, Y. Lee, D.-H. Lee, J. S. Woertink, A. A. Narducci Sarjeant, E. I. Solomon, K. D. Karlin, *Chem. Commun.* **2010**, *46*, 91; c) T. Ohta, T. Tachiyama, K. Yoshizawa, T. Yamabe, T. Uchida, T. Kitagawa, *Inorg. Chem.* **2000**, *39*, 4358; d) Y. Lee, D.-H. Lee, G. Y. Park, H. R. Lucas, A. A. Narducci Sarjeant, M. T. Kieber-Emmons, M. A. Vance, A. E. Milligan, E. I. Solomon, K. D. Karlin, *Inorg. Chem.* **2010**, *49*, 8873.
[17] E. A. Ambundo, M.-V. Deydier, A. J. Grall, N. Aguera-Vega, L. T. Dressel, T. H. Cooper, M. J. Heeg, L. A. Ochrymowycz, D. B. Rorabacher, *Inorg. Chem.* **1999**, *38*, 4233.
[18] D.-H. Lee, L. Q. Hatcher, M. A. Vance, R. Sarangi, A. E. Milligan, A. A. N. Sarjeant, C. D. Incarvito, A. L. Rheingold, K. O. Hodgson, B. Hedman et al., *Inorg. Chem.* **2007**, *46*, 6056.
[19] P. Josephs, *dissertation* **2017**, University Paderborn.
[20] M. Schatz, V. Raab, S. P. Foxon, G. Brehm, S. Schneider, M. Reiher, M. C. Holthausen, J. Sundermeyer, S. Schindler, *Angew. Chem.* **2004**, *43*, 4360.
[21] T. Rotärmel, J. Becker, S. Schindler, *Faraday Discuss.* **2022**, *234*, 70.
[22] H. Sterckx, B. Morel, B. U. W. Maes, *Angew. Chem.* **2019**, *58*, 7946.
[23] a) N. W. Aboelella, B. F. Gherman, L. M. R. Hill, J. T. York, N. Holm, V. G. Young, C. J. Cramer, W. B. Tolman, *J. Am. Chem. Soc.* **2006**, *128*, 3445; b) I. Castillo, V. M. Ugalde-Saldívar, L. A. Rodríguez Solano, B. N. Sánchez Eguía, E. Zeglio, E. Nordlander, *Dalton Trans.* **2012**, *41*, 9394; c) M. Gennari, M. Tegoni, M. Lanfranchi, M. A. Pellinghelli, M. Giannetto, L. Marchiò, *Inorg. Chem.* **2008**, *47*, 2223.
[24] a) M. Wern, T. Hoppe, J. Becker, S. Zahn, D. Mollenhauer, S. Schindler, *Eur. J. Inorg. Chem.* **2016**, *2016*, 3384; b) M. E. Helton, D. Maiti, L. N. Zakharov, A. L. Rheingold, J. A. Porco, K. D. Karlin, *Angew. Chem.* **2006**, *45*, 1138; c) D. Maiti, J. S. Woertink, M. A. Vance, A. E. Milligan, A. A. N. Sarjeant, E. I. Solomon, K. D. Karlin, *J. Am. Chem. Soc.* **2007**, *129*, 8882.
[25] B.-J. Liaw, T. S. Lobana, Y.-W. Lin, J.-C. Wang, C. W. Liu, *Inorg. Chem.* **2005**, *44*, 9921.
[26] a) E. A. Ambundo, M. V. Deydier, L. A. Ochrymowycz, D. B. Rorabacher, *Inorg. Chem.* **2000**, *39*, 1171; b) F. Jiang, M. A. Siegler, E. Bouwman, *Inorg. Chim. Acta* **2019**, *486*, 135; c) E. C. M. Ording-Wenker, M. A. Siegler, M. Lutz, E. Bouwman, *Dalton Trans.* **2015**, *44*, 12196.
[27] a) M. Weitzer, S. Schindler, G. Brehm, S. Schneider, E. Hörmann, B. Jung, S. Kaderli, A. D. Zuberbühler, *Inorg. Chem.* **2003**, *42*, 1800; b) C. X. Zhang, S. Kaderli, M. Costas, E.-I. Kim, Y.-M. Neuhold, K. D. Karlin, A. D. Zuberbühler, *Inorg. Chem.* **2003**, *42*, 1807.
[28] a) A. Hoffmann, M. Wern, T. Hoppe, M. Witte, R. Haase, P. Liebhäuser, J. Glatthaar, S. Herres-Pawlis, S. Schindler, *Eur. J. Inorg. Chem.* **2016**, *2016*, 4744; b) M. Lerch, M. Weitzer, T.-D. J. Stumpf, L. Laurini, A. Hoffmann, J. Becker, A. Miska, R. Göttlich, S. Herres-Pawlis, S. Schindler, *Eur. J. Inorg. Chem.* **2020**, 3143.

4. Syntheses and investigation of metal complexes with macrocyclic polythioether ligands

This work has been published in

Faraday Discussions

Thomas Rotärmel, Jonathan Becker, and Siegfried Schindler

Faraday Discuss., **2022**, 234, 70-85

Faraday Discussions

Cite this: *Faraday Discuss.*, 2022, **234**, 70

ROYAL SOCIETY OF CHEMISTRY

PAPER

View Article Online
View Journal | View Issue

Syntheses and investigation of metal complexes with macrocyclic polythioether ligands†

Thomas Rotärmel, Jonathan Becker and Siegfried Schindler *

Received 6th September 2021, Accepted 14th October 2021
DOI: 10.1039/d1fd00062d

Copper(I) complexes with the macrocyclic thioether ligands 1,4,8,11-tetrathiacyclotetradecane (tetrathiacyclam, 14-S_4) and 1,8-dithia-4,11-diazacyclotetradecane (dithiacyclam, 14-N_2S_2) were synthesised and structurally characterised. While the copper(I) complexes showed no reactivity towards dioxygen, the formation of "dioxygen adduct complexes" could be spectroscopically detected with ozone using low temperature stopped-flow techniques. Furthermore, it was possible to synthesise and characterise iron(II) and cobalt(II) complexes with the tetrathiacyclam ligand. No "dioxygen adduct" intermediates were observed when these complexes were reacted with dioxygen or ozone. Depending on the reaction conditions, the coordination of the metal ions could be controlled (*endo- vs. exo*-coordination and *cis- vs. trans*-coordination) and in addition to mononuclear complexes, also coordination polymers were obtained.

Introduction

With regard to gaining a better understanding of important selective oxidation/oxygenation reactions there has been a large number of investigations of copper and iron complexes that can be regarded as model compounds for corresponding metalloenzymes.[1] In particular, more recently interest increased in the analysis of the active site of the copper monooxygenases peptidylglycine-α-hydroxylating mono-oxygenase (PHM) and dopamine β-monooxygenase (DβM), enzymes that are important for the synthesis of neuropeptides and hormones.[2] Only in 2004, structural characterisation of a copper dioxygen complex in PHM could show unambiguously a mononuclear *end-on*-superoxido copper complex in the active site.[3] While up to then model compounds had supported the formation of such a species spectroscopically it finally was possible to structurally characterise an *end-on* copper superoxido complex with the tripodal ligand

Institut für Anorganische und Analytische Chemie, Justus-Liebig-Universität Gießen, Heinrich-Buff-Ring 17, 35392 Gießen, Germany. E-mail: siegfried.schindler@ac.jlug.de

† Electronic supplementary information (ESI) available. CCDC 2107318–2107328. For ESI and crystallographic data in CIF or other electronic format see DOI: 10.1039/d1fd00062d

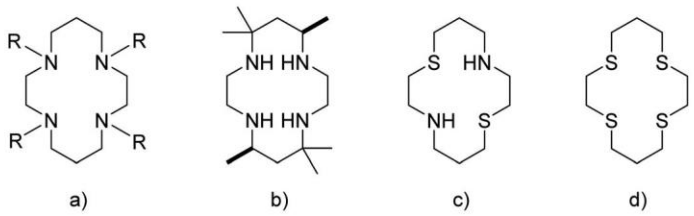

Scheme 1 Macrocyclic ligands (a) cyclam (R = H), TMC (R = CH_3), (b) tet b, (c) 14-N_2S_2 and (d) 14-S_4.

tris(tetramethylguanidino)tren (TMG_3tren).[4] Alternatively, dioxygen can be coordinated as a *side-on* superoxide which has been thoroughly described previously by Kitajima and Tolman;[5] however, this is not a binding mode so far observed in nature. In an effort to get closer to modelling the active site of PHM, Itoh and co-workers[6] used tridentate ligands instead of tetradentate tripodal ligands. However, while most of these compounds were based on all nitrogen ligands,[7] PHM and DβM contain thioether ligand residues, such as cysteine (Cys) and methionine (Met).[3,7,8] The coordination of Met plays an important role in copper dioxygen chemistry and is of high interest for understanding how thioether-ligation influences the structure, spectroscopy and reactivity.[3,9] Therefore, in previous work, a number of different thioether ligands already have been studied.[10] Bhadra *et al.* recently described the synthesis of an *end-on* superoxido copper complex system with a $^{TMG}N_3S$ thioether ligand (a derivative of TMG_3tren). It is the first reported *end-on* superoxido copper complex with an experimentally proven Cu–S bond which also possesses demonstrated hydrogen atom abstraction (HAA) reactivity.[11]

Based on earlier work by Valentine and co-workers, we have been successful in spectroscopically observing the formation of an *end-on* superoxido copper complex with the ligand tet b (*rac*-5,5,7,12,12,14-hexamethyl-1,4,8,11-tetraazacyclotetradecane), a derivative of the well-known macrocyclic ligand cyclam (Scheme 1).[12,13] With regard to these results we decided to investigate the reactivity of copper complexes with the known sulfur containing derivatives of cyclam (Scheme 1) 14-N_2S_2 (1,8-dithia-4,11-diazacyclotetradecane, dithiacyclam) and 14-S_4 (1,4,8,11-tetrathiacyclotetradecane, tetrathiacyclam) towards dioxygen and ozone.[14,15]

Results and discussion

As observed by us[16] and reported previously by Nam, Karlin and co-workers, the copper(I) complex with TMC as ligand does not react with dioxygen.[17] In contrast, as described above, the complex $[Cu(tet\ b)]^+$ reacts with dioxygen to form an *end-on* superoxido complex.[12]

More recently we started to use ozone as an oxidant to trap an oxygen adduct complex, *e.g.* to obtain an iron(IV) oxido complex with the ligand TMC, an approach based on earlier work by Wieghardt and co-workers as well as by Pestovsky *et al.*[18] Furthermore, the oxygenation with ozone is well known for iron and manganese porphyrinoid complexes.[19] However, to the best of our knowledge,

studies on the reactions of ozone and copper(I) complexes to trap an "oxygen adduct" have not been reported so far. Therefore, we thought it might be useful to extend our investigations on the reactions of copper(I) complexes with ozone.

Interestingly, formation of the superoxido complex $[(\text{tet b})\text{Cu}(\text{O}_2)]^+$ is still observed (characteristic absorbance maxima at 410 nm, Fig. 1) if the reaction is performed with ozone, however, much faster decomposition takes place in comparison with the reaction with pure dioxygen. Low temperature stopped-flow measurements allowed obtaining the time resolved UV-vis spectra presented in Fig. 1.

Because ozone is always applied together with dioxygen, with our ozone generator a mixture of 6–14% ozone and 86–94% dioxygen is obtained (depending on the gas pressure, time and current settings), the direct reaction with dioxygen is still occurring. However, the presence of ozone obviously does lead to a fast decomposition of the superoxido complex. Interestingly, even in the presence of ozone, we did not observe a reaction of $[\text{Cu}(\text{TMC})]^+$ with either dioxygen or ozone (under the applied stopped-flow conditions).

Synthesis and characterisation of copper(I) complexes with the ligands 14-S_4 and 14-N_2S_2

In order to better understand the effect of sulfur in the TMC ligand system, the two derivatives 14-S_4 and 14-N_2S_2 were synthesised. While 14-S_4 was commercially available, 14-N_2S_2 had to be prepared in a multi-step synthesis according to the literature.[15]

Previous work was reported on copper complexes with the 14-S_4 ligand in order to investigate the importance of the geometry of copper(I/II)-complexes in copper redox chemistry and revealed a polymeric crystal structure for the copper(I) complex where each copper(I)-ion is coordinated to four sulfur atoms, three of them originating from one ligand and the fourth one from an adjacent ligand.[20]

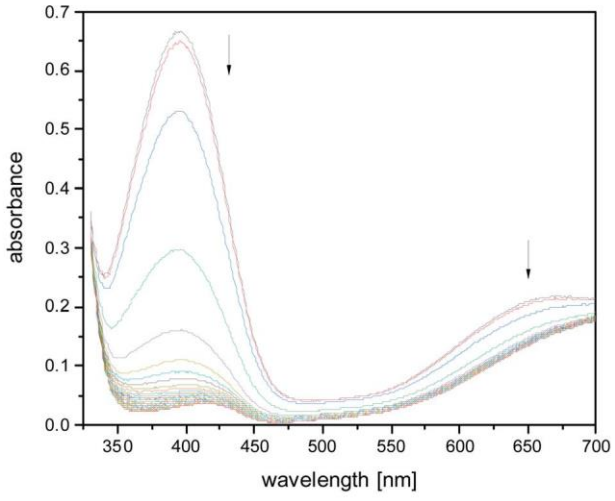

Fig. 1 Time-resolved UV/vis spectra of the reaction of ozone/dioxygen with $[\text{Cu}^{\text{I}}(\text{tet b})]PF_6$ in acetone ($c_{\text{complex}} = 0.4$ mmol L^{-1} after mixing) at −90 °C, total time: 0.3 s.

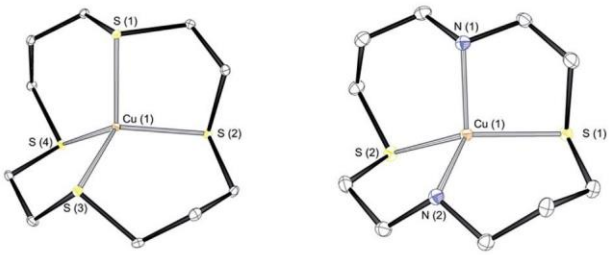

Fig. 2 Molecular structures of $[Cu^{I}(14\text{-}S_4)]^+$ and $[Cu^{I}(14\text{-}N_2S_2)]^+$ in ORTEP representations at 50% probability. H atoms and counterions were omitted for clarity.

The ability of the 14-S_4 ligand to maintain four coordinating bonds to a single copper(I)-ion was indicated in solution by NMR measurements.[21] In contrast to these previous results we were able to prepare and structurally characterise the monomeric copper species with different copper salts. The reaction of the 14-S_4 ligand with $[Cu(MeCN)_4]OTf$ in THF generated a colourless solid in high yield. The formation of $[Cu^{I}(14\text{-}S_4)]OTf$ was confirmed by electrospray-ionisation mass-spectrometry (ESI-MS), revealing the characteristic peak at $m/z = 330.975$ for the $[Cu^{I}(14\text{-}S_4)]^+$ cation. Moreover, we obtained suitable single crystals for X-ray structural characterisation. The crystal structure revealed that the copper(I)-ion is coordinated in a distorted tetrahedron by four sulfur-donor atoms. The molecular structure of $[Cu^{I}(14\text{-}S_4)]OTf$ is presented in Fig. 2 (crystallographic data are reported in ESI†) and selected bond lengths and angles are given in Table 1. Furthermore, it was possible to synthesise and structurally characterise $[Cu^{I}(14\text{-}S_4)]PF_6$ and $[Cu^{I}(14\text{-}S_4)]BPh_4$ (see ESI†) which only differ with regard to the anions.

Changing the solvent in the reaction with the 14-S_4 ligand and a copper salt from a non-coordinating solvent such as THF or dichloromethane to a well-coordinating solvent, *e.g.* MeCN, also led to the formation of a 1-dimensional polymeric structure. However, this polymer is different to the one reported previously and described above. In this new polymer, the copper(I)-ion is *exo*-coordinated in a distorted tetrahedral geometry by three sulfur-donor atoms and

Table 1 Selected bond lengths/Å and angles/° for $[Cu^{I}(14\text{-}S_4)]OTf$ and $[Cu^{I}(14\text{-}N_2S_2)]OTf$

$[Cu^{I}(14\text{-}S_4)]OTf$		$[Cu^{I}(14\text{-}N_2S_2)]OTf$	
Bond length		**Bond length**	
Cu(1)–S(1)	2.270(4)	Cu(1)–S(1)	2.257(6)
Cu(1)–S(2)	2.281(4)	Cu(1)–S(2)	2.266(5)
Cu(1)–S(3)	2.262(4)	Cu(1)–N(1)	2.091(17)
Cu(1)–S(4)	2.283(4)	Cu(1)–N(2)	2.096(17)
Bond angle		**Bond angle**	
S(1)–Cu(1)–S(2)	95.8°(16)	S(1)–Cu(1)–S(2)	146.4°(2)
S(1)–Cu(1)–S(3)	126.2°(16)	S(1)–Cu(1)–N(1)	90.8°(5)
S(1)–Cu(1)–S(4)	112.4°(16)	S(1)–Cu(1)–N(2)	106.4°(5)
S(2)–Cu(1)–S(3)	111.3°(16)	S(2)–Cu(1)–N(1)	106.3°(5)
S(2)–Cu(1)–S(4)	118.5°(16)	S(2)–Cu(1)–N(2)	91.2°(5)
S(3)–Cu(1)–S(4)	94.6°(15)	N(1)–Cu(1)–N(2)	117.7°(7)

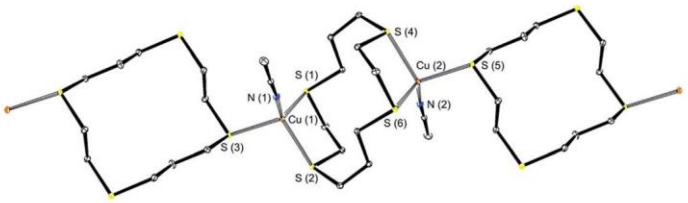

Fig. 3 Excerpt of the crystal structure of $\{[Cu^{I}(14\text{-}S_4)(MeCN)PF_6]\}_n$ in ORTEP representation at 50% probability. H atoms and counterions were omitted for clarity.

one nitrogen-donor atom from MeCN. The three S–Cu bonds arising from two different ligands coordinate alternately in a monodentate and bidentate fashion. A section of the polymer chain is presented in Fig. 3 (crystallographic data are reported in the ESI†).

In contrast to the reaction with the 14-S_4 ligand, no solvent effect was observed for the formation of copper(I) complexes with the 14-N_2S_2 ligand. It therefore seems that the coordination of the complex (*endo- vs. exo*-coordination) depends on the donor-atoms (two *vs.* four sulfur-atoms) and the type of solvent (non- *vs.* good-coordinating solvent) used in the reaction. In fact, sulfur-containing macrocycles often show metal coordination in an *exo*-fashion, caused by the torsion arrangements from the donor atoms.[22] However, with the "right" reaction conditions it is possible to force the ligand to coordinate the metal-ion inside the cavity (*endo*-coordination).

A copper(I) complex with the 14-N_2S_2 ligand, $[Cu^{I}(14\text{-}N_2S_2)]$OTf, was easily obtained and the molecular structure is presented in Fig. 2 (crystallographic data are reported in the ESI†). The structure of its cation is nearly identical to the molecular structure of the cation of the complex $[Cu^{I}(14\text{-}N_2S_2)]PF_6$ which had been reported previously.[23]

In both complexes, $[Cu^{I}(14\text{-}S_4)]$OTf as well as $[Cu^{I}(14\text{-}N_2S_2)]$OTf, the copper ion is four-coordinated either by four sulfur atoms or by two sulfur atoms and two nitrogen atoms in a distorted tetrahedral geometry. However, the complexes differ in bond lengths and angles (Table 1). For example, comparing the 14-S_4 complex to the 14-N_2S_2 complex the S–Cu–S angle decreases by ~28° based on the shorter Cu–N bond lengths, which are incorporated in the 14-N_2S_2 complex, while the Cu–S bond lengths in both complexes are almost identical.

Reactivity of the copper(I) complexes $[Cu^{I}(14\text{-}S_4)]$OTf and $[Cu^{I}(14\text{-}N_2S_2)]$OTf towards dioxygen and ozone

Similar to the reaction of the copper(I) complex with the ligand TMC described above, copper complexes $[Cu^{I}(14\text{-}S_4)]$OTf and $[Cu^{I}(14\text{-}N_2S_2)]$OTf did not react with dioxygen. The coordinated sulfur atoms might even lead to a higher stability towards oxidation due to the fact that sulfur containing ligand systems can form quite stable Cu(I) complexes that are inert to dioxygen.[7] Furthermore, no reaction was observed under stopped-flow conditions in dichloromethane at −80 °C. In contrast, the reaction of $[Cu^{I}(14\text{-}S_4)]$OTf with ozone at −80 °C in dichloromethane immediately led to a lime green species. Warming the solution led to the formation of a light green coloured suspension. The light green solid could be

separated, however, up to now we did not succeed in characterising this product. Time-resolved UV-vis spectra obtained in a low temperature stopped-flow experiment are shown in Fig. 4.

Absorbance maxima at 402 nm and 627 nm are consistent with the formation of an *end-on* superoxido copper complex (compare with Fig. 1).[7] However, as can be seen in Fig. 4 (inset), the complex was not stable enough to allow isolation/crystallisation of this transient intermediate.

Still, in an effort to obtain crystals, in one approach (sample stored for 6 months in a freezer at −80 °C) the colour of the solution turned from a lime green to a purple colour and a few red purple crystals were obtained, suitable for X-ray structural characterisation. The molecular structure revealed formation of the copper(II) complex $[Cu^{II}(14\text{-}S_4)]OTf_2$ (molecular structure and crystallographic data are presented in the ESI†). The copper(II) ion is *endo*-coordinated by the macrocyclic ligand system with additional two triflate ions coordinated in axial positions. The molecular structure is very similar to the perchlorate analogue reported previously.[24]

The overall finding is quite important because it shows that it is possible to obtain a transition metal superoxido complex by applying ozone as an oxidant.

In contrast to the reaction of $[Cu^{I}(14\text{-}S_4)]OTf$ with ozone, $[Cu^{I}(14\text{-}N_2S_2)]OTf$ produced immediately a dark green species with ozone in dichloromethane at −80 °C. Warming up the solution led to the formation of a light green suspension. Again, the light green solid was separated, but could not be characterised so far. Stopped-flow measurements of the reaction of the copper(I) complex with ozone at low temperature were performed and time resolved UV-vis spectra are shown in Fig. 5. These investigations confirmed the formation of a short-lived "oxygen adduct" complex. A characteristic UV absorbance band around 386 nm could be detected, which in comparison with literature data most likely indicates the formation of a *side-on* peroxido copper(II) complex.[7,17] Unfortunately, in a series of

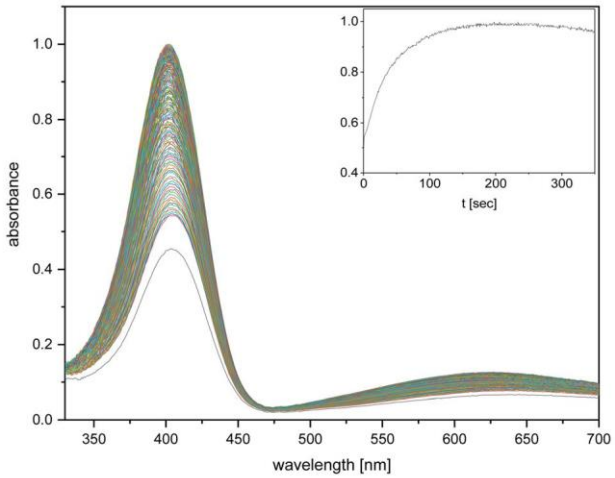

Fig. 4 Time-resolved UV/vis-spectra of the reaction of ozone with $[Cu^{I}(14\text{-}S_4)]OTf$ in dichloromethane ($c_{complex}$ = 0.2 mmol L^{-1} after mixing) at −80 °C, total time: 375 s. Inlay (timetrace): absorbance *vs.* time at 402 nm.

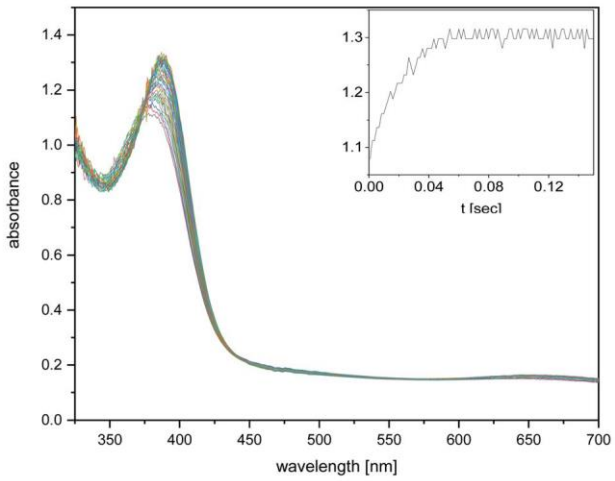

Fig. 5 Time-resolved UV/vis-spectra of the reaction of ozone with [Cu^{I}(14-N_2S_2)]OTf in dichloromethane ($c_{complex}$ = 0.2 mmol L^{-1} after mixing) at −80 °C, total time: 0.15 s. Inlay (timetrace): absorbance *vs.* time at 386 nm.

crystallisation approaches no crystals could be obtained for a further characterisation of this complex.

Unfortunately, it was not possible (due to the instability of the complexes and the special setup for ozone chemistry) to characterise the postulated complexes [(14-S_4)Cu(O_2)]OTf and [(14-N_2S_2)Cu(O_2)Cu[(14-N_2S_2)](OTf)$_2$ further, however, the UV-vis spectra in combination with the results for the copper tet b complex system strongly support this assignment. In contrast to the iron complexes described above, we think that the formation of a copper(III) oxido or copper(II) oxygenyl complex is less likely during the reaction with ozone. However, we cannot completely exclude it so far. Instead, we propose the mechanism shown in Scheme 2 for the formation of the copper superoxido and copper peroxido complex.

The quite labile copper ozonido complex can react with dioxygen (that is present in excess) leading to the copper superoxido complex [(14-S_4)Cu(O_2)]OTf. The opposite reaction is well known for the synthesis of alkali metal ozonido complexes. Thus, potassium and rubidium ozonido salts are prepared from the corresponding superoxido compounds and ozone.[25] If there is no steric hindrance the copper superoxido complex can react further with another copper(I) complex, leading to the corresponding dinuclear copper peroxido complex. Further side

$$[Cu^{I}(L)]^{+} + O_3 \longrightarrow [Cu^{II}(L)O_3]^{+} \quad (1)$$

$$[Cu^{II}(L)O_3]^{+} + O_2 \longrightarrow [Cu^{II}(L)O_2]^{+} + O_3 \quad (2)$$

$$[Cu^{II}(L)O_2]^{+} + [Cu^{I}(L)]^{+} \longrightarrow [(L)Cu^{II}(O_2)Cu^{II}(L)]^{2+} \quad (3)$$

Scheme 2 Proposed reaction mechanism for the formation of a copper superoxido and copper peroxide complex.

reactions occur due to the fact that we observe decomposition of the formed complexes as well as precipitation of a so far not identified product in more concentrated solutions.

Synthesis and characterisation of iron(II) complexes with the 14-S_4 ligand

Hughes *et al.* reported the first investigations of iron(II) complexes with the 14-S_4 ligand.[26] The authors already were quite successful in describing the reaction between the 14-S_4 ligand and FeI_2, however, without reporting a crystal structure of the complex. They prepared $[Fe^{II}(14\text{-}S_4)(MeCN)_2]FeI_4$ and analysed the complex by Mössbauer spectroscopy, elemental analysis and IR spectroscopy. We now could crystallise $[Fe^{II}(14\text{-}S_4)(MeCN)_2]FeI_4$ by reacting FeI_2 and 14-S_4 in a ratio of 2 : 1. The molecular structure is presented in Fig. 6 (crystallographic data are reported in the ESI†).

The Fe^{II} center is *endo*-coordinated and octahedrally surrounded by the 14-S_4 ligand and two additional acetonitrile molecules, which are coordinated in *cis* positions. Furthermore, the successful complexation was supported by ESI-MS revealing the characteristic mass peak at $m/z = 161.989$ for the $[Fe(14\text{-}S_4)]^{2+}$ fragment.

Moreover, we succeeded in synthesising the complex $[Fe^{II}(14\text{-}S_4)(MeCN)_2][(FeI_3)_2(14\text{-}S_4)]$ in a reaction between FeI_2 and 14-S_4 in a ratio of 1 : 1. The molecular structure presented in Fig. 7 (crystallographic data are reported in the ESI†) is quite interesting, because of the fact that the ligand is involved both as a cation as well as an anion and on the one hand in *exo*- and on the other hand in *endo*-coordination. In comparison to $[Fe^{II}(14\text{-}S_4)(MeCN)_2]FeI_4$ the acetonitrile molecules are coordinated in *trans* positions. The formation of the expected Fe^{II} complex was also confirmed by ESI-MS revealing a mass peak at $m/z = 161.989$ for the $[Fe(14\text{-}S_4)]^{2+}$ fragment.

A comparison of the molecular structure between both iron(II) complexes shows almost the same bond lengths and angles (bond lengths and angles are presented in Table 2). In addition, an iron(II) complex could be prepared with $[Fe(MeCN)_4](PF_6)_2$ and 14-S_4 followed by an anion exchange with $AgBAr_4^F$. The

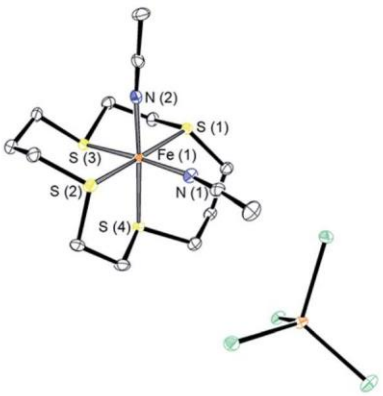

Fig. 6 Molecular structure of $[Fe^{II}(14\text{-}S_4)(MeCN)_2]FeI_4$ in ORTEP representation at 50% probability. H atoms were omitted for clarity.

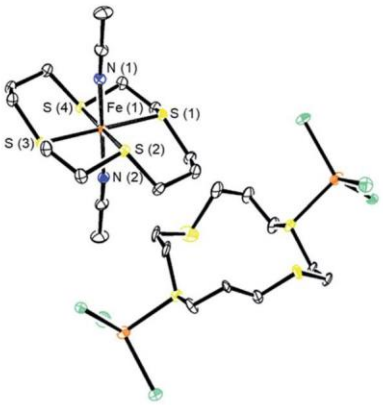

Fig. 7 Molecular structure of $[Fe^{II}(14\text{-}S_4)(MeCN)_2][(FeI_3)_2(14\text{-}S_4)]$ in ORTEP representation at 50% probability. H atoms were omitted for clarity.

molecular structure of $[Fe^{II}(14\text{-}S_4)(MeCN)_2](BAr_4{}^F)_2$ is presented in the ESI† and shows the same octahedral geometry as the complex $[Fe^{II}(14\text{-}S_4)(MeCN)_2][(FeI_3)_2(14\text{-}S_4)]$.

Bench-top experiments at different temperatures for the reaction of the iron complexes with dioxygen and ozone did not provide evidence for the formation of

Table 2 Selected bond lengths/Å and angles/° for *cis* Fe^{II} complex and *trans* Fe^{II} complex

Cis Fe^{II} complex		*Trans* Fe^{II} complex	
Bond length		**Bond length**	
Fe(1)–S(1)	2.252(9)	Fe(1)–S(1)	2.249(11)
Fe(1)–S(2)	2.249(10)	Fe(1)–S(2)	2.246(11)
Fe(1)–S(3)	2.233(9)	Fe(1)–S(3)	2.253(11)
Fe(1)–S(4)	2.240(9)	Fe(1)–S(4)	2.246(11)
Fe(1)–N(1)	1.945(3)	Fe(1)–N(1)	1.923(4)
Fe(1)–N(2)	1.955(3)	Fe(1)–N(2)	1.926(4)
Bond angle		**Bond angle**	
N(1)–Fe(1)–N(2)	89.7°(11)	N(1)–Fe(1)–N(2)	179.1°(15)
N(1)–Fe(1)–S(1)	91.2°(9)	N(1)–Fe(1)–S(1)	87.4°(11)
N(1)–Fe(1)–S(2)	86.2°(9)	N(1)–Fe(1)–S(2)	86.1°(11)
N(1)–Fe(1)–S(3)	175.4°(9)	N(1)–Fe(1)–S(3)	92.5°(11)
N(1)–Fe(1)–S(4)	90.8°(9)	N(1)–Fe(1)–S(4)	93.6°(11)
N(2)–Fe(1)–S(1)	87.9°(8)	N(2)–Fe(1)–S(1)	92.7°(11)
N(2)–Fe(1)–S(2)	88.4°(3)	N(2)–Fe(1)–S(2)	94.9°(11)
N(2)–Fe(1)–S(3)	94.8°(8)	N(2)–Fe(1)–S(3)	92.5°(11)
N(2)–Fe(1)–S(4)	176.5°(9)	N(2)–Fe(1)–S(4)	85.5°(11)
S(1)–Fe(1)–S(2)	175.5°(4)	S(1)–Fe(1)–S(2)	89.5°(4)
S(1)–Fe(1)–S(3)	88.4°(3)	S(1)–Fe(1)–S(3)	179.6°(5)
S(1)–Fe(1)–S(4)	95.5°(3)	S(1)–Fe(1)–S(4)	90.1°(4)
S(2)–Fe(1)–S(3)	94.6°(4)	S(2)–Fe(1)–S(3)	90.1°(4)
S(2)–Fe(1)–S(4)	88.2°(3)	S(2)–Fe(1)–S(4)	179.5°(5)
S(3)–Fe(1)–S(4)	84.7°(3)	S(3)–Fe(1)–S(4)	90.3°(4)

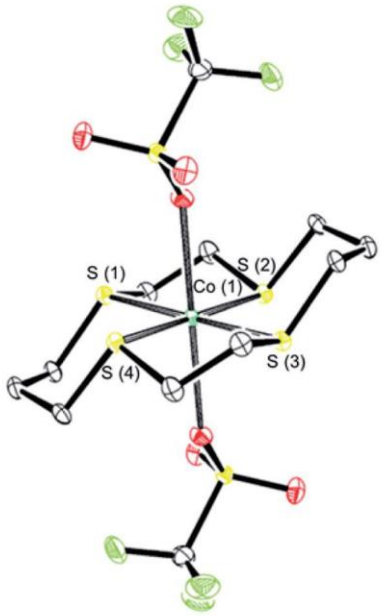

Fig. 8 Molecular structure of $[Co^{II}(14\text{-}S_4)(OTf)_2]$ in ORTEP representation at 50% probability. H atoms were omitted for clarity.

an "oxygen adduct" complex as an intermediate. This was furthermore supported by cyclic voltammetry, which showed irreversible redox reactions (ESI†).

Synthesis and characterisation of cobalt(II) complexes with the 14-S_4 ligand

Furthermore, a cobalt(II) complex could be prepared with $Co^{II}(OTf)_2$ and the 14-S_4 ligand in THF. In previous work cobalt(II) complexes have already been synthesised with the cyclam and 14-N_2S_2 ligand.[27,28] Nevertheless, to the best of our knowledge, this is the first synthesised and structurally characterised cobalt(II) complex with the 14-S_4 ligand. The successful complexation was supported by ESI-MS revealing the characteristic mass peaks at $m/z = 163.489$ and 475.924 for the $[Co(14\text{-}S_4)]^{2+}$ and $[Co(14\text{-}S_4)OTf]^{+}$ fragments. The molecular structure, presented in Fig. 8 (crystallographic data are reported in the ESI†), shows an octahedral geometry. Selected bond lengths and angles are reported in Table 3. A comparison of the cobalt(II) complexes with cyclam,[27] 14-N_2S_2 (ref. 28) and 14-S_4 ligand systems shows similarities in terms of bond angles, lengths and geometry.

However, it is interesting to note, that while the previous reported cobalt(II) complexes showed no solvent dependency with regard to the *exo- vs. endo*-coordination of the cobalt(II) ion, this is the case for the cobalt(II) 14-S_4 complex. Similar to the solvent dependency of the copper(I) complexes described above, the same effect could be observed with cobalt(II) ions and the 14-S_4 ligand.

If the reaction is carried out in MeCN, a polymeric structure could be obtained revealing an *exo*-coordination of the cobalt(II)-ions (molecular structures and crystallographic data are reported in the ESI†).

Table 3 Selected bond lengths/Å and angles/° for $[Co^{II}(14\text{-}S_4)](OTf)_2$

$[Co^{II}(14\text{-}S_4)](OTf)_2$			
Bond length		**Bond angle**	
Co(1)–S(1)	2.2262(5)	S(1)–Co(1)–S(2)	90.2°(18)
Co(1)–S(2)	2.2262(5)	S(1)–Co(1)–S(3)	180.0°
Co(1)–S(3)	2.2206(5)	S(1)–Co(1)–S(4)	89.8°(18)
Co(1)–S(4)	2.2206(5)	S(2)–Co(1)–S(3)	89.8°(18)
Co(1)–O(1)	2.357(14)	S(2)–Co(1)–S(4)	180.0°
Co(1)–O(2)	2.357(14)	S(3)–Co(1)–S(4)	90.2°(18)
		S(1)–Co(1)–O(2)	89.8°(4)
		S(3)–Co(1)–O(2)	90.2°(4)
		S(2)–Co(1)–O(2)	96.9°(4)
		S(4)–Co(1)–O(2)	83.1°(4)
		S(1)–Co(1)–-O(1)	90.2°(4)
		S(3)–Co(1)–O(1)	89.8°(4)
		S(2)–Co(1)–O(1)	83.1°(4)
		S(4)–Co(1)–O(1)	96.9°(4)
		O(1)–Co(1)–O(2)	180.0°

Furthermore, as with the iron complexes, cyclic voltammetry of $[Co^{II}(14\text{-}S_4)](OTf)_2$ only showed irreversible redox behaviour (ESI†).

Experimental section

All reagents and solvents used were of p.a. quality and were purchased from Sigma Aldrich and AcrosOrganics. The solvents were purified by distillation with a drying agent by standard procedures. The ligand $14\text{-}N_2S_2$,[15,29] $[Cu(TMC)]PF_6$ (ref. 17) and $[Cu(tet\ b)]PF_6$ (ref. 30) were synthesised according to literature protocols. The air sensitive syntheses of the metal complexes were performed under inert conditions in an MBraun glove box (equipped with water and dioxygen sensors; H_2O and O_2 concentrations less than 0.1 ppm) under an argon atmosphere. Stopped-flow measurements were carried out with a HI-Tech SF-61SX2 and CSF-61DX2 low-temperature stopped-flow unit equipped with a diode array spectrophotometer. NMR measurements were performed with a Bruker Avance II 400 MHz (AV II 400). For electrospray-ionisation MS (ESI-MS) measurements a Bruker microTOF mass spectrometer was used. UV/vis spectra were recorded with an Agilent 8453 spectrometer. Experimental data in single-crystal X-ray diffraction measurements were collected by using a Bruker D8 Venture system, equipped with dual IμS-sources (Mo(Cu)), a PHOTON 100 detector and an Oxford Cryostream 700 low temperature system (details are described in the ESI†). Cyclic voltammetry measurements were performed with a glassy carbon electrode as working electrode, a platinum/titanium electrode (counter electrode) and an Ag/AgCl reference electrode. MeCN was used as solvent and NBu_4BF_4 was applied as conducting salt. Ferrocene was used as standard and the electrochemical data were recorded with an e-corder 410 edaq (eDAQ, Colorado Springs, US) and the program eChem. The CHN elemental analysis was performed using the CHN-Analysator: Thermo FlashEA – 1112 Series.

Ozonolysis of copper complexes

Ozonolysis was performed with the OZONOSAN PM 83 K. For the reactions with ozone and the copper complexes absolute dry glassware was used. The complex solutions were prepared in a glove box. Approximately 100 mg of the copper complexes were dissolved in 2 mL DCM for the reaction at −80 °C. Ozone was bubbled for 5 min through the complex solution with a glass cannula, which allowed bubbling ozone through the complex solution without any contact with the metal of the syringe needle. After the reaction with ozone, the complex solutions were stored in a −80 °C freezer.

Synthesis of [Cu(14-S_4)]OTf

A solution of $[Cu(MeCN)_4]OTf$ (69.3 mg, 0.184 mmol) in THF (2 mL) was added dropwise to a solution of 14-S_4 (50.0 mg, 0.186 mmol) in THF (2 mL). The colourless solution was stirred overnight at room temperature. Slow evaporation of the solvent led to colourless crystals that were suitable for X-ray structural characterisation. Yield: 73.5 mg (83%). HRMS (ESI): *m*/*z* calcd for $C_{10}H_{20}CuS_4^+$: 330.973; found: 330.975 $[M + L]^+$. EA: calcd for $[C_{11}H_{20}CuF_3O_3S_5]$: C, 27.46%; H, 4.19%; found: C, 27.81%; H, 4.21%.

Synthesis of [Cu(14-S_4)]PF_6

A solution of $[Cu(MeCN)_4]PF_6$ (65.9 mg, 0.177 mmol) in THF (2 mL) was added dropwise to a solution of 14-S_4 (50.0 mg, 0.186 mmol) in THF (2 mL). The colourless solution was stirred overnight at room temperature. Slow evaporation of the solvent led to colourless crystals that were suitable for X-ray structural characterisation. Yield: 67.5 mg (80%). HRMS (ESI): *m*/*z* calcd for $C_{10}H_{20}CuS_4^+$: 330.973; found: 330.972 $[M + L]^+$. EA: calcd for $[C_{10}H_{20}CuF_6PS_4 + 0.25CH_3CN]$: C, 25.88%; H, 4.29%; N, 0.72%; found: C, 26.19%; H, 4.14%; N, 0.57%.

Synthesis of [Cu(14-S_4)]BPh_4

A solution of $[Cu(MeCN)_4PF_6$ (67.5 mg, 0.181 mmol) in DCM/acetone (1/1, 2 mL) was added dropwise to a solution of 14-S_4 (50.0 mg, 0.186 mmol) in DCM/acetone (1/1, 2 mL). The colourless solution was stirred for 30 minutes at room temperature. An acetone solution (2 mL) of sodium tetraphenylborate (61.9 mg, 0.181 mmol) was added to the reaction mixture and stirred at room temperature overnight. On the next day, the formed colourless solid was filtrated and 2 mL diethyl ether was added to the solution. The precipitated solid was filtrated, washed with diethyl ether and dried. Colourless crystals suitable for X-ray structural characterisation were obtained by slow diffusion of diethyl ether into a DCM solution of the complex at −30 °C for one day. Yield: 38.2 mg (32%). HRMS (ESI): *m*/*z* calcd for $C_{10}H_{20}CuS_4^+$: 330.973; found: 330.970 $[M + L]^+$. EA: calcd for $[C_{34}H_{40}BCuS_4]$: C, 62.70%; H, 6.19%; found: C, 62.21%; H, 6.02%.

Synthesis of $\{[Cu(14\text{-}S_4)(MeCN)PF_6]\}_n$

A solution of $[Cu(MeCN)_4]PF_6$ (69.3 mg, 0.177 mmol) in a THF/MeCN mixture (1/1, 2 mL) was added dropwise to a solution of 14-S_4 (50.0 mg, 0.186 mmol) in THF (2 mL). The colourless solution changed to a milky suspension after the solution of the copper-salt was added. The colourless solid was filtrated and a small amount

of the solid was dissolved again. Slow evaporation of the solvent led to colourless crystals that were suitable for X-ray structural characterisation. Yield: 44.8 mg.

Synthesis of [Cu(14-N_2S_2)]OTf

A solution of [Cu(MeCN)$_4$]OTf (63.7 mg, 0.169 mmol) in THF (2 mL) was added dropwise to a solution of 14-N_2S_2 (40.0 mg, 0.171 mmol) in THF (2 mL). The colourless solution was stirred overnight at room temperature. Slow evaporation of the solvent led to colourless crystals that were suitable for X-ray structural characterisation. Yield: 55.2 mg (73%). HRMS (ESI): *m*/*z* calcd for $C_{10}H_{22}CuN_2S_2^+$: 297.051; found: 297.051 $[M + L]^+$. EA: calcd for $[C_{11}H_{22}CuF_3N_2O_3S_3 + 0.1C_4H_8O]$: C, 30.14%; H, 5.06%; N, 6.17%; found: C, 30.49%; H, 4.90%; N, 6.11%.

Synthesis of [Cu(14-N_2S_2)]PF_6

A solution of [Cu(MeCN)$_4$]PF_6 (62.2 mg, 0.167 mmol) in DCM/THF (1/1, 2 mL) was added dropwise to a solution of 14-N_2S_2 (40.0 mg, 0.171 mmol) in DCM (2 mL). The colourless solution was stirred overnight at room temperature. Slow evaporation of the solvent led to colourless crystals that were suitable for X-ray structural characterisation. Yield: 62.1 mg (84%). HRMS (ESI): *m*/*z* calcd for $C_{10}H_{22}CuN_2S_2^+$: 297.051; found: 297.051 $[M + L]^+$. EA: calcd for $[C_{10}H_{20}CuF_6N_2PS_2 + 0.1C_4H_8O]$: C, 27.75%; H, 5.11%; N, 6.22%; found: C, 27.79%; H, 4.95%; N, 6.23%.

Synthesis of [Fe(14-S_4)(MeCN)$_2$]FeI_4 [26]

To a stirred solution of FeI_2 (116 mg, 0.373 mmol) in MeCN (2 mL), a solution of 14-S_4 (50.0 mg, 0.186 mmol) in DCM (2 mL) was added. The reaction mixture was heated at 50 °C for 4 h in order to start the reaction. Subsequently the reaction mixture was stirred for two days at room temperature. Slow evaporation of the solvent led to purple crystals that were suitable for X-ray structural characterisation. Yield: 20.2 mg (7%). HRMS (ESI): *m*/*z* calcd for $C_{10}H_{20}FeS_4^{2+}$: 161.989; found: 161.989 $[M + L]^{2+}$. EA: calcd for $[C_{14}H_{26}Fe_2I_4N_2S_4 + CH_2Cl_2]$: C, 17.08%; H, 2.68%; N, 2.66%; found: C, 16.80%; H, 2.45%; N, 2.26%.

Synthesis of [Fe(14-S_4)(MeCN)$_2$][(FeI_3)$_2$(14-S_4)]

To a stirred solution of 14-S_4 (50.0 mg, 0.186 mmol) in THF (2 mL), a solution of FeI_2 (57.6 mg, 0.186 mmol) in MeCN (2 mL) was added dropwise. The reaction mixture was heated at 50 °C for 4 h in order to start the reaction. Subsequently the reaction mixture was stirred for two days at room temperature. Slow evaporation of the solvent led to purple crystals that were suitable for X-ray structural characterisation. Yield: 34.5 mg (19%). HRMS (ESI): *m*/*z* calcd for $C_{10}H_{20}FeS_4^{2+}$: 161.989; found: 161.989 $[M + L]^{2+}$. EA: calcd for $[C_{24}H_{46}Fe_3I_6N_2S_8 + 3CH_3CN + FeI_2]$: C, 18.19%; H, 2.80%; N, 3.54%; found: C, 18.30%; H, 2.60%; N, 3.90%.

Synthesis of [Fe^{II}(14-S_4)(MeCN)$_2$](BAr_4^F)$_2$

To a stirred solution of 14-S_4 (50.0 mg, 0.186 mmol) in THF (2 mL), FeI_2 (57.6 mg, 0.186 mmol) in MeCN (2 mL) was added dropwise. The reaction mixture was heated at 50 °C and stirred for one day. After one day $AgBAr_4^F$ (404 mg, 0.372 mmol) was added and the suspension was stirred for 6 h. The colourless

precipitate was filtered off. Slow evaporation of the solvent led to purple crystals that were suitable for X-ray structural characterisation. Yield: 19.8 mg (5%). HRMS (ESI): *m*/*z* calcd for $C_{10}H_{20}FeS_4^{2+}$: 161.989; found: 161.989 $[M + L]^{2+}$. EA: calcd for $[C_{78}H_{50}B_2F_{48}FeN_2S_4 + 3.5CH_3CN]$: C, 44.85%; H, 2.68%; N, 3.38%; found: C, 44.88%; H, 2.21%; N, 3.76%.

Synthesis of $\{[Co(14\text{-}S_4)(MeCN)(Cl)_2]\}_n$

A suspension of $CoCl_2$ (24.2 mg, 0.186 mmol) in MeCN/THF (1/1, 2 mL) was added dropwise to a solution of 14-S_4 (50.0 mg, 0.186 mmol) in THF (2 mL) and stirred overnight. Unreacted $CoCl_2$ was filtrated and slow evaporation of the blue solvent led to blue crystals that were suitable for X-ray structural characterisation. Yield: 39.3 mg.

Synthesis of $[Co(14\text{-}S_4)(OTf)_2]$

A solution of $Co(OTf)_2$ (66.4 mg, 0.186 mmol) in THF (2 mL) was added dropwise to a solution of 14-S_4 (50.0 mg, 0.186 mmol) in THF (2 mL) and stirred at 60 °C over 3 days. After 3 days the solvent was evaporated and the pink solid was redissolved in MeCN. The orange/pink suspension was filtrated and the orange filtrate-solution was retained for evaporation. Slow evaporation of the solvent led to orange crystals that were suitable for X-ray structural characterisation. Yield: 10.0 mg (9%). HRMS (ESI): *m*/*z* calcd for $C_{10}H_{20}CoS_4^{2+}$: 163.488; found: 163.489 $[M + L]^{2+}$, $C_{11}H_{20}CoF_3O_3S_5^{+}$: 475.929; found: 475.924 $[M + L + OTf]^{+}$. EA: calcd for $[C_{12}H_{20}CoF_6O_6S_6]$: C, 23.04%; H, 3.22%; found: C, 23.30%; H, 3.00%.

Conclusions

Within this report, we describe the synthesis and characterisation of a series of mononuclear metal complexes (M = Cu, Fe, Co) containing the thioether ligands 14-S_4 and 14-N_2S_2. The iron and the cobalt complexes have been prepared mainly to investigate the coordination behaviour and solvent dependency and did not form "dioxygen adduct" complexes when reacted with either dioxygen or ozone. All complexes with the 14-S_4 ligand showed interesting metal ion coordination behaviour depending on the conditions. The copper(I) complexes were synthesise especially to investigate their reactivity towards different oxidants (dioxygen and ozone). Both copper(I) complexes, $[Cu^I(14\text{-}S_4)]OTf$ and $[Cu^I(14\text{-}N_2S_2)]OTf$, showed no reactivity towards dioxygen, similar to the copper(I) TMC complex. In contrast, both complexes reacted with ozone to form either an *end-on* superoxido or a *side-on* peroxido complex, an important finding with regard to opening a new possibility to prepare these complexes. Low temperature stopped-flow measurements showed that these complexes were not stable over time and therefore it was not possible to isolate and to crystallise them. However, by applying a suitable ligand system it should be possible to obtain more inert/stable "dioxygen adduct" complexes this way.

Conflicts of interest

There are no conflicts to declare.

Acknowledgements

We gratefully acknowledge support by the Justus-Liebig-Universität Gießen and the Deutsche Forschungsgemeinschaft for financial support (SS, SCHI 377/18-1). Furthermore, we would like to thank Stefan Schaub for his help in the laboratory with ozone handling.

Notes and references

1 D. A. Quist, D. E. Diaz, J. J. Liu and K. D. Karlin, *J. Biol. Inorg. Chem.*, 2017, **22**, 253.
2 S. T. Prigge, A. S. Kolhekar, B. A. Eipper, R. E. Mains and L. M. Amzel, *Science*, 1997, **278**, 1300.
3 S. T. Prigge, B. A. Eipper, R. E. Mains and L. M. Amzel, *Science*, 2004, **304**, 864.
4 C. Würtele, E. Gaoutchenova, K. Harms, M. C. Holthausen, J. Sundermeyer and S. Schindler, *Angew. Chem.*, 2006, **118**, 3951.
5 (*a*) K. Fujisawa, M. Tanaka, Y. Moro-oka and N. Kitajima, *J. Am. Chem. Soc.*, 1994, **116**, 12079; (*b*) A. M. Reynolds, B. F. Gherman, C. J. Cramer and W. B. Tolman, *Inorg. Chem.*, 2005, **44**, 6989.
6 A. Kunishita, M. Kubo, H. Sugimoto, T. Ogura, K. Sato, T. Takui and S. Itoh, *J. Am. Chem. Soc.*, 2009, **131**, 2788–2789.
7 L. M. Mirica, X. Ottenwaelder and T. D. P. Stack, *Chem. Rev.*, 2004, **104**, 1013.
8 (*a*) E. I. Solomon, D. E. Heppner, E. M. Johnston, J. W. Ginsbach, J. Cirera, M. Qayyum, M. T. Kieber-Emmons, C. H. Kjaergaard, R. G. Hadt and L. Tian, *Chem. Rev.*, 2014, **114**, 3659; (*b*) R. E. Cowley, L. Tian and E. I. Solomon, *Proc. Natl. Acad. Sci. U. S. A.*, 2016, **113**, 12035.
9 G. Y. Park, Y. Lee, D.-H. Lee, J. S. Woertink, A. A. Narducci Sarjeant, E. I. Solomon and K. D. Karlin, *Chem. Commun.*, 2010, **46**, 91.
10 (*a*) S. Kim, J. W. Ginsbach, A. I. Billah, M. A. Siegler, C. D. Moore, E. I. Solomon and K. D. Karlin, *J. Am. Chem. Soc.*, 2014, **136**, 8063; (*b*) S. Kim, J. Y. Lee, R. E. Cowley, J. W. Ginsbach, M. A. Siegler, E. I. Solomon and K. D. Karlin, *J. Am. Chem. Soc.*, 2015, **137**, 2796; (*c*) J. Y. Lee and K. D. Karlin, *Curr. Opin. Chem. Biol.*, 2015, **25**, 184.
11 M. Bhadra, W. J. Transue, H. Lim, R. E. Cowley, J. Y. C. Lee, M. A. Siegler, P. Josephs, G. Henkel, M. Lerch, S. Schindler, *et al.*, *J. Am. Chem. Soc.*, 2021, **143**, 3707.
12 M. Nappa, J. S. Valentine, A. Miksztal, H. J. Schugar and S. S. Isied, *J. Am. Chem. Soc.*, 1979, **101**, 7744.
13 T. Hoppe, S. Schaub, J. Becker, C. Würtele and S. Schindler, *Angew. Chem., Int. Ed.*, 2013, **52**, 870.
14 (*a*) X. Liang and P. J. Sadler, *Chem. Soc. Rev.*, 2004, **33**, 246; (*b*) M. Studer and T. A. Kaden, *Helv. Chim. Acta*, 1986, **69**, 2081.
15 T. L. Walker, W. Malasi, S. Bhide, T. Parker, D. Zhang, A. Freedman, J. M. Modarelli, J. T. Engle, C. J. Ziegler, P. Custer, *et al.*, *Tetrahedron Lett.*, 2012, **53**, 6548.
16 S. Schindler, Unpublishedresults.
17 I. Garcia-Bosch, R. E. Cowley, D. E. Díaz, M. A. Siegler, W. Nam, E. I. Solomon and K. D. Karlin, *Chem.–Eur. J.*, 2016, **22**, 5133.

18 (*a*) C. A. Grapperhaus, B. Mienert, E. Bill, T. Weyhermüller and K. Wieghardt, *Inorg. Chem.*, 2000, **39**, 5306; (*b*) O. Pestovsky, S. Stoian, E. L. Bominaar, X. Shan, E. Münck, L. Que and A. Bakac, *Angew. Chem.*, 2005, **117**, 7031; (*c*) S. Schaub, A. Miska, J. Becker, S. Zahn, D. Mollenhauer, S. Sakshath, V. Schünemann and S. Schindler, *Angew. Chem.*, 2018, **130**, 5453.
19 R. A. Baglia, J. P. T. Zaragoza and D. P. Goldberg, *Chem. Rev.*, 2017, **117**, 13320.
20 E. R. Dockal, L. L. Diaddario, M. D. Glick and D. B. Rorabacher, *J. Am. Chem. Soc.*, 1977, **99**, 4530.
21 M. M. Bernardo, M. J. Heeg, R. R. Schroeder, L. A. Ochrymowycz and D. B. Rorabacher, *Inorg. Chem.*, 1992, **31**, 191.
22 (*a*) S. Park, S. Y. Lee, K.-M. Park and S. S. Lee, *Acc. Chem. Res.*, 2012, **45**, 391; (*b*) M. Heller, *Z. Anorg. Allg. Chem.*, 2006, **632**, 441.
23 T. L. Walker, S. Mula, W. Malasi, J. T. Engle, C. J. Ziegler, A. van der Est, J. Modarelli and M. J. Taschner, *Dalton Trans.*, 2015, **44**, 20200.
24 M. D. Glick, D. P. Gavel, L. L. Diaddario and D. B. Rorabacher, *Inorg. Chem.*, 1976, **15**, 1190.
25 W. Schnick and M. Jansen, *Angew. Chem., Int. Ed. Engl.*, 1985, **24**, 54.
26 D. L. Hughes, M. Jimenez-Tenorio, G. J. Leigh, A. Houlton and J. Silver, *J. Chem. Soc., Dalton Trans.*, 1992, 2033.
27 J. F. Endicott, J. Lilie, J. M. Kuszaj, B. S. Ramaswamy, W. G. Schmonsees, M. G. Simic, M. D. Glick and D. P. Rillema, *J. Am. Chem. Soc.*, 1977, **99**, 429.
28 L. Iffland, D. Siegmund and U.-P. Apfel, *Z. Anorg. Allg. Chem.*, 2020, **646**, 746.
29 P. Gerschel, K. Warm, E. R. Farquhar, U. Englert, M. L. Reback, D. Siegmund, K. Ray and U.-P. Apfel, *Dalton Trans.*, 2019, **48**, 5923.
30 M. Wern, T. Hoppe, J. Becker, S. Zahn, D. Mollenhauer and S. Schindler, *Eur. J. Inorg. Chem.*, 2016, **2016**, 3384.

5. Summary

The selective oxidation of organic molecules plays an important role in the chemical industry for many years. Most reactions that use molecular dioxygen or alternative oxidants require a catalyst for the oxidation of organic substrates. Although many processes are long established in the chemical industry, catalysts are far from achieving 100% selectivity of the desired target products. Harsh reaction conditions, high resource consumption, and the formation of numerous by-products reflect several disadvantages that can arise during most reactions. Inspired by the reaction behavior of copper-containing enzymes, which can activate atmospheric dioxygen and selectively transfer it to organic molecules under mild reaction conditions, the focus is to reproduce the reaction behavior of copper-containing enzymes with oxidants, such as dioxygen, by synthesizing model complexes and stabilizing the oxygen species by appropriate ligand systems. A particular focus was placed on the PHM enzyme and its active site (*end-on* copper(II) superoxido complex).

In the first part of this research, based on the TMPA and TMG_3tren ligands, different sulfur-containing N_3S ligands were synthesized, and the corresponding copper(I) complexes were investigated in regard to their reactivity towards dioxygen using low-temperature stopped-flow technique. While the reaction of the copper(I) complexes with the TMPA derivatives showed reversible dioxygen binding with the formation of a *trans*-*μ*-1,2-peroxido species at −80 °C, specific ligand modification of the copper(I) complex with the TMG_3tren derivatives stabilized the *end-on* copper(II) superoxido complex at temperatures above −90 °C and allowed it to be kinetically studied using the stopped-flow technique. Similar systems known from the literature showed the formation of the *end-on* copper(II) superoxido complex at temperatures below −130 °C. The results show that even minimal changes to the ligand system can have a large effect on the reaction behavior and stability of the complex, and that oxygen species can be stabilized by specific ligand modification.

In the second part of this research, the sulfur-containing macrocyclic ligand systems N_2S_2 and S_4 were synthesized based on the cyclam ligand. This time, the corresponding copper(I) complexes showed no reactivity towards oxygen due to the increased stability of the copper(I) complexes by sulfur donor atoms. Due to this fact, ozone was investigated as another oxidant that is more reactive compared to

dioxygen. Using the stopped-flow technique, it was shown that the copper(I) complexes form oxygen adducts with ozone at low temperatures. While the copper(I) complex forms a *side-on* peroxido copper(II) complex with the N_2S_2 ligand and ozone, the copper(I) complex with the S_4 ligand reacts with ozone at −90 °C to form an *end-on* copper(II) superoxido complex, thus providing a model complex for the active site of the PHM enzyme. A possible mechanism for the reaction of the copper(I) complex with ozone was also established. The use of ozone as an oxidant offers the possibility of activating copper(I) complexes, which are inert to dioxygen, and form oxygen adducts.

Zusammenfassung

Die selektive Oxidation organischer Moleküle spielt seit vielen Jahren eine wichtige Rolle in der chemischen Industrie. Dabei benötigen die meisten Reaktionen, die molekularen Sauerstoff oder alternative Oxidationsmittel verwenden, einen Katalysator für die Oxidation organischer Substrate. Obwohl viele Prozesse in der chemischen Industrie bereits lange etabliert sind, erzielen die Katalysatoren bei weitem keine hundertprozentige Selektivität der gewünschten Zielprodukte. Harsche Reaktionsbedingungen, hoher Ressourcenverbrauch und die Entstehung zahlreicher Nebenprodukte spiegeln eine Reihe an Nachteilen wider, die während der meisten Reaktionen auftauchen können. Inspiriert vom Reaktionsverhalten kupferhaltiger Enzyme, die atmosphärischen Sauerstoff aktivieren und selektiv unter milden Reaktionsbedingungen auf organische Moleküle übertragen können, liegt der Fokus darauf, das Reaktionsverhalten kupferhaltiger Enzyme mit Oxidationsmitteln, wie Sauerstoff, durch die Synthese von Modellkomplexen zu reproduzieren und die Sauerstoffspezies durch entsprechende Liganden-Systeme zu stabilisieren. Ein besonderer Fokus wurde dabei auf das PHM Enzym und dessen aktiven Zentrum (*end*-on Superoxidokomplex) gelegt.

Im ersten Teil dieser Forschungsarbeit wurden basierend auf den TMPA und TMG_3tren Liganden verschiedene schwefelhaltige N_3S Liganden synthetisiert und die entsprechenden Kupfer(I)-Komplexe auf ihre Reaktivität gegenüber Sauerstoff mittels Tieftemperatur-Stopped-Flow-Technik untersucht. Während die Reaktion der Kupfer(I)-Komplexe mit den TMPA-Derivaten eine reversible Sauerstoffanbindung unter Ausbildung einer *trans*-Peroxidospezies bei −80 °C zeigten, konnte durch gezielte Liganden-Modifikation des Kupfer(I)-Komplexes mit dem TMG_3tren Derivaten der *end*-on Superoxidokomplex bei Temperaturen über −90 °C stabilisiert werden und mittels Stopped-Flow-Technik kinetisch untersucht werden. Ähnliche literaturbekannte Systeme zeigten die Ausbildung des *end*-on Superoxidokomplexes bei Temperaturen unter −130 °C. Die Ergebnisse verdeutlichen, dass bereits minimale Änderungen am Liganden-System einen großen Effekt auf das Reaktionsverhalten und die Stabilität des Komplexes haben können und dass durch gezielte Liganden-Modifikation die Sauerstoffspezies stabilisiert werden kann.

Im zweiten Teil dieser Forschungsarbeit wurden die schwefelhaltigen, makrozyklischen Liganden-Systeme N_2S_2 und S_4 aufbauend auf dem Cyclam

Liganden synthetisiert. Die entsprechenden Kupfer(I)-Komplexe zeigten diesmal keine Reaktivität gegenüber Sauerstoff aufgrund einer erhöhten Stabilität der Kupfer(I)-Komplexe durch Schwefel-Donor-Atome. Aufgrund dieser Tatsache wurde mit Ozon ein weiteres Oxidationsmittel untersucht, welches im Vergleich zu Sauerstoff reaktiver ist. Dabei konnte mittels Stopped-Flow-Technik gezeigt werden, dass die Kupfer(I)-Komplexe bei tiefen Temperaturen mit Ozon Sauerstoff-Addukte bilden. Während der Kupfer(I)-Komplex mit dem N_2S_2 Liganden und Ozon einen *side-on* Peroxidokomplex ausbildet, reagiert der Kupfer(I)-Komplex mit dem S_4 Liganden und Ozon bei −90 °C unter Ausbildung eines *end-on* Superoxidokomplexes und stellt somit ein Modelkomplex für das aktive Zentrum des PHM Enzyms dar. Es konnte außerdem ein möglicher Mechanismus für die Reaktion des Kupfer(I)-Komplexes mit Ozon aufgestellt werden. Die Verwendung von Ozon als Oxidationsmittel bietet die Möglichkeit Kupfer(I)-Komplexe, die gegenüber Sauerstoff inert sind, zu aktivieren und Sauerstoff-Addukte auszubilden.

6. References

[1] F. Cavani, *Catal. Today* **2010**, *157*, 8.

[2] J. N. Armor, *Catal. Today* **2011**, *163*, 3.

[3] a) M. Damm, B. Gutmann, C. O. Kappe, *ChemSusChem* **2013**, *6*, 978; b) M. Dugal, G. Sankar, R. Raja, J. M. Thomas, *Angew. Chem. Int. Ed.* **2000**, *39*, 2310.

[4] U. Schuchardt, D. Cardoso, R. Sercheli, R. Pereira, R. S. Da Cruz, M. C. Guerreiro, D. Mandelli, E. V. Spinacé, E. L. Pires, *Appl. Catal. A: Gen.* **2001**, *211*, 1.

[5] K. C. Hwang, A. Sagadevan, *Science* **2014**, *346*, 1495.

[6] Y. Yuan, H. Ji, Y. Chen, Y. Han, X. Song, Y. She, R. Zhong, *Org. Process Res. Dev.* **2004**, *8*, 418.

[7] a) L. Boisvert, K. I. Goldberg, *Acc. Chem. Res.* **2012**, *45*, 899; b) T. Punniyamurthy, S. Velusamy, J. Iqbal, *Chem. Rev.* **2005**, *105*, 2329.

[8] a) A. Decker, E. I. Solomon, *Curr. Opin. Chem. Biol.* **2005**, *9*, 152; b) X. Huang, J. T. Groves, *Chem. Rev.* **2018**, *118*, 2491.

[9] S. Hippeli, E. F. Elstner, *FEBS Lett.* **1999**, *443*, 1.

[10] C. L. Hill, I. A. Weinstock, *Nature* **1997**, *388*, 332.

[11] M. DeRosa, R. J. Crutchley, *Coord. Chem. Rev.* **2002**, *233-234*, 351.

[12] A. Greer, *Acc. Chem. Res.* **2006**, *39*, 797.

[13] E. J. Corey, M. M. Mehrotra, A. U. Khan, *J. Am. Chem. Soc.* **1986**, *108*, 2472.

[14] P. D. Bartlett, G. D. Mendenhall, D. L. Durham, *J. Org. Chem.* **1980**, *45*, 4269.

[15] M. Suzuki, *Acc. Chem. Res.* **2007**, *40*, 609.

[16] L. M. Mirica, X. Ottenwaelder, T. D. P. Stack, *Chem. Rev.* **2004**, *104*, 1013.

[17] R. E. Cowley, L. Tian, E. I. Solomon, *Proc. Natl. Acad. Sci. USA* **2016**, *113*, 12035.

[18] M. Momenteau, C. A. Reed, *Chem. Rev.* **1994**, *94*, 659.

[19] a) S. Aluri, S. P. de Visser, *J. Am. Chem. Soc.* **2007**, *129*, 14846; b) W.-D. Woggon, *Acc. Chem. Res.* **2005**, *38*, 127; c) S. Fetzner, R. A. Steiner, *Appl. Microbiol. Biotechnol.* **2010**, *86*, 791.

[20] S. S. Stahl, *Angew. Chem.* **2004**, *43*, 3400.

[21] I. S. MacPherson, M. E. P. Murphy, *Cell. Mol. Life Sci.* **2007**, *64*, 2887.

[22] K. I. Tishchenko, E. K. Beloglazkina, A. G. Mazhuga, N. V. Zyk, *Ref. J. Chem.* **2016**, *6*, 49.

[23] E. I. Solomon, U. M. Sundaram, T. E. Machonkin, *Chem. Rev.* **1996**, *96*, 2563.

[24] a) E. I. Solomon, R. Sarangi, J. S. Woertink, A. J. Augustine, J. Yoon, S. Ghosh, *Acc. Chem. Res.* **2007**, *40*, 581; b) P. Gamez, P. G. Aubel, W. L. Driessen, J. Reedijk, *Chem. Soc. Rev.* **2001**, *30*, 376; c) A. Chaudhari, M. Mahfouz, A. M. Fialho, T. Yamada, A. T. Granja, Y. Zhu, W. Hashimoto, B. Schlarb-Ridley, W. Cho, T. K. Das Gupta, A. M. Chakrabarty, *Biochemistry* **2007**, *46*, 1799.

[25] J. A. Guckert, M. D. Lowery, E. I. Solomon, *J. Am. Chem. Soc.* **1995**, *117*, 2817.

[26] P. M. Colman, H. C. Freeman, J. M. Guss, M. Murata, V. A. Norris, J. A. M. Ramshaw, M. P. Venkatappa, *Nature* **1978**, *272*, 319.

[27] H. B. Gray, B. G. Malmström, R. J. Williams, *J. Biol. Inorg. Chem.* **2000**, *5*, 551.

[28] I. A. Koval, P. Gamez, C. Belle, K. Selmeczi, J. Reedijk, *Chem. Soc. Rev.* **2006**, *35*, 814.

[29] a) J. A. Tainer, E. D. Getzoff, J. S. Richardson, D. C. Richardson, *Nature* **1983**, *306*, 284; b) J. A. Tainer, E. D. Getzoff, K. M. Beem, J. S. Richardson, D. C. Richardson, *J. Mol. Biol.* **1982**, *160*, 181; c) J. P. Klinman, *Chem. Rev.* **1996**, *96*, 2541; d) N. Ito, S. E. Phillips, K. D. Yadav, P. F. Knowles, *J. Mol. Biol.* **1994**, *238*, 794.

[30] N. Ito, S. E. Phillips, C. Stevens, Z. B. Ogel, M. J. McPherson, J. N. Keen, K. D. Yadav, P. F. Knowles, *Nature* **1991**, *350*, 87.

[31] A. Volbeda, W. G. Hol, *J. Mol. Biol.* **1989**, *209*, 249.

[32] C. Gerdemann, C. Eicken, B. Krebs, *Acc. Chem. Res.* **2002**, *35*, 183.

[33] a) A. Volbeda, W. G. Hol, *J. Mol. Biol.* **1989**, *206*, 531; b) Y. Matoba, T. Kumagai, A. Yamamoto, H. Yoshitsu, M. Sugiyama, *J. Biol. Chem.* **2006**, *281*, 8981; c) T. Klabunde, C. Eicken, J. C. Sacchettini, B. Krebs, *Nat. Struct. Mol. Biol.* **1998**, *5*, 1084.

[34] a) W. P. J. Gaykema, W. G. J. Hol, J. M. Vereijken, N. M. Soeter, H. J. Bak, J. J. Beintema, *Nature* **1984**, *309*, 23; b) M. E. Cuff, K. I. Miller, K. E. van Holde, W. A. Hendrickson, *J. Mol. Biol.* **1998**, *278*, 855; c) K. A. Magnus, H. Ton-That, J. E. Carpenter, *Chem. Rev.* **1994**, *94*, 727.

[35] A. L. Hughes, *Immunogenetics* **1999**, *49*, 106.

[36] K. D. Karlin, S. Itoh, S. Rokita, *Copper-oxygen chemistry*, Wiley, Hoboken, N.J., **2013**.

[37] D. A. Quist, D. E. Diaz, J. J. Liu, K. D. Karlin, *J. Biol. Inorg. Chem.* **2017**, *22*, 253.

[38] J. J. Liu, D. E. Diaz, D. A. Quist, K. D. Karlin, *Isr. J. Chem.* **2016**, *56*, 9.

[39] B. Hazes, K. A. Magnus, C. Bonaventura, J. Bonaventura, Z. Dauter, K. H. Kalk, W. G. Hol, *Protein Sci.* **1993**, *2*, 597.

[40] R. R. Jacobson, Z. Tyeklar, A. Farooq, K. D. Karlin, S. Liu, J. Zubieta, *J. Am. Chem. Soc.* **1988**, *110*, 3690.

[41] Z. Tyeklar, R. R. Jacobson, N. Wei, N. N. Murthy, J. Zubieta, K. D. Karlin, *J. Am. Chem. Soc.* **1993**, *115*, 2677.

[42] P. Gamez, I. A. Koval, J. Reedijk, *Dalton Trans.* **2004**, 4079.

[43] N. Kitajima, K. Fujisawa, Y. Morooka, K. Toriumi, *J. Am. Chem. Soc.* **1989**, *111*, 8975.

[44] N. Kitajima, K. Fujisawa, C. Fujimoto, Y. Morooka, S. Hashimoto, T. Kitagawa, K. Toriumi, K. Tatsumi, A. Nakamura, *J. Am. Chem. Soc.* **1992**, *114*, 1277.

[45] J. A. Halfen, S. Mahapatra, E. C. Wilkinson, S. Kaderli, V. G. Young, L. Que, A. D. Zuberbühler, W. B. Tolman, *Science* **1996**, *271*, 1397.

[46] S. Mahapatra, J. A. Halfen, E. C. Wilkinson, G. Pan, X. Wang, V. G. Young, C. J. Cramer, L. Que, W. B. Tolman, *J. Am. Chem. Soc.* **1996**, *118*, 11555.

[47] W. B. Tolman, *Acc. Chem. Res.* **1997**, *30*, 227.

[48] K. Fujisawa, M. Tanaka, Y. Moro-oka, N. Kitajima, *J. Am. Chem. Soc.* **1994**, *116*, 12079.

[49] C. Würtele, E. Gaoutchenova, K. Harms, M. C. Holthausen, J. Sundermeyer, S. Schindler, *Angew. Chem. Int. Ed.* **2006**, *118*, 3951.

[50] M. Becker, F. W. Heinemann, S. Schindler, *Chem. Eur. J.* **1999**, *5*, 3124.

[51] a) J. L. DuBois, P. Mukherjee, A. M. Collier, J. M. Mayer, E. I. Solomon, B. Hedman, T. D. P. Stack, K. O. Hodgson, *J. Am. Chem. Soc.* **1997**, *119*, 8578; b) V. Mahadevan, Z. Hou, A. P. Cole, D. E. Root, T. K. Lal, E. I. Solomon, T. D. P. Stack, *J. Am. Chem. Soc.* **1997**, *119*, 11996.

[52] G. Tian, J. A. Berry, J. P. Klinman, *Biochemistry* **1994**, *33*, 226.

[53] S. O. Pember, K. A. Johnson, J. J. Villafranca, S. J. Benkovic, *Biochemistry* **1989**, *28*, 2124.

[54] D. J. Merkler, R. Kulathila, A. P. Consalvo, S. D. Young, D. E. Ash, *Biochemistry* **1992**, *31*, 7282.

[55] K. D. Karlin, N. Wei, B. Jung, S. Kaderli, A. D. Zuberbühler, *J. Am. Chem. Soc.* **1991**, *113*, 5868.

[56] S. T. Prigge, B. A. Eipper, R. E. Mains, L. M. Amzel, *Science* **2004**, *304*, 864.

[57] S. Itoh, *Acc. Chem. Res.* **2015**, *48*, 2066.

[58] A. Hoffmann, M. Wern, T. Hoppe, M. Witte, R. Haase, P. Liebhäuser, J. Glatthaar, S. Herres-Pawlis, S. Schindler, *Eur. J. Inorg. Chem.* **2016**, *2016*, 4744.

[59] E. A. Lewis, W. B. Tolman, *Chem. Rev.* **2004**, *104*, 1047.

[60] a) E. I. Solomon, P. Chen, M. Metz, S.-K. Lee, A. E. Palmer, *Angew. Chem. Int. Ed.* **2001**, *40*, 4570; b) D. W. Randall, D. R. Gamelin, L. B. LaCroix, E. I. Solomon, *J. Biol. Inorg. Chem.* **2000**, *5*, 16.

[61] S. Kim, J. Y. Lee, R. E. Cowley, J. W. Ginsbach, M. A. Siegler, E. I. Solomon, K. D. Karlin, *J. Am. Chem. Soc.* **2015**, *137*, 2796.

[62] a) P. Chen, E. I. Solomon, *J. Am. Chem. Soc.* **2004**, *126*, 4991; b) P. Chen, J. Bell, B. A. Eipper, E. I. Solomon, *Biochemistry* **2004**, *43*, 5735.

[63] E. A. Ambundo, M.-V. Deydier, A. J. Grall, N. Aguera-Vega, L. T. Dressel, T. H. Cooper, M. J. Heeg, L. A. Ochrymowycz, D. B. Rorabacher, *Inorg. Chem.* **1999**, *38*, 4233.

[64] E. A. Ambundo, M. V. Deydier, L. A. Ochrymowycz, D. B. Rorabacher, *Inorg. Chem.* **2000**, *39*, 1171.

[65] N. W. Aboelella, B. F. Gherman, L. M. R. Hill, J. T. York, N. Holm, V. G. Young, C. J. Cramer, W. B. Tolman, *J. Am. Chem. Soc.* **2006**, *128*, 3445.

[66] L. Zhou, K. M. Nicholas, *Inorg. Chem.* **2008**, *47*, 4356.

[67] G. Y. Park, Y. Lee, D.-H. Lee, J. S. Woertink, A. A. Narducci Sarjeant, E. I. Solomon, K. D. Karlin, *Chem. Commun.* **2010**, *46*, 91.

[68] a) L. Zhou, D. Powell, K. M. Nicholas, *Inorg. Chem.* **2006**, *45*, 3840; b) L. Zhou, D. Powell, K. M. Nicholas, *Inorg. Chem.* **2007**, *46*, 7789.

[69] L. Q. Hatcher, D.-H. Lee, M. A. Vance, A. E. Milligan, R. Sarangi, K. O. Hodgson, B. Hedman, E. I. Solomon, K. D. Karlin, *Inorg. Chem.* **2006**, *45*, 10055.

[70] D.-H. Lee, L. Q. Hatcher, M. A. Vance, R. Sarangi, A. E. Milligan, A. A. N. Sarjeant, C. D. Incarvito, A. L. Rheingold, K. O. Hodgson, B. Hedman, E. I. Solomon, K. D. Karlin, *Inorg. Chem.* **2007**, *46*, 6056.

[71] I. Castillo, V. M. Ugalde-Saldívar, L. A. Rodríguez Solano, B. N. Sánchez Eguía, E. Zeglio, E. Nordlander, *Dalton Trans.* **2012**, *41*, 9394.

[72] T. Hoppe, P. Josephs, N. Kempf, C. Wölper, S. Schindler, A. Neuba, G. Henkel, *Z. Anorg. Allg. Chem.* **2013**, *639*, 1504.

[73] S. Kim, J. W. Ginsbach, A. I. Billah, M. A. Siegler, C. D. Moore, E. I. Solomon, K. D. Karlin, *J. Am. Chem. Soc.* **2014**, *136*, 8063.

[74] M. Bhadra, W. J. Transue, H. Lim, R. E. Cowley, J. Y. C. Lee, M. A. Siegler, P. Josephs, G. Henkel, M. Lerch, S. Schindler, A. Neuba, K. O. Hodgson, B. Hedman, E. I. Solomon, K. D. Karlin, *J. Am. Chem. Soc.* **2021**, *143*, 3707.

[75] a) D. Maiti, H. C. Fry, J. S. Woertink, M. A. Vance, E. I. Solomon, K. D. Karlin, *J. Am. Chem. Soc.* **2007**, *129*, 264; b) M. Bhadra, J. Y. C. Lee, R. E. Cowley, S. Kim, M. A. Siegler, E. I. Solomon, K. D. Karlin, *J. Am. Chem. Soc.* **2018**, *140*, 9042; c) D. E. Diaz, D. A. Quist, A. E. Herzog, A. W. Schaefer, I. Kipouros, M. Bhadra, E. I. Solomon, K. D. Karlin, *Angew. Chem. Int. Ed.* **2019**, *131*, 17736; d) R. L. Peterson, R. A. Himes, H. Kotani, T. Suenobu, L. Tian, M. A. Siegler, E. I. Solomon, S. Fukuzumi, K. D. Karlin, *J. Am. Chem. Soc.* **2011**, *133*, 1702; e) J. S. Woertink, L. Tian, D. Maiti, H. R. Lucas, R. A. Himes, K. D. Karlin, F. Neese, C. Würtele, M. C. Holthausen, E. Bill, J. Sundermeyer, S. Schindler, E. I. Solomon, *Inorg. Chem.* **2010**, *49*, 9450; f) R. L. Peterson, J. W. Ginsbach, R. E. Cowley, M. F. Qayyum, R. A. Himes, M. A. Siegler, C. D. Moore, B. Hedman, K. O. Hodgson, S. Fukuzumi, E. I. Solomon, K. D. Karlin, *J. Am. Chem. Soc.* **2013**, *135*, 16454.

[76] L. Q. Hatcher, K. D. Karlin, *J. Biol. Inorg. Chem.* **2004**, *9*, 669.

[77] X. Ottenwaelder, D. J. Rudd, M. C. Corbett, K. O. Hodgson, B. Hedman, T. D. P. Stack, *J. Am. Chem. Soc.* **2006**, *128*, 9268.

[78] Y. Funahashi, T. Nishikawa, Y. Wasada-Tsutsui, Y. Kajita, S. Yamaguchi, H. Arii, T. Ozawa, K. Jitsukawa, T. Tosha, S. Hirota, T. Kitagawa, H. Masuda, *J. Am. Chem. Soc.* **2008**, *130*, 16444.

[79] a) Z. Chen, T. J. Meyer, *Angew. Chem.* **2013**, *52*, 700; b) M.-T. Zhang, Z. Chen, P. Kang, T. J. Meyer, *J. Am. Chem. Soc.* **2013**, *135*, 2048; c) T. Zhang, C. Wang, S. Liu, J.-L. Wang, W. Lin, *J. Am. Chem. Soc.* **2014**, *136*, 273.

[80] a) D. Maiti, H. C. Fry, J. S. Woertink, M. A. Vance, E. I. Solomon, K. D. Karlin, *J. Am. Chem. Soc.* **2007**, *129*, 264; b) J. Y. Lee, R. L. Peterson, K. Ohkubo, I. Garcia-Bosch, R. A. Himes, J. Woertink, C. D. Moore, E. I. Solomon, S. Fukuzumi, K. D. Karlin, *J. Am. Chem. Soc.* **2014**, *136*, 9925.

[81] a) E. Kimura, *Tetrahedron* **1992**, *48*, 6175; b) J. J. Christensen, D. J. Eatough,R. M. Izatt, *Chem. Rev.* **1974**, *74*, 351; c) K. P. Wainwright, *Coord. Chem. Rev.* **1997**, *166*, 35.

[82] D. K. Cabbiness, D. W. Margerum, *J. Am. Chem. Soc.* **1969**, *91*, 6540.

[83] E. K. Barefield, *Coord. Chem. Rev.* **2010**, *254*, 1607.

[84] a) J. Cho, S. Jeon, S. A. Wilson, L. V. Liu, E. A. Kang, J. J. Braymer, M. H. Lim, B. Hedman, K. O. Hodgson, J. S. Valentine, E. I. Solomon, W. Nam, *Nature* **2011**, *478*, 502; b) J.-U. Rohde, J.-H. In, M. H. Lim, W. W. Brennessel, M. R. Bukowski, A. Stubna, E. Münck, W. Nam, L. Que, *Science* **2003**, *299*, 1037; c) M. T. Kieber-Emmons, J. Annaraj, M. S. Seo, K. M. van Heuvelen, T. Tosha, T. Kitagawa, T. C. Brunold, W. Nam, C. G. Riordan, *J. Am. Chem. Soc.* **2006**, *128*, 14230; d) J. Cho, J. Woo, J. Eun Han, M. Kubo, T. Ogura, W. Nam, *Chem. Sci.* **2011**, *2*, 2057; e) J. Cho, J. Woo, W. Nam, *J. Am. Chem. Soc.* **2010**, *132*, 5958.

[85] S. Schaub, A. Miska, J. Becker, S. Zahn, D. Mollenhauer, S. Sakshath, V. Schünemann, S. Schindler, *Angew. Chem. Int. Ed.* **2018**, *130*, 5453.

[86] R. A. Baglia, J. P. T. Zaragoza, D. P. Goldberg, *Chem. Rev.* **2017**, *117*, 13320.

[87] a) C. A. Grapperhaus, B. Mienert, E. Bill, T. Weyhermüller, K. Wieghardt, *Inorg. Chem.* **2000**, *39*, 5306; b) O. Pestovsky, S. Stoian, E. L. Bominaar, X. Shan, E. Münck, L. Que, A. Bakac, *Angew. Chem. Int. Ed.* **2005**, *117*, 7031.